Hypothalamic melanocortin system in the regulation of the energy homeostasis: studies in aging rats and in SHR animals

DOCTORAL (Ph.D.) THESIS

NÓRA FÜREDI

Head of Doctoral School: Prof. Erika Pinter M.D., Ph.D., D.Sc

Head of the Doctoral Program: Prof. Erika Pinter M.D., Ph.D., D.Sc

Supervisors: Erika Petervari M.D., Ph.D. and Balazs Gaszner M.D., Ph.D.

INSTITUTE FOR TRANSLATIONAL MEDICINE and

DEPARTMENT OF ANATOMY

MEDICAL SCHOOL, UNIVERSITY OF PECS

2018

1. INTRODUCTION 4
2. LITERATURE REVIEW 6
2.1. Central peptidergic regulation of the energy homeostasis 6
2.1.1. Regulation of the energy balance: hypothalamus and the main regulatory peptides 6
2.1.1.1. The main catabolic system of the hypothalamus: the melanocortins 8
2.1.1.1.1. Alpha-melanocyte stimulating hormone (alpha-MSH) 13
2.1.1.1.2. Agouti-related peptide (AgRP) 15
2.1.1.1.3. Selective melanocortin-4 receptor antagonist - HS024 16
2.1.2. Interaction between the regulation of the energy homeostasis and blood pressure (BP) 17
2.1.2.1. Hypothalamic MC system and blood pressure control 17
2.1.2.2. Neuropeptide Y and blood pressure control 18
2.1.2.3. Dysregulation of the energy homeostasis and blood pressure in SHR 18
2.1.2.3.1. Neuropeptides in SHR 19
2.2. Age-related alterations in the central peptidergic regulation of the energy homeostasis: the potential crucial role of melanocortins 20
3. AIMS AND HYPOTHESES 27
4. MATERIALS AND METHODS
4.1. Animals 30
4.2. Body composition measurements 31
4.2.1. Body composition assessment by micro-CT 31
4.2.2. Measurements of skinfold thickness (ST), repeatability and reproducibility 32
4.2.3. *Post mortem* analysis 32
4.3. Measurement of blood pressure 32
4.4. Surgeries and drug administration 33
4.5. Measurement of food consumption of rats 34
4.6. Metabolic and thermoregulatory assessment 35
4.7. Immunohistochemistry (IHC) 36
4.7.1. Tissue sampling for immunohistochemistry 36

4.7.2. Double labeling immunofluorescence for alpha-MSH and MC4R 36
4.7.3. Single immunofluorescence for AgRP 37
4.7.4. Immunofluorescence for NPY 37
4.7.5. Antiserum characterization and immunofluorescent controls 38
4.7.6. Microscopy and morphometry 38
4.8. Quantitative Real-Time Polymerase Chain Reaction (qRT-PCR) 39
4.8.1. Sampling for qRT-PCR 39
4.9. Statistical analysis 40
5. RESULTS AND DISCUSSION
5.1.Hypothesis I 42
5.1.1. Body composition (BC) measurements 42
5.1.1.1. Results of BC analysis 42
5.1.1.2. Discussion of the results of the BC analysis 49
5.1.2. Age-related changes in the hypothalamic MC system: *in vivo* investigation of catabolic responsiveness to exogenous melanocortin in Wistar rats 53
5.1.2.1. Results of *in vivo* experiments 53
5.1.2.2. Discussion of *in vivo* experiments 58
5.1.3. Age-related changes in the hypothalamic MC system: *in vitro* analysis of the endogenous activity in Wistar rats 60
5.1.3.1. Results of *in vitro* analysis 60
5.1.3.1. Discussion of *in vitro* results in view of our *in vivo* observations 66
5.2. Hypothesis II 71
5.2.1. Dysregulation in SHR rats 71
5.2.1.1. Results of *in vivo* and *in vitro* experiments 71
5.2.1.2. Discussion of *in vivo* and *in vitro* experiments 79
6. SUMMARY (MAIN FINDINGS) 83
7. CONCLUSIONS 84
8. ACKNOWLEDGEMENT 86
9. ABBREVIATIONS 87
10. REFERENCES 89
11. PUBLICATIONS 110

1. INTRODUCTION

Obesity, as a common risk factor for numerous diseases became in the last decades a major epidemiological and general healthcare challenge in Western countries (WHO 2012, 2014, 2015).

While middle-aged populations tend to become obese (Cameron et al. 2003; Rautiainen et al. 2016), old age is rather characterized by anorexia and consequent loss of active tissues (muscle) leading to sarcopenia (Morley et al. 2001; Landi et al. 2016; Ballyuzek et al. 2015). As both trends are also observed in other mammals (Tardif et al. 2011) common endogenous regulatory alterations may contribute to their development (Scarpace et al. 2001; Rautiainen et al. 2016; Landi et al. 2016; Ballyuzek et al. 2015). As similar trends were also observed in male laboratory mice (Blackwell et al. 1995) and rats (Balaskó et al. 2013), the idea arises that changes observed in humans and other mammals may share their biological background. Moreover, due to the current obesogenic environment, young adult populations and even children show increasing incidence of obesity leading to an early onset of cardiometabolic syndrome (Khoury et al. 2016) and a rise in premature mortality. Although these are well-known epidemiological observations, our knowledge on its neurobiological background is still insufficient.

The main goal of this Ph.D. research program was to gain deeper insight into the hypothalamic control of energy homeostasis. As the hypothalamic melanocortin (MC) system is a major central regulator of the energy homeostasis, we hypothesized that age-related shifts in the balance of melanocortins play an important role in long-term trends of body weight (BW) during the course of aging (*i.e*. middle-aged obesity and aging anorexia).

We analyzed the age-related changes in the effects and endogenous activity of the MC system using *in vivo* [*i.e.* measurement of BW, food intake (FI) and metabolic rate (MR), body composition (BC)] and *in vitro* (*i.e.* qRT-PCR and immunohistochemistry) techniques on hypothalamic samples of male Wistar rats of different age-groups.

The MC system influences via activation of the sympathetic nervous system not only the energy homeostasis but also the blood pressure (BP) regulation. The strong interaction between these two homeostatic systems was observed in spontaneously hypertensive rats (SHR). They have high sympathetic tone and progressive hypertension (Judy et al. 1976). Chronic calorie-restriction was able to prevent their hypertension (Dolinsky et al. 2010). Their FI and BW are lower than in normotensive controls, even on a high-fat diet, suggesting a dysregulation of energy homeostasis in these animals (Oliveira et al. 2009).

Therefore, we hypothesized that the dysregulation of the hypothalamic MC system may contribute both to the development of hypertension and altered energy homeostasis in SHR. As a part of this Ph.D. project the activity of the MC system of SHR was compared with that of Wistar rats in order to understand how the dysregulation of the MC system contributes to the characteristic phenotype of SHR rats.

2. LITERATURE REVIEW

2.1. Central peptidergic regulation of the energy homeostasis

2.1.1. Regulation of the energy balance: hypothalamus and the main regulatory peptides

The main components of energy balance are food intake (FI), metabolic rate (MR) and heat loss (HL). The balance between FI and MR determines on the short-term the actual feeding state (hunger vs. satiety) while on the long-term it determines the body weight (BW, nutritional state). The balance between the MR and the HL determines the body temperature and provides the stability of the core temperature (Tc). These two closely related regulatory circles control together the energy homeostasis (Székely and Szelényi 2005) (**Figure 1**).

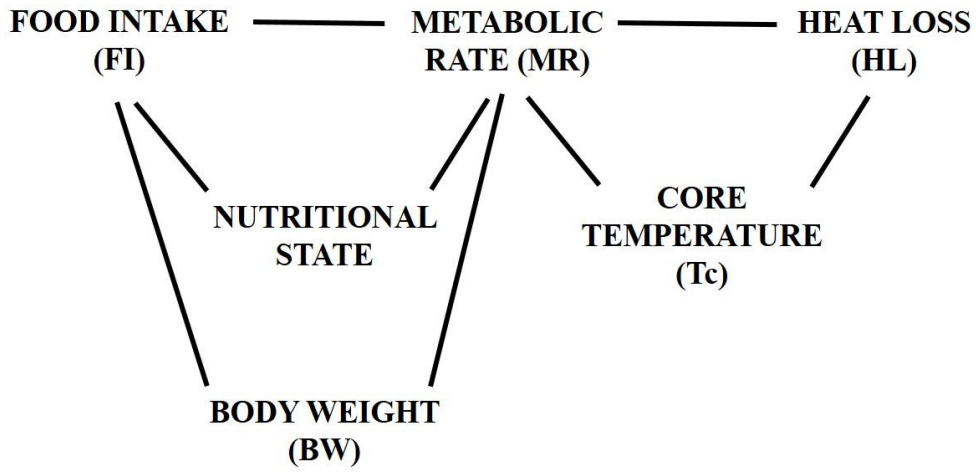

Figure 1: The main components of the energy homeostasis. The regulatory circles interact with each other: environmental temperature and internal thermoregulatory changes influence the FI, while the nutritional state and the BW affect the control of body temperature. If the balance between FI and the MR is overturned, BW change occurs, resulting either in weight gain/obesity or in malnutrition.

Both, the regulation of the BW and that of body temperature are orchestrated by hypothalamic neuropeptidergic centers. Peptides based on their effects on the FI may be classified as orexigenic (increase the FI) or anorexigenic (decrease the FI) mediators. To assess the general effect of a particular neuropeptide on energy balance one has to consider its influence on the MR as well. From the aspect of energy balance, the orexigenic/anorexigenic effects on FI can be evaluated as coordinated, if they are coupled with concomitant regulatory changes in the MR and body temperature, which act in the same direction of energy balance. For instance, hyperphagia with hypometabolism (decreased MR) is an anabolic state (results in

weight gain), in contrast to the catabolic effect, *i.e.* hypophagia with hypermetabolism (increased MR) resulting in weight loss (**Figure 2**).

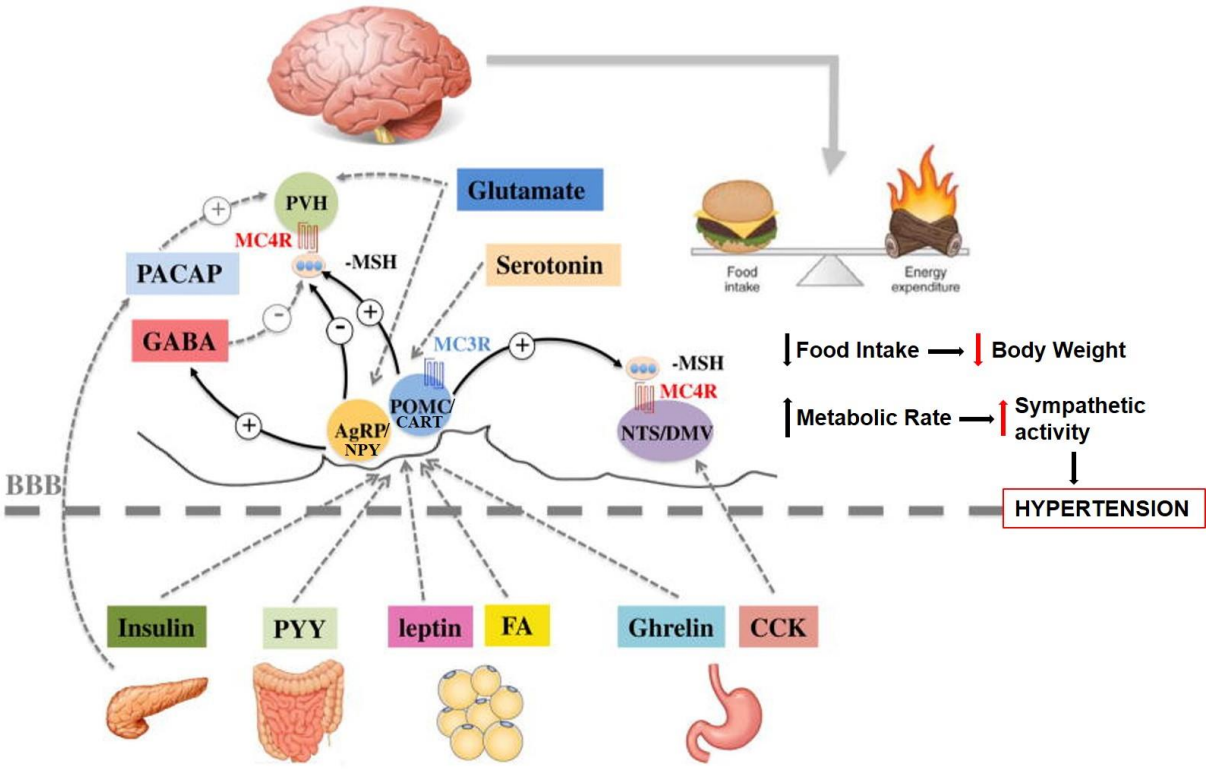

Figure 2: Neural regulation of energy homeostasis in the arcuate nucleus (ARC). The ARC contains two feeding-related neuronal groups: the agouti-reated peptide (AgRP) / neuropeptide Y (NPY) expressing neurons with orexigenic and hypometabolic properties (stimulate food intake and decrease energy expenditure) and the pro-opiomelanocortin (POMC)/ cocaine and amphetamine-regulated transcript (CART) neurons with anorexigenic and hypermetabolic features (inhibit food intake and increase energy expenditure). Insulin and leptin among other peripheral signals, provide information on the energetic status of the organism. They stimulate the POMC/CART neurons while they inhibit AgRP/NPY nerve cells. On the other hand, during fasting, the activation of AgRP/NPY expressing neurons is characteristic, while POMC/CART neurons get inhibited. Alpha-melanocyte stimulating hormone (a post-translational derivate of POMC) by its catabolic activity (inhibits the food intake, increases the metabolic rate) decreases the body weight and stimulates the sympathetic activity leading to elevation of BP. Ghrelin is an orexigenic gastric peptide which stimulates the food intake by direct activation of AgRP/NPY neurons.

These two feeding-related first-order neuron groups of the ARC transmit the signals to the second order neurons via NPY- and melanocortin receptors. Abbreviations: PYY, peptide YY; FA, fatty acids; CCK, cholecystokinin; MC3R/MC4R, melanocortin 3/4 receptor; PVH: paravetricular nucleus; NTS, nucleus tractus solitarius; DMV, dorsal motor nucleus of the vagus; PACAP, pituitary adenylate cyclase-activating polypeptide; GABA, gamma-aminobutyric acid; BBB, blood-brain barrier. (Own figure, based on work of Shen et al. 2017)

2.1.1.1. The main catabolic system of the hypothalamus: the melanocortins

The hypothalamic MC system including adrenocorticotrop-hormone (ACTH), beta-endorphin, beta-lipotropine, corticotropin-like intermediate-lobe-protein (CLIP) as well as alpha-, beta-, and gamma-melanocyte-stimulating hormones (MSH) has well established and important role in the regulation of energy homeostasis. Five distinct types of MC receptors (MC1R-MC5R) have been identified involved in a wide range of biological functions. They are expressed in various types of tissues as detailed in **Table 1/Panel A** (Garfield et al. 2009). All the MC receptors are coupled to Gs proteins (GPCR) (Gantz and Fong 2003; Mountjoy et al. 1992) and signalize through the cyclic AMP (cAMP) pathway by activating adenylate cyclase resulting in increased intracellular cAMP levels (Konda et al 1994; Manna et al. 1998; Blondet et al. 2004). MC receptors are involved in diverse biological functions, such as memory (Giuliani et al. 2015; Shen et al. 2016; Giuliani et al. 2017; Scantlebury et al. 2017), nociception (Pan et al. 2013; Ye et al. 2014; Hellard et al. 2017), both anti- and pro-inflammatory processes (Bhardwaj et al. 1996; Redondo et al. 1998; Ichiyama et al. 1999; Mountjoy et al. 2003; Caruso et al. 2004; Catania et al. 2004; Maaser et al. 2006), mood control (Yilmaz et al. 2014, 2015) and addiction (Bruijnzeel 2017).

Some features of the MC receptors are briefly listed below. Taking the significant role of MC3R and MC4R in energy homeostasis in consideration, they will be highlighted.

MC1R possesses anti-inflammatory effects in neutrophils, monocytes, macrophages, dendritic cells, B lymphocytes, glial cells, and endothelial cells (Catania et al. 2004; Catania et al. 2010) by binding alpha-MSH.

MC2R is a highly sensitive and highly specific receptor for ACTH wich is also known as ACTH receptor. Its major function is to stimulate the cells of the zona fasciculata in the adrenal cortex to synthesize and secrete glucocorticoid hormones. Glucocorticoids influence a wide range of biological functions including energy homeostasis (So et al. 2009; Lee et al. 2014), immune system (Lindsay et al. 2016) and stress response (Whirledge and Cidlowski 2013; Myers et al. 2014). Mutations in MC2R gene accounts for 25% of all cases of the familial glucocorticoid deficiency (FGD), a rare autosomal recessive disorder characterized by a severe glucocorticoid deficiency, associated with failure of adrenal responsiveness to ACTH (Thisthlethwaite et al. 1975; Chung et al. 2008; Clark et al. 1998). In addition, ACTH has a permissive effect on zona glomerulosa cells to secrete mineralocorticoids and zona reticularis cells to secrete adrenal androgens.

MC2Rs are also able to bind alpha-MSH, but with lower potential. MC2R is also present in human skin cells (Slominski et al. 1996) which are activated by ACTH inducing cortisol production in the skin (Slominski et al. 2000; Ito et al. 2005) and also regulates hair growth (Ito at el. 2005). MC2R is also expressed in mouse adipocytes (Norman et al. 2003; Boston et al. 1996; Cho et al. 2005; Moller et al. 2011), where it was suggested to regulate lipolysis (Boston 1999).

MC3Rs and MC4Rs are central players in the hypothalamic regulation of energy balance conveying anorexigenic/hypermetabolic effects (Balthasar et al. 2005).

MC3Rs are expressed primarily in the brain such as in the arcuate nucleus of the hypothalamus (ARC), ventromedial hypothalamic nucleus (VMH), ventral tegmental area (VTA). Moderate expression of MC3R was detected in anteroventral preoptic nucleus, lateral and posterior hypothalamic area and paraventricular nucleus of the hypothalamus (PVN) (Roselli-Rehfuss et al. 1993; Gantz et al 1993; Cone 2006) (**Table 1/Panel C)**. In the periphery, MC3Rs are present on the surface of macrophages and B lymphocytes influencing the inflammatory responses (Gettings et al. 2000). They also occur in the placenta, heart, and the mesenteric microcirculation (Leoni et al. 2008). It has a potent effect on the energy homeostasis, shaping the thermoregulation response (Verty et al. 2010) by creating a thermogenic tone via brown adipose tissue (BAT) activity.

MC3R null mice are mildly obese (Butler et al. 2000). Genetic variation of human MC3R may contribute to the obesity (Feng et al. 2005; Renquist et al. 2011). Mutations of the *Mc3r* gene frequently cause type 2 diabetes mellitus and obesity (Mountjoy 2010). In accordance with this, *Mc3r* polymorphisms were shown to be associated with increased risk of childhood obesity (Feng et al. 2005; Mencarelli et al. 2011; Savastano et al. 2009; Zegers et al. 2011).

The MC4R is the most important receptor type concerning the regulation of energy homeostasis (Balthasar et al. 2005).

MC4Rs are expressed in the CNS, primarily in hypothalamic regions, such as anteroventral periventricular nucleus, dorsal hypothalamic area, but the most emphasized site of MC4R expression is the PVN (Kishi et al. 2003) (**Table 1/Panel C)**. Stimulation of central MC4R induces anorexigenic response by decreasing appetite and FI (Cowley 2003; Ellacotte and Cone 2004; Adan et al. 2006), while the inhibition leads to orexigenic effects (*i.e*. increased appetite and FI) (Scarlet and Marks 2005; DeBoer and Marks 2006; Nicholson et al. 2006). Deletion of MC4R in mice results in hyperphagia, associated with increased fat and lean mass, increased body length, reduced activity, and reduced MR leading to obesity (Huszar et al. 1997;

Balthasar et al. 2005). Mutations of the human *Mc4r* gene are responsible for up to 6% of morbid obesity cases (Loos 2011).

Previous studies have also shown, that MC4R gene mutation or deletion could contribute to obesity in rodents and also in humans (Vaisse et al. 2000; Ste Marie et al. 2000; Farooqi et al. 2003). The disruption of MC4R signaling resulted in a late-onset obesity with severe complications like hyperglycemia and hyperinsulinemia (Huszar et al. 1997).

MC4R-related obesity may be of diverse molecular background. For instance, reduced MC4R function caused by genetic mutations or polymorphisms at the *Mc4r* gene (Farooqi et al. 2003; Loos et al. 2008; Vaisse et al. 1998; Yeo et al. 1998), as well as the absence or the low level of the endogenous agonist (Krude et al. 1998), or inactivation of pro-opiomelanocortin (POMC) neurons was shown to cause early-onset obesity characterized by hyperphagia and reduced energy expenditure in humans (Yeo et al. 1998; Vaisse et al. 1998; Krude et al. 1998). MC3R and MC4R share their ligands: alpha-MSH is an agonist while AgRP possesses the characteristics of an inverse agonist of these receptors (Tao 2014). MC4Rs exist in the peripheral nervous system as well (Gautron et al. 2010) influencing sexual behavior and erectile function (Martin and MacIntyre 2004; Wikberg and Mutulis 2008).

The MC5R was found to be expressed in a variety of organs and tissues. These receptors in mice contribute to the regulation of exocrine glandular secretion (Chen et al. 1997), glucose uptake (Enriori 2016), fatty acid oxidation in muscle tissues (An et al. 2007). MC5R occurs in rat liver involved in the cell protection during acute phase response (Malik et al. 2012). Another group published that melanocortins stimulate the lipid production in human sebaceous glands through MC5R (Zang et al. 2011). In line with this, MC5R KO mice were shown to exert deficiency in the function of exocrine glands including sebaceous glands. MC5R is present in the immune system as it activates T-lymphocytes (Lee and Taylor 2011; Taylor and Namba 2001; Taylor et al. 2006; Taylor and Lee 2010), conveys immunomodulatory signals to B lymphocytes (Buggy 1998) and induces cytokine secretion. Metabolic actions involve promoted lipolysis and reduced fatty acid re-esterification in adipocytes (Jun et al. 2010; Boston and Cone 1996; MØller et al. 2011; Rodrigues et al. 2013).

A

Receptor	Distribution	Endogenous agonists	Endogenous antagonists	Function
MC1R	dermal fibroblasts keratinocytes melanocytes neutrophils monocytes B lymphocytes macrophages endothelial cells dendritic cells glial cells astrocytes	**alpha-MSH, beta-MSH, ACTH**, gamma-MSH	Agouti	nociception anti-inflammatory skin pigmentation
MC2R	adrenal cortex, melanocytes, keratinocytes, adipose tissue, bone cells	**ACTH**	Agouti	steroidogenesis
MC3R	ARC, VMH, VTA, PVN, lateral hypothalamic area, posterior hypothalamic area, stomach, duodenum, kidneys, placenta, heart, monocytes, macrophages	**alpha-MSH, beta-MSH, gamma-MSH, ACTH**	**AgRP**	**energy homeostasis** **food intake** anti-inflammatory
MC4R	cortex, thalamus, hypothalamus, hippocampus, brainstem spinal cord, astrocytes heart, lung, kidney, testis	**alpha-MSH, beta- MSH, ACTH**, gamma-MSH	Agouti **AgRP**	**energy homeostasis** **food intake** anti-inflammatory nociception memory mood disorders neuroprotection drug addiction drug tolerance sexual behavior
MC5R	skin, spleen, lung, gut, sexual organs, bone marrow, adipose tissue	**alpha-MSH,** beta-MSH, ACTH, gamma-MSH	Agouti	exocrine secretion lipid mobilization

B

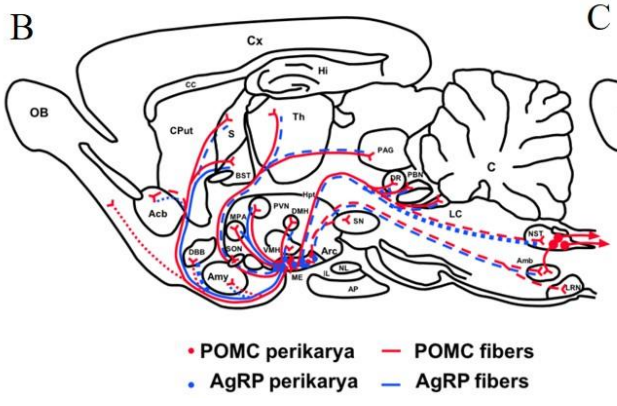

C

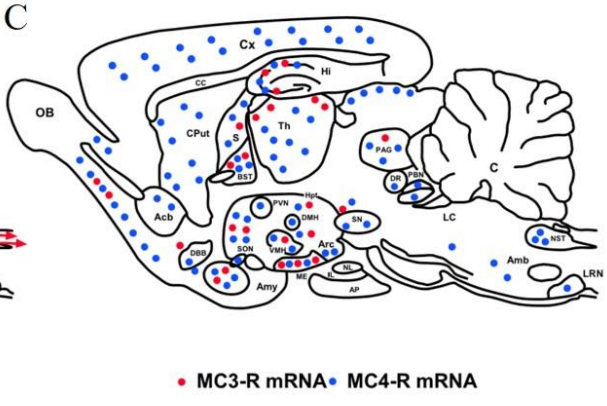

Table 1/Panel A: Melanocortin receptors (MCR) and their ligands. Bold characters mark the high-affinity ligands of the corresponding receptors. The table is focused on the metabolic control-related features of these mediators, as these functions are relevant for this PhD thesis. **Panel B:** represents the sagittal section of rat brain focusing the distribution of POMC and AgRP neuronal system. **Panel C**: Shows the distribution of MC3R and MC4R mRNA in the rat brain. (B and C: Jégou et al. Handbook of biologically active peptides, book chapter 111.)

The MC system implements its catabolic effect: weight loss inducing action by decreasing FI and increasing the MR via activation of sympathetic nervous system with simultaneously elevated body temperature (Tc) (Krashes et al. 2016; Moehlecke et al. 2016).

Melanocortins may be classified into two main groups. The endogenous agonists (*i.e.* alpha-, beta-, gamma-MSH and ACTH) convey an excitatory effect. On the other hand, two naturally present endogenous antagonists, more precisely inverse antagonists are the agouti protein and agouti-related peptide (AgRP) (Tao 2014) occurring in the central nervous system.

Among the ligands of the MC receptors, the excitatory melanocortins are derived from a post-translational processing of POMC, which is coded by the *Pomc* gene (Brzoska et al. 2008; Butler 2006; Catania et al. 2000). The *Pomc* gene is expressed significantly in various mammalian tissues, such as in the anterior and intermediate lobe of pituitary, in the immune system and skin. Centrally, the hypothalamus, amygdala, and the cerebral cortex were shown to contain the *Pomc* gene product, but it was not detectable in midbrain or cerebellar RNA samples (Smith and Blalock 1981; Bertagna 1994; Castro and Morison 1997; Civelli et al. 1982). Post-translationally, POMC is cleaved by serine-type proteinase prohormone convertase 1 and 2 (PC1, PC2) into a variety of smaller peptides such as ACTH, beta-endorphin, beta-lipotropine, CLIP as well as alpha-, beta-, and gamma-melanocyte-stimulating hormones (MSH) (Crine et al. 1979; Mains and Eipper 1979; Loh 1979). The post-translational modification of the POMC peptide is site-specific, which is explained by the expression patterns of PC1 and PC2 enzymes. PC1 is found in corticotroph cells of the anterior pituitary and cleaves POMC to generate shorter peptide chain derivative hormones. In the intermediate pituitary melanotroph cells express both PC1 and PC2. PC1 splits POMC into ACTH, while PC2 cleaves ACTH further yielding to alpha-MSH (Chretien and Mbikay 2016). As beta- and gamma-MSH were found to play a significant role in fish, here we do not provide detailed information on these messengers (Dores and Baron 2011).

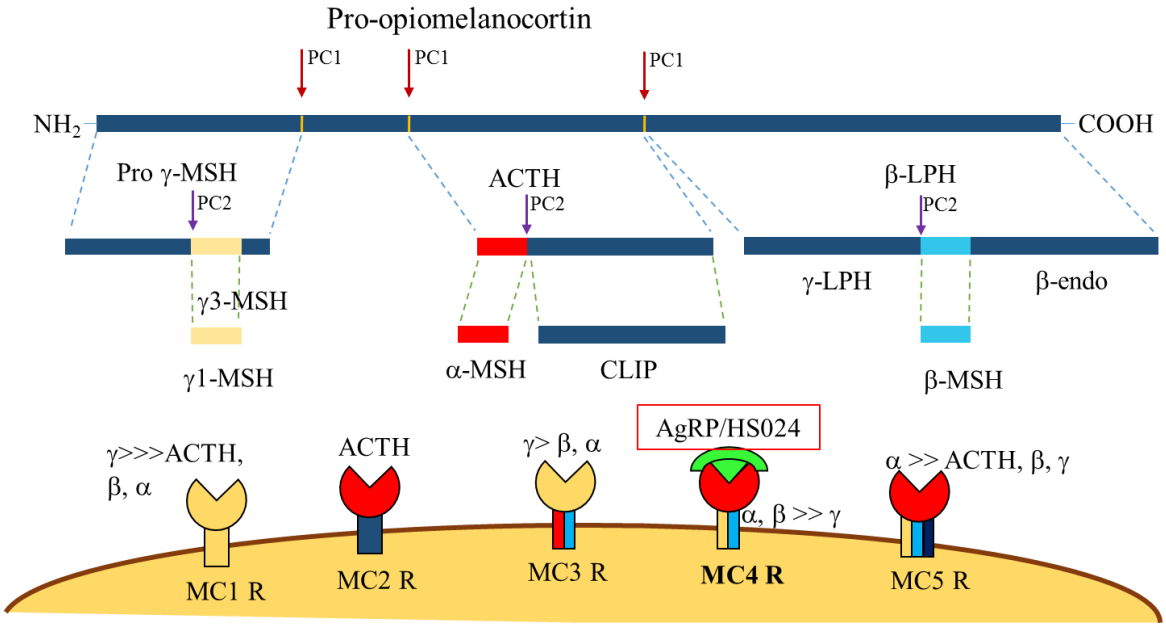

Figure 3: Schematic overview of the melanocortin system. PC1: proconvertase, PC2: proconvertase 2, ACTH: adrenocotricotrop hormone, LPH: lipotropin hormone, AgRP: agouti-related peptide, MC1/2/3/4/5: melanocortin receptors, CLIP: corticotropin-like intermediate-lobe-protein, β-endo: β-endorphin, MSH: melanocyte-stimulating hormone. Angle bracket symbolizes the difference in affinity of ligands to the MC receptors (own figure, based on Ramachandrappa et al. 2013).

2.1.1.1.1. Alpha-melanocyte-stimulating hormone (alpha-MSH)

Alpha-MSH (Ser-Tyr-Ser-Met-Glu-His-Phe-Arg-Trp-Gly-Lys-Pro-Val) is cleaved as a thirteen amino acid N-terminal peptide segment of the POMC derived ACTH (Brzoska et al. 2008; Butler 2006; Catania et al. 2000). Alpha-MSH is a peptide of basic characteristic which is acetylated at the N-terminus and amidated at the C-terminus (Seidah and Chretien 1994; Benjannet et al. 1991).

The POMC mRNA was detected by Northern blot in hypothalamus, amygdala and the cerebral cortex (Civelli et al. 1982) samples of adult rodents. Later on, the POMC was also identified in the nucleus tractus solitarii (NTS) and lateral reticular formation of the rat brainstem by ACTH immunohistochemistry (Joseph et al. 1983; Schwartzberg and Nakane 1983) and by *in situ* hybridization (Bronstein et al. 1992). Nevertheless, the main expression site is the hypothalamic ARC. Here, POMC neurons express both alpha-MSH (Morton et al. 2006) and another anorexigenic peptide, CART.

Using reporter mice expressing green-fluorescent protein (GFP) under POMC promoter revealed that almost 100% of the GFP cells contain POMC in the ARC. In other brain regions,

GFP was not expressed (Pinto et al. 2004). Padilla et al. in 2012 have concluded comparing three techniques (POMC-Cre, POMC-GFP, *in situ* hybridization) that POMC expression in the adult mouse brain is restricted to ARC and NTS (Padilla et al. 2012).

In this work we focused on the hypothalamic peptidergic control of the energy homeostasis, therefore NTS-POMC expressing neurons will not be detailed in this thesis.

POMC neurons are heavily interconnected within the ARC, and they project widely in- and outside the hypothalamus (Eskay et al. 1979; Chen and Pelletier 1983; Kiss and Williams 1983). POMC/CART and AgRP/NPY neurons show similar connectivity. They project to several areas within the hypothalamus, such as the medial preoptic area, PVN) lateral hypothalamic area (LH), VMH, dorsomedial (DMH) and posterior hypothalamus (Bagnol et al. 1999). Furthermore, POMC neurons in the ARC send projections to the bed nucleus of stria terminalis (BNST), lateral septum, nucleus accumbens, lateral parabrachial nucleus (LPB), the periaqueductal gray, and the dorsal vagal nuclear complex (DMV) outside the hypothalamus (Singru 2005; Lechnan and Fekete 2006). Projections to the hindbrain preganglionic sympathetic neurons of the NTS, DMV may play important role in the effects on appetite, SNS activity and arterial pressure, since they are all important sites for autonomic regulation (**Table 1/Panel B**).

POMC, and consequently alpha-MSH production in the ARC is triggered by peripheral signals (*i.e*. leptin, insulin and glucose) providing information about the feeding/nutritional state and BW (Leinninger 2009) (**Figure 2** and **4**). The ablation of ARC-POMC neurons using diphtheria toxin results in hyperphagia, decreased energy expenditure obesity (Zhan et al. 2013). Chronic optogenetic stimulation of POMC neurons in ARC was found to reduce FI and cause weight loss (Aponte et al. 2011; Zhan et al. 2013). In case of acute chemical stimulation of ARC POMC has been shown to promote feeding by endocannabinoids, which may be responsible for the delayed response of ARC-POMC neurons, but not that of NTS-POMC cells (Koch et al. 2015).

POMC producing neurons release alpha-MSH. To express its effects on energy balance, the peptide induces cAMP elevation via Gs protein coupled MC3R and MC4R receptors expressed in the PVN (Li et al. 2013).

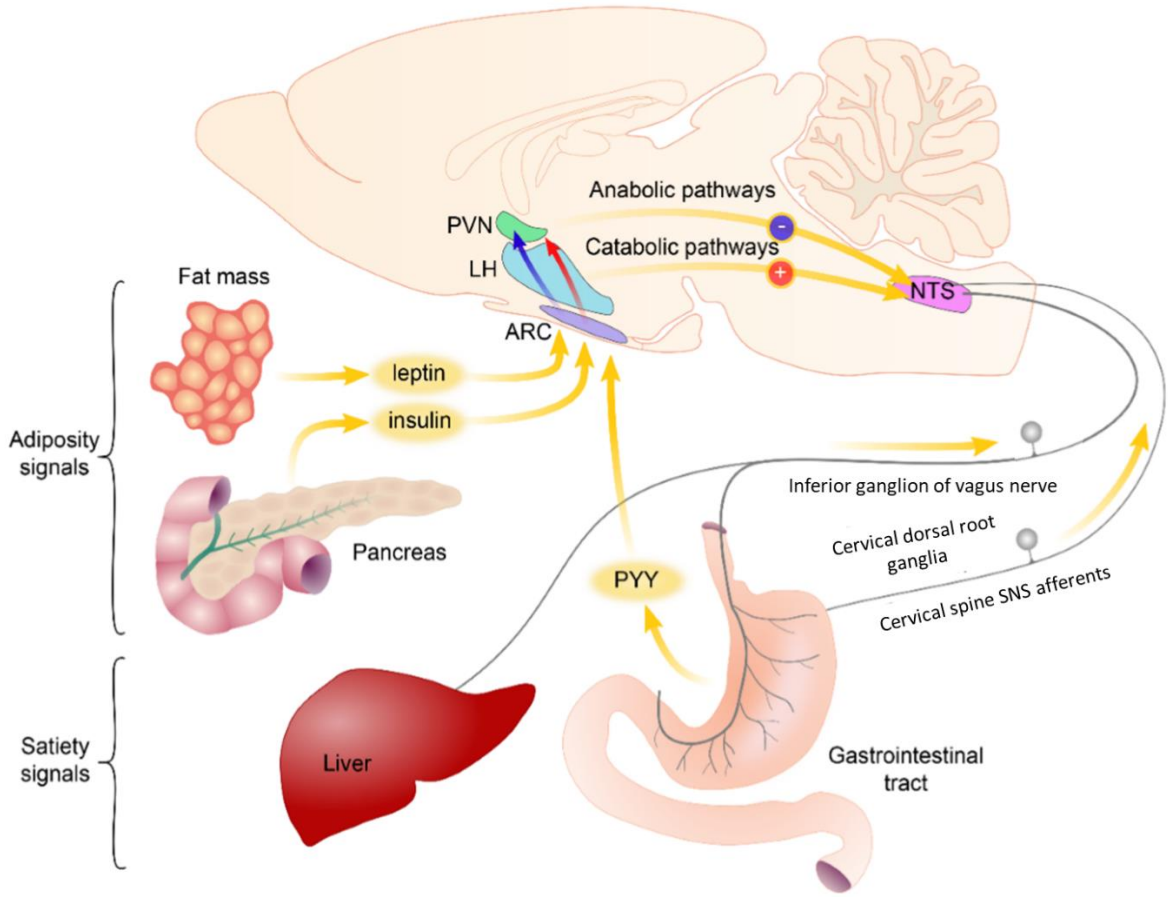

Figure 4: Schematic illustration of pathways transmitting energy homeostasis-related signals from the peripheral organs to the central nervous system. The circulating blood contains satiety-related hormones like PYY released from the gastrointestinal tract and adiposity hormones like leptin and insulin. The primary central target of these hormones is the arcuate nucleus (ARC). Neurons of the ARC sense and integrate these signals and transmit toward second order neuronal groups like the hypothalamic paraventricular nucleus (PVN) and the lateral hypothalamus (LH). The vagus nerve and the sympathetic nerves carry information about the amount and the quality of the consumed food sensed by mechano- and chemosensitive receptors and by detecting locally released hormones. Axons of these nerves terminate on the neurons of the nucleus tractus solitarii (NTS). Descending pathways from the hypothalamus influence the sensitivity of the NTS neurons to vagus derived inputs. Modified from Barsh and Schwartz Nature, 2002.

2.1.1.1.2. Agouti-related peptide (AgRP)

AgRP, an analog of agouti (agouti signaling protein) was discovered in 1997. Expression mapping revealed that the main central AgRP expression site is the ARC. In the periphery, it is predominantly found in the adrenal gland (Fong et al. 1997; Graham et al. 1997; Ollmann et al.

1997) but its low expression was demonstrated in the lung, kidney, testis and ovaries (Shutter et al. 1997; Ollman et al. 1997) as well.

Ninety percent of AgRP neurons in the ARC co-express another potent orexigenic messenger, neuropeptide Y (NPY). AgRP neurons located in the ARC project to many hypothalamic nuclei including PVN, LH, VMH, posterior hypothalamus, DMH, and medial preoptic area (Bagnol et al. 1999). These neurons also innervate extrahypothalamic areas like the BNST, and the LPB, central nucleus of the amygdala (CEA), and periaqueductal gray (PAG) (Singru et al. 2012; Betley et al. 2013; Wang et al. 2015; Zséli et al. 2016).

AgRP binds with high affinity both to MC3R and MC4R (Chai et al. 2003) as a competitive antagonist of alpha-MSH (Ollmann et al. 1997), furthermore, it is an inverse agonist of MC4R by decreasing cAMP levels attributed to the constitutive activity of MC4R (Haskell-Luevano and Monck 2001; Nijenhuis et al. 2001; Chai et al. 2003). Besides these, a low affinity to MC1R has been shown (Ollmann et al. 1997).

The mRNA expression level of AgRP in the ARC measured by *in situ* hybridization depends on the nutritional state in mice (Swart et al. 2002). From our recent study we demonstrated that after 48 hours fasting period the peptide level of AgRP is increased not only in the ARC but also in the centrally projecting Edinger-Wesphal nucleus (Füredi et al. 2017). Intracerebroventricular (ICV) injection of AgRP increases FI for up to a week. Co-injection of AgRP with alpha-MSH quenches the orexigenic effects of the AgRP. In line with these, it has been shown that a 48-h fasting period increased the level of AgRP in human blood samples also affecting BC and nutritional state. Interestingly, elevated AgRP plasma concentrations were shown both in obese children (Vehapoğlu et al. 2016) and in adults (Hazell et al. 2016).

2.1.1.1.3. Selective melanocortin-4 receptor antagonist -HS024

AgRP and alpha-MSH are believed to be the natural antagonist and agonist of MC3R and MC4R, respectively. Recently, the MCs and their receptors have been targeted for drug-based treatment of pathological processes (especially obesity), therefore a number of synthetic MC ligands have been developed.

The most effective synthetic, selective MC4R antagonist HS024 shows 20-fold selectivity and very high affinity (Ki = 0.29 nM) to the MC4R. This antagonist (cyclic [AcCys3, Nle4, Arg5, D-Nal7, Cys-NH2(11)] alpha-MSH-(3-11)) is composed of 29-membered atom ring structure, including an Arg in position 5. HS024 caused a dose-dependent increase in FI in free

feeding rats, with a maximum response (4-fold increase) at a 1 nmol dose injected ICV (Kask et al. 1998). Based on these data we decided to use this compound in our experiments.

2.1.2. Interaction between the regulation of energy homeostasis and blood pressure (BP)

Besides regulating energy balance, certain hypothalamic neuropeptides are involved in the BP regulation. This connection of these two regulatory systems may partially explain, that obesity frequently co-exists with hypertension. The most potent hypothalamic neuropeptides such as alpha-MSH and NPY are involved in the regulation of energy balance and sympathetic nervous system (SNS) activity, possibly contributing to BP elevation.

High BP does not cause conspicuous symptoms for a long time, but later it can lead to serious cardiovascular, cerebrovascular, renal complications or even to death (Kirk and Klein 2009). The World Health Organization has identified hypertension as the leading cause of cardiovascular mortality. Hypertension is defined as BP persistently higher than 140/90 mmHg in adults, even at rest. This condition affects about one third the Hungarian population (Bodo et al. 2008), thereby it means a burden of public health and health care finance. These epidemiological data support both its priority in research and the high importance of reliable animal models. The most often used animal model of hypertension research is the spontaneously hypertensive rat (SHR) strain.

2.1.2.1. Hypothalamic MC system and blood pressure control

Peptide fragments cleaved from POMC play crucial roles in multiple physiological functions including cardiovascular regulation, such as control of BP and heart rate (HR). An increasing body of evidence corroborates that melanocortins influence these through MCRs in the SNS.

For instance, ICV injection of alpha-MSH was shown to cause activation of SNS resulting in an elevation of BP (Ni et al. 2006; Matsumura et al. 2002; Hill and Dunbar 2002). In contrast, intravenously (IV) given alpha-MSH did not affect BP (Matsumura et al. 2002; Hill and Dunbar 2002). The effect of centrally administered alpha-MSH on BP depends on the manipulated brain area: the BP was decreased if the peptide was injected into the DMV or NTS (Pavia et al. 2003; Tai et al. 2007). This phenomenon was attenuated by MC4R antagonists. The main line considering alpha-MSH is that the peptide activates SNS, inducing hypertension (Ye and Li 2011; Barzel et al. 2016). Li and co-worker in 2013 showed that the activation of MC3/4Rs in the PVN increases the sympathetic outflow and thereby the BP via the cAMP-protein kinase A

pathway. Additionally, MC3/4R antagonist (SHU9119) infusion decreases HR and mean arterial pressure (MAP).

2.1.2.2. Neuropeptide Y and blood pressure control

Besides the described effects of NPY in energy balance, its role in BP regulation is also well known. NPY is a Ca^{2+}-dependent local vasoconstrictor released with norepinephrine from perivascular sympathetic nerves (Crnkovic et al. 2014; Hartl et al. 2015). NPY is involved in the regulation of norepinephrine release as well as the sympathetic control of atrial contractility and coronary blood flow (Pernow et al. 1986). In addition to the effects of peripheral NPY, the contribution of the central NPY to the BP regulation has also been shown. In a recent study, ARC stimulation decreased the MAP and sympathetic nerve activity via Y1 receptors located in the PVN of male Wistar rats. However, a conversion of these inhibitory effects to excitatory effects was also observed when the baseline MAP was lower than normal. In case of low baseline MAP, increases in MAP and HR induced by ARC stimulation were mediated via MC3/4 receptors in the PVN (Kawabe et al. 2012).

2.1.2.3. Dysregulation of the energy homeostasis and blood pressure in SHR

Spontaneously hypertensive rats (SHR) are the most often used rodent models to study hypertension (Pinto et al. 1998) and human metabolic syndrome (Miesel et al. 2010). These animals are widely used also to study of cardiovascular complications. For instance, numerous antihypertensive agents were tested in them. Agents acting on the renin-angiotensin system, calcium channel blockers and direct vasodilators such as hydralazine displayed good efficacy, while diuretics and endothelin antagonists showed lower BP reducing potential. Uncertain effects of beta-blockers were shown (Pinto et al. 1998).

The model was invented by Kozo Okamoto and Kyuzo Aoki who described the breeding of SHR from Wistar Kyoto (WKY) strain in 1963. The essence of this breeding process was to mate male rats which showed permanently high blood pressure (HBP) (150-175 mmHg) from the 7^{th} week of age with females, whose BP was above the average (130-140 mmHg). Subsequently, F1 to F6 generations with hypertension were selected for the brother-sister coupling. In later generations of this breeding protocol the BP of rats became higher and the hypertension developed earlier (F4: 185 mmHg, F5: 196 mmHg). In the 4-6^{th} week of their life these rats develop hypertension which increases with age. In some extreme cases, the systolic parameter may reach or exceed the value of 180-200 mmHg (Pinto et al. 1998).

The sympathetic tone (Judy et al. 1976) and locomotor activity of SHR is higher than those of the normotensive control rats (Henry 1990), thereby they are also used as a model of attention-deficit hyperactivity disorder (Arime et al. 2011; Hsieh and Yang 2008; Meneses et al. 2011). Porter et al. in 2011 described that reduced excitation and/or exaggerated inhibition of neurons in the rostral CEA and the dysregulation of corticotropin-releasing factor (CRF) positive cells in the caudal CEA possibly contribute to the exaggerated cardiovascular response to stress in the SHR rats.

Although this strain has long been and far-reaching used for experiments, concerning their energy balance and metabolic regulation a number of contradictory data exist, *i.e.* regarding their BW development, insulin resistance (Sato et al. 1995) and their reaction to the high-fat diet. Several groups have found lower BW in SHR than in normal rats of the same age (Oliveira et al. 2009). Importantly, the hypertension of this rat strain could be prevented by caloric restriction (Dolinsky et al. 2010). The mechanism has not yet been elucidated. Their spontaneous caloric intake and BW values are lower than those of age- and BW-matched controls (Woo et al. 1993; Sato et al. 1995; Oliveira et al. 2009). These rats cannot reach the BW of normally fed controls even on a high-calorie diet also suggesting a deficit in their regulation of feeding and BW (Oliveira et al. 2009). All these observations suggest that the central control of energy homeostasis in SHR rats is also altered, which might underlie the phenotype of this strain.

2.1.2.3.1. Neuropeptides in SHR

Various lines of evidence suggest that certain peptides participate not only in the regulation of feeding behavior but also of the cardiovascular and sympathetic systems. Hypothalamic MCs are known to have strong catabolic effect mainly via MC4Rs: they reduce FI (anorexigenic effect) and increase MR, thereby inducing loss of BW (MacNeil et al. 2002). The major MC agonist, alpha-MSH, acting at the MC4R also induces sympathetic activity and may contribute to the development of elevated BP (Dunbar and Lu 1999). In addition to alpha-MSH, agouti-related peptide (AgRP) also binds to MC4R as an endogenous antagonist (Sánchez et al. 2009). Activation of MC3 and MC4 receptors in the PVN increases the sympathetic outflow and BP via the cAMP-protein kinase A pathway (Li et al. 2013). In the SHR strain, the activity of the hypothalamic MC system seems to be enhanced: a MC3/4R antagonist (*i.e.* SHU9119) could reduce MAP to a greater extent in SHR than in controls. This suggests that high endogenous activity of the MC system contributes to the maintenance of

adrenergic tone and elevated arterial pressure in SHR even though the mRNA levels for pro-opiomelanocortin (POMC, pre-hormone of MCs) and for MC4R in the mediobasal hypothalamus were not increased as compared to controls (da Silva et al. 2008). In contrast, POMC mRNA was found to be increased in the ARC of SHR that may be related to the genesis of their spontaneous hypertension (Yin et al. 1997).

The observations of da Silva and coworkers suggested also alterations in the regulation of energy balance in SHR (da Silva et al. 2008). Their results showed different feeding responses to chronic MC4R antagonism in SHR as compared with control rats.

On the other hand, NPY (the major hypothalamic orexigenic neuropeptide known to induce FI and to suppress MR, thereby increasing BW in addition to eliciting hypotension and bradycardia when administered ICV) counteracts all the above mentioned MC-mediated effects (Morley et al. 1987; Fuxe et al. 1989; Williams et al. 2004). Several studies confirmed higher expression levels of NPY and of endogenous MC antagonist AgRP, in the SHR strain (McLean et al. 1996; Sweerts et al. 2001; da Silva et al. 2008). Despite higher NPY gene expression, similar hypothalamic NPY-like immunoreactivity concentrations and similar brain NPY receptor densities were found in SHR and normotensive controls (Pavia and Morris 1994; McLean et al. 1996).

Concerning data in the literature about the production and the effects of different neuropeptides on the regulation of FI, BW and BP are controversial. These neuropeptides might provide a pathophysiological link between hypertension and excess BW (Baltatzi et al. 2008).

In our study we aimed to analyze the dysregulation of energy homeostasis in SHR rats and to investigate the potential role of major anorexigenic (MC system) and orexigenic (NPY and AgRP) peptides in the dysregulation of feeding and BW of this rat strain.

2.2. Age-related alterations in the central peptidergic regulation of energy homeostasis: the potential crucial role of melanocortins

Changes in BC associated with aging in men from middle to old age include a progressive increase in fat mass. Especially visceral adiposity associated with elevated plasma insulin and leptin levels as well as insulin resistance should be pointed out. A decrease in lean body mass associated with a decline in muscle mass (sarcopenia) and strength; and a reduction in bone mineral density associated with an increased risk for osteoporosis and bone fractures were also found (Tenover 1999). Aging is also associated with alterations in the regulation of energy balance and BW, characterized by reduced spontaneous FI and hunger (Rolls et al. 1995),

impaired FI and BW homeostasis following caloric restriction or overfeeding (Roberts et al. 1994), and a decline in energy expenditure associated with decreased activity and exercise (Swinburn and Ravussin 1994).

Age-related changes in BC and energy regulation contribute significantly to reduced physical function, decreased quality of life, increased risk of disease (*i.e.* diabetes and atherosclerotic cardiovascular disease associated with visceral adiposity and insulin resistance) and an increased susceptibility to frailty and its consequences (*i.e.* disability and loss of independence, psychological and socioeconomic consequences, institutionalization and death). With extreme old age and the onset of age-related pathology, more severe anorexia, malnutrition and weight loss may occur and result in significant morbidity and mortality. The mechanisms underlying these important age-associated alterations involve neuropeptides in the control of energy balance, BW and BC (Balaskó et al. 2014; Kmiec et al. 2013; Pétervári et al. 2011; Székely et al. 2016). Here we discuss just the major neuropeptides of the most investigated systems with a potential role in age-related changes of BW regulation.

Peripheral hormones, such as leptin and insulin are important neuroendocrine regulators of energy intake and BW in animals. Our research group found characteristic age-dependent changes in the responsiveness to centrally applied leptin infusion in male Wistar rats (Pétervári et al. 2014). Measurements of spontaneous cumulative FI during a 7-day infusion revealed a significant anorexigenic effect in all examined age-groups (*i.e.* 3-, 6-, 12-, 18- and 24-month of age). This effect of leptin attenuated by the age of 18 months, to become more pronounced again in the oldest group. Interestingly, the decline in BW values occurred in the 3-,6- and again in 24-month-old rats, while the weight reducing effect of leptin diminished in middle-aged and aging (12- and 18-month-old) animals. In contrast, when other components of the catabolic features of leptin were tested, the heart rate (HR, indicating metabolic rate) and the Tc raised significantly only in younger age-groups (Pétervári et al. 2014), *i. e.* the hypermetabolic/hyperthermic effects of leptin gradually declined with aging. These data confirmed previous observations concerning development of leptin resistance in the course of aging (Scarpace 2002; Shek 2000). More recently, we found similar age-related patterns concerning acute catabolic action of a leptin injection in Wistar rats of various age. Leptin injection suppressed the re-feeding FI upon 48-h fasting strongly in young adult (3-month-old) rats, but not in younger (6-month-old) or older (12-month) middle-aged and in aging (18-month) rats. However, anorexigenic leptin effects reached statistical significance in old (24-month) rats again. Contrastly, anorexia and hypermetabolism changed also in this study in disparate way with aging. The leptin-induced hypermetabolism showed again a monotonous

age-related decline and disappeared by old age. The expression of leptin receptor (Ob-Rb) mRNA was found to decline until 12 months of age followed by a partial recovery in 18- and 24-month-old groups. On the other hand, the expression of signal transduction inhibitor suppressor of cytokine signaling 3 (SOCS3), which is cytokine-inducible negative regulator of cytokine signaling was elevated in 6- and 18-month-old and to some extent in old rats (24-month) rats (Rostás et al. 2016). Age-related alterations of Ob-Rb and SOCS3 expression in the ARC may partly contribute to the explanation of age-related variations in anorexigenic but not hypermetabolic leptin effects. According to these experimental results, the age-related pattern shown by leptin-induced anorexia may contribute to the explanation of middle-aged obesity, and partly to that of aging anorexia (Petervari et al. 2014; Rostás et al. 2016).

Cholecystokinin (CCK), another important anorexigenic peripheral peptide was studied by different research groups, but controversial data have been reported concerning the contribution of CCK to the maintenance of energy balance. Akimoto and Miyasaka in 2010 found, that CCK and CCK-B receptor mRNA in the hypothalamus did not differ when young (5.5-10-months) and old (25-29-months) rats were compared. Unlike the hypothalamic CCK-A receptor mRNA expression, which was significantly decreased in old rats compared to the young group. In contrast, the inhibitory effect of CCK on FI was significantly greater in old rats (Akimoto and Miyasaka 2010). Previous observations suggest a possible contribution of CCK to the development of age-related alterations in energy balance despite some controversial findings concerning the changes in the CCK system/levels in old populations. Although the plasma concentration of CCK was not analyzed in many age-groups, the fasting peptide level was found to be higher or at least maintained in aged individuals compared to that in young ones (Chapman et al. 2002; Di Francesco et al. 2005; Serra-Prat et al. 2009; Winkels et al. 2011). Postprandial CCK-release was also found to be similarly diminished in cachectic and normal weight elderly volunteers compared to that of young people (Serra-Prat et al. 2009). In animal studies the CCK release in brain samples was smaller in old than in young rats, although the CCK content rather increased (Ohta et al. 1995).

In addition to the amount, the efficacy of the peptide may also be different in various age-groups. During fasting, a similar level of CCK was associated with diminished hunger in elderly human volunteers (Serra-Prat et al. 2009). The satiety-inducing effect of exogenous CCK was also more pronounced in old than in young persons or animals (MacIntosh et al. 2001; Silver et al. 1988). Our results confirmed earlier data according to which the anorexigenic effect of CCK increases in the old age-group, supporting the view that CCK possibly contributes to the negative energy balance characterizing old age. However, the data also provide evidence that –

as compared with young adults – the CCK-effect is minimal in the later middle-aged group, suggesting that the lack of satiety effect may contribute to the positive energy balance and weight gain in this especially obesity-prone age group (Balaskó et al. 2013).

Concerning the central hypothalamic systems, activity of the neuropeptides involved in the downstream of leptin actions also show characteristic age-related patterns. Leptin inhibits the orexigenic NPY, the major anabolic regulator of the ARC, which has been reported to decline with aging (Kmiec et al. 2013). In animal models of aged rodents, and also in brain samples from individuals with neurodegenerative disease, levels of NPY and NPY receptors are decreased in several brain areas, including hypothalamic nuclei (Botelho and Cavadas 2015; Baranowska et al. 2006), but opposing data were also found by others in human studies (Martinez et al. 1993; Escobar et al. 2004). Matsumoto and his coworkers found that aging male Brown Norway (BN) rats have increased peripheral and visceral adiposity associated with increased insulin and leptin levels, and decreased relative lean body mass and muscle mass. These rats exhibited reduced FI and BW gain associated with decreased hypothalamic NPY gene expression in the ARC, both during *ad libitum* feeding and after a 72-h fast (Matsumoto et al. 2000; Gruenewald et al. 1996). At protein level, Kowalski et al. found a gradual age-related decrease in the NPY content in the whole hypothalamus of young (4-month-old), mature (18-month-old) and senescent (26-month-old) male Wistar rats (Kowalski et al. 1992). In agreement with these results, Fuxe et al. have shown that a marked loss of NPY immunoreactivity occurs in the nerve terminals of the PVN as well as a drop in the NPY concentrations in many hypothalamic nuclei in the 24-month-old rat (Fuxe et al. 1990).

Blanton et al. compared the responsiveness of 8-months and 24-30-months aged male Fischer 344 rats to ICV NPY and found, that the feeding response is diminished in senescent rats that are undergoing terminal weight loss (Blanton et al. 2001).

Wolden-Hanson and his coworkers found age-related changes in FI response to NPY in four age-groups when young (3-4 months), middle-aged (13 months), old (24 months) and very old (33 months) male BN rats received one ICV injection of NPY (Wolden-Hanson et al. 2004). According to their data, NPY stimulated feeding at 4 h after third ventricular injections in all age-groups, however, by 24 h the effect of NPY was abolished in all groups except for the young animals suggesting a blunted effect of NPY in aging animals. In contrast, earlier experiments on young rats of our laboratory have been shown, that NPY injected in the lateral ventricle induces acute prompt increase in daytime spontaneous FI followed by a rebound decrease in cumulative 24-h FI (Székely et al. 2005). In an other study, the stimulatory effect of NPY on FI was compared among young (4 months), adult (11 months) and old (24-27

months) male Wistar rats and an age-related decline was found, with no effects in old rats (Akimoto-Takano et al. 2005). The NPY neurons in the ARC and orexin-A producing neurons in the LH have reciprocal functional connections important in feeding. In the same study of Akimoto-Takano et al., the stimulatory effect of orexin-A on FI also declined in association with age (Akimoto-Takano et al. 2005). 1 nmol orexin-A significantly increased FI in young (4-months-old) rats, while 3 nmol was required for the significant effect in adult middle-aged (11-months-old) rats. No significant increase was observed in old (24-27-months-old) rats, even when higher doses (1 and 3 nmol) were applied. This group reported earlier, that the decrease in the specific orexin-A receptor (OX1R) protein level in the hypothalamus could be responsible for the lack of the stimulatory effect of orexin-A on FI in old rats (Takano et al. 2004). In contrast, NPY was shown to maintain its FI stimulatory efficacy in old mice, compared to adults (Morley et al. 1987).

As it has been introduced earlier, besides NPY, the other main target of the leptin in the ARC, the melanocortin system plays significant role in the control of energy homeostasis. The final control signal on energy homeostasis may depend strongly on the balance of melanocortins possessing physiologically opposing agonistic (*i.e.* alpha-MSH) and antagonistic (*i.e.* AgRP) effects. We hypothesized that age-related shifts in this balance play an important role in long-term trends of BW during the course of aging. In our previous *in vivo* studies the anorexigenic effects of an ICV injected alpha-MSH or a 7-day alpha-MSH infusion in male Wistar rats were shown to be age-dependent: the effects of the peptide were strong in young and again in old rats but they were weak in the middle-aged groups (Pétervári et al. 2010; 2011). Our research group found that such a 7 day-long ICV infusion of alpha-MSH was able to reduce the BW in 2- and 3-4-month-old (young) groups, had hardly any effect on BW in the 12-month-old (middle-aged) animals, but it was most effective in the 24-month-old rats (Pétervári et al. 2011). In contrast, the hypermetabolic effect was still high in the oldest group, but low in the younger groups. These findings were in accord with the robust MC infusion-induced response of old male F344×Brown Norway rats reported by Zhang and co-workers (Zhang et al. 2004). However, other previous *in vitro* studies failed to reveal an unequivocal age-related pattern in the endogenous activity of the hypothalamic MC system as indicated by gene expression of POMC: either decreased (Gruenewald and Matsumoto 1991; Kappeler et al. 2003; Nelson et al. 1988; Arens et al. 2003; Lloyd et al. 1991; Rigamonti et al. 2006) or unchanged MC activity was described in old rodents (McShane et al. 1999; Wolden-Hanson et al. 2004; Zhang et al. 2004). A study on the transcription levels of energy balance-related hypothalamic neuropeptides described that besides unchanged POMC mRNA massage, the arcuate AgRP

gene expression decreased while CART increased in the course of aging in BN rats. Interestingly, the centrally administered AgRP injection showed the most potent orexigenic effect in very old, 33-month-old animals, *i.e.* the aging melanocortin system is able to respond appropriately to exogenous AgRP, whereas at the same time showing blunted responses to NPY. Fasting-induced changes in gene expression of all neuropeptides studied (rise in AgRP or decrease in POMC and CART) were attenuated with aging (Wolden-Hanson et al. 2004). These data suggest that age-associated decrements in levels of orexigenic signaling through AgRP/NPY neurons in the ARC are accompanied by increased levels of anorexigenic signaling through POMC/CART neurons (incomplete suppression of anorexigenic drive to fasting). This pattern of neuropeptide gene expression may contribute to a loss of appetite and the anorexia of aging.

Hypothalamic CRF lays downstream to catabolic melanocortins and at least partly mediates their catabolic effects. We found that the age-related pattern of alterations in anorexia induced by a CRF-infusion and consequent weight loss (Tenk et al. 2017) appears to be similar to that previously described in case of central catabolic effects of a melanocortin infusion (Pétervári et al. 2011), *i.e.*, significant responsiveness in the young adult, followed by a suppression of catabolic effects in the middle-aged and a recovery of the anorexigenic efficacy in the old age groups. Retroperitoneal fat mass was found to be reduced by CRF-infusion only in the latter group. We showed that the CRF gene expression increases with age in the PVN until 18 months (*i.e*. aging rats) also suggesting the potential contribution of endogenous CRF effects to aging anorexia. Hypermetabolic effects of the CRF infusion were weak and did not show remarkable age-related variations (Tenk et al. 2017). Thus, unlike hyperthermia/hypermetabolism induced by ICV infusions of alpha-MSH, where increases of corresponding parameters were strong in young adult and middle-aged rats and declined thereafter (Pétervári et al. 2011), hyperthermic effects of CRF appeared only in the young adult animals and failed to develop in the older groups (Tenk et al. 2017). When the effects of acute CRF injection were tested, we found that the CRF-induced anorexia declined with aging whereas hypermetabolic/hyperthermic actions were maintained in all age-groups (Tenk et al. 2016). Acute hypermetabolic/hyperthermic effects of a central alpha-MSH injection in different age-groups of rats have not been investigated yet.

Accordingly, earlier studies concerning age-related changes in the activity/function of the hypothalamic MC system show contradictory results. To date, no detailed systematic analysis was carried out across more than three age-groups. Therefore, we aimed to systematically

investigate the age-related dynamics of the MC system including those of alpha-MSH, AgRP and MC4R across different age groups of rats from young to old age.

3. AIMS AND HYPOTHESIS

Our aim was to investigate the key role of the hypothalamic melanocortin system in the regulation of energy homeostasis.

Hypothesis I.

Activity of the MC system shows characteristic age-related pattern. Decreased activity of the hypothalamic melanocortin system contributes to the development of middle-aged obesity, but later the melanocortin activity increases leading to anorexia and weight loss in old age.

We aimed to test this hypothesis in our male Wistar rat strain in 3 settings of experiments.

1) In order to **demonstrate middle-aged obesity** and **aging sarcopenia** in our rat model, we measured **BW** and assessed **BC** of Wistar rats of **different age-groups**. Most of the methods currently used among animals are not suitable for long-term *in vivo* monitoring of BC. We aimed to provide evidence on changes of BC during aging by applying three different methods for the assessment of BC. In addition to *post mortem* body composition analysis (PMA), we aimed to assess BC also *in vivo.* We evaluated abdominal micro-computed tomography (CT) scan restricted to the L1-L3 region (micro-$CT_{(L1-L3)}$, a scan of previously untested abdominal region in rats) and a skinfold thickness-based method (STM) with regard to whole-body micro-CT scan in rats. The whole-body micro-CT is a widely used reliable, high-resolution imaging method for *in vivo* body fat assessment in small laboratory animals (Hildebrandt et al. 2002; Judex et al. 2010). STM is a general technique in humans, however, in small rodents it is not a widely used and validated method (Wells and Fewtrell 2006; Lean et al. 1996; Colman et al. 1999; Latshaw and Bishop 2001; Caroprese et al. 2006; Dhungel et al. 2009; Brock et al. 2013). We also put forward to compare and validate these three approaches for future *in vivo* studies where the aging-related dynamics of BC should be quantified.

With regard to the above described techniques, we aimed to test the following assumptions:

- Abdominal micro-$CT_{(L1-L3)}$ with short scanning time is an equally useful tool as whole-body micro-CT.
- The simple and non-invasive total skinfold thickness-based method (STM) is also suitable to detect differences and follow changes in fat mass.
- Visceral fat measured by micro-$CT_{(L1-L3)}$ and subcutaneous fat assessed by STM would show similar age-related differences.

- *Post mortem* measurement of retroperitoneal fat reflect age-related differences in body fat better than measurement of epididymal fat.

2) ***In vivo*** **investigation of hypothalamic responsiveness to exogenous melanocortin in Wistar rats:**

We hypothesized that the acute short-term metabolic/thermoregulatory effects of alpha-MSH may also show age-related alterations similar to those of the anorexigenic melanocortin effects (Pétervári et al. 2010; 2011). Therefore, we analyzed the acute hypermetabolic/hyperthermic effects of a central alpha-MSH injection in different age-groups of rats. In addition, we aimed to analyze complex acute catabolic (hypermetabolic and anorexigenic) effects of this exogenous MC agonist in five age-groups of male Wistar rats from young adult to old age with special regard to the BW development curve.

3) ***In vitro*** **analysis of the endogenous hypothalamic melanocortin system in Wistar rats:**

We investigated the age-related dynamics of the endogenous MC system including those of alpha-MSH, AgRP and MC4R in the ARC and PVN using quantitative reverse transcriptase polymerase chain reaction (qRT-PCR) and a semiquantitative immunohistochemical approach. Then, dynamics of these age-related changes were systematically compared with those of the *in vivo* results.

Hypothesis II.

Spontaneously hypertensive rats **do not show characteristic middle-aged obesity** seen in Wistar rats: their BW is lower than that of normotensive (NT) controls, even on a high-fat diet, suggesting a dysregulation of energy homeostasis (Oliveira et al. 2009). High activity of the hypothalamic MC system contributes to the maintenance of adrenergic tone and elevated arterial pressure of SHR.

We assumed, that enhanced activity of hypothalamic anorexigenic melanocortins and diminished tone of orexigenic NPY may contribute to their BW dysregulation.

We aimed to test this hypothesis in 2 settings of experiments.

1) ***In vivo*** **investigation of hypothalamic responsiveness to exogenous peptides in SHR:**

To test our hypothesis, we treated male 3-months-old, ICV cannulated SHRs with exogenous alpha-MSH, AgRP or NPY injections in an acute model and with HS024 infusion

in a chronically (7-day long) treated setup. We aimed to analyze the effects of the peptides on the FI and BW.

2) ***In vitro*** **analysis of the endogenous hypothalamic systems in SHR:**

To semi-quantify the (endogenous) activity of the above described peptidergic system, immunohistochemistry was applied.

4. MATERIALS AND METHODS

4.1. Animals

Five age groups [*i.e.* young adult (3-month-old), adult (6-month-old), middle-aged (12-month-old), aging (18-month-old) and old (24-month-old)] of male Wistar were used to test *Hypothesis I.* In certain thermoregulatory experiments, a juvenile (2-month-old) group was also applied.

For investigating *Hypothesis II*, besides the 3-month-old Wistar rats as controls, age-matched SHR rats were subjected. Rats of both strains used in these experiments were bred at the Animal Facilities of the Department of Anatomy and the Institute for Translational Medicine at Pécs University, Hungary.

Hypothesis I:

Cohorts of non-treated male Wistar rats were used for body composition (micro-CT, PMA, STM) measurements (n= 14-17/age group).

Two further cohorts of rats were subjected to ICV cannula implantation surgery (see below) for

a) food intake assessment (n = 6-14/age-group)

b) metabolic/thermoregulatory measurements (n = 6-16/age-group).

Other two cohorts of intact rats were used for

c) immunohistochemistry (n = 5-8/age-group)

d) qRT-PCR (n = 5-9/age-group).

Due to the well-known greater variability of biological measures and the higher mortality in old age, a greater number of rats was subjected in these groups.

Hypothesis II:

For *in vivo* experiments the following cohorts were used (6-8 rats/group):

Cohorts of rats [including SHR and normotensive Wistar rats (NT)] were subjected to implantation of an ICV cannula connected to Alzet osmotic minipump in order to measure the effect of HS024 (infusion) on the cumulative FI and BW.

Three further cohorts of NT and SHR were subjected to ICV cannula implantation surgery in order

a) to measure the orexigenic effect of AgRP (injection) on the daytime FI

b) to measure the orexigenic effect of NPY (injection) on the daytime FI

c) to measure the anorexigenic effect of alpha-MSH (injection) on 12-h cumulative spontaneous nighttime FI.

For *in vitro* experiments the following cohorts were used:
Cohorts of non-treated male NT and SHR rats were used for

a) qRT-PCR (NT: n=6; SHR: n=5) to measure the relative expression of POMC mRNA in the ARC.
b) immunohistochemistry (NT: n=6; SHR: n=6) to measure the number of alpha-MSH producing cells as well as the peptide level of alpha-MSH and NPY in ARC. Alpha-MSH signal density was also evaluated in PVN.

Animals were housed in standard polycarbonate cages with woodchip bedding at an ambient temperature (23-26°C) and humidity controlled environment. Lights were on between 06:00 and 18:00 h. Rats had free access to tap water and for the standard laboratory rat chow (CRLT/N rodent chow, Szindbád Kft., Gödöllő, Hungary, 11 kJ/g). Animals were weighed manually on a daily basis. Intact rats were housed three per cage, whereas following cannula implantation, animals were housed singly. All experiments and interventions were approved by the National Ethical Council for Animal Research (Permit numbers: BA 02/200-11/2011, BA 02/2000-25/2011 valid for 5 years). They were also in accord with the directives of the European Communities Council on the protection of animals used for scientific purposes (86/609/EEC, Directive 2010/63/EU of the European Parliament and of the Council).

4.2. Body composition measurements

4.2.1. Body composition assessment by micro-CT

Micro-CT scan was performed under intraperitoneal (IP) ketamine-xylazine [78 mg/kg (Calypsol, Richter) + 13 mg/kg (Sedaxylan, Eurovet)] anesthesia that provided 1.5-2 hours of deep sleep. Rats were immediately placed into the micro-CT scanner (Skyscan 1176 high resolution *in vivo* micro-CT, Kontich, Belgium) and scanned using the following settings: 80 kV tube voltage, 300 μA tube current, 75 msec exposure time, 0.7 degree rotational step, 2 frames averaged in each step. The center of the scanned field of view was aligned at the level of the L2 and default width of field of view was used with offset scan settings. Overall scan time was 14-15 minutes during analyses of abdominal region between L1-L3 and 60-75 minutes when whole body micro-CT (from the base of the skull to the distal end of the tibia; Luu et al. 2009) scan was applied. Datasets were reconstructed with the following settings: post-alignment compensation: 0; beam hardening: 30; ring artefact compensation: 5; smoothing: 5; and analyzed using CT AN software (Skyscan, Kontich, Belgium). The three components (fat and bone percentage, other soft tissue) of the body composition were measured and calculated

among rats with this method. For the statistical analysis only fat percentage values were used. Based on the L1-L3 abdominal scan, visceral and subcutaneous fat percentages were also determined. The region of interest was determined within the body by the abdominal and back muscle(s) (m./mm.) (*mm. obliquus abdominis, m. rectus abdominis, m. erector spinae*). Then with the help of the analyzing software, the right voxels typical of fat tissues were selected. These selected volumes were aggregated to determine the total fat percentage of the slices. The results had been divided based on the previously captured region of interest to visceral or subcutaneous fat depending on whether the selected fat volumes were in the region of interest, or not. Analyses were done in collaboration with the Department of Pharmacology and Pharmacotherapy, Janos Szentagothai Research Centre & Neuroscience Centre, University of Pecs.

4.2.2. Measurement of skinfold thickness (ST), repeatability and reproducibility

For skinfold thickness measurements (STM), a short ether anesthesia was sufficient. These values were measured in five locations with Lange caliper: four landmarks were determined according to Marshall (1969) (right scapular, right abdominal, right triceps brachii, right leg) and an additional site was chosen at the right iliac crest. All ST values were added to calculate the total ST. In order to analyze STM repeatability and reproducibility two assessments (in mornings and afternoons) were applied on the same animals (n=10) by two experienced professionals (observers 1 and 2). Measurements were performed in collaboration with the Institute of Sport Science and Physical Education, University of Pecs.

4.2.3. *Post mortem* analysis

After an overdose of urethane (3 g/kg, IP, Reanal), indicators of body fat (epididymal, retroperitoneal fat pads) and indicator of muscle mass (wet weight of 1. *m. tibialis anterior*, 2. *m. soleus*, 3. *m. extensor hallucis longus*, 4. *m. extensor digitorum longus*) from the left side of the animals were removed and weighed with centesimal accuracy in gramm (g). These indicators were calculated for 100 g BW.

4.3. Measurement of blood pressure

For the *Hypothesis II*, before the experiments we had to confirm the hypertension of SHR and the normal blood pressure (BP) of controls. For this, their systolic blood pressure was

measured non-invasively using a tail cuff device (LE 5100; PanLab, Harvard Apparatus, Petriz et al. 2015).

Animals were anesthetized by IP ketamine + xylazine (see at 4.4) and placed into a black box in complete rest. Twenty minutes after, systolic BP was measured. Ten value of every rats were averaged. From these values we got the average systolic BP in every group of rats.

4.4. Surgeries and drug administration

Upon reaching the appropriate age and BW, rats were operated for the purpose of implanting a leading guide cannula into the right lateral cerebral ventricle for ICV injections or an ICV cannula (Alzet Brain Infusion Kit) for ICV infusion. Animals were anesthetized by IP ketamine + xylazine administration [78 mg/kg Calypsol (Richter) + 13 mg/kg Sedaxylan (Eurovet), respectively], and they also received Gentamycin injection (2 mg IP) for prophylaxis. After fixing the head of rats in a stereotaxic apparatus, desinfection was done before the skin of the skull was incised. The bone was cleaned and two holes were drilled for two miniature screws. A further hole was made for the stereotaxic implantation of a 22-gauge stainless-steel leading cannula with its tip at A: -1.0 mm (posterior to Bregma), L: 1.5 mm (to midline), V: 3.5 mm (ventral to dura mater). Coordinates were determined according to the rat brain atlas of Paxinos and Watson (2005). Dental cement was applied to fix the screw-cannula complex to the bone. A stylet closed the lumen of this cannula, which was replaced by an injection cannula (extending 0.5 mm below the guide cannula) with a polyethylene tube attachment when injection of substances were given.

During acute tests a single 5 μL ICV injection of alpha-MSH [Bachem AG Switzerland, 5 μg dissolved in pyrogen-free saline (PFS)], NPY (Bachem AG Switzerland, 5 μg) and AgRP (Phoenix Europe GmBH, 5 μg) or pyrogen-free saline (PFS) as control was given in random order as described earlier Pétervári et al. 2010. These doses were chosen according to earlier observations (Balaskó et. al. 2010; Pétervári et al. 2010; Székely et al. 2005; Kim et al. 2002). Five-to-seven days later the substances (*i.e*. the tested peptide and PFS) were switched and the measurements were repeated.

For chronic administration of high-dose HS024, a selective antagonist of the MC4R [Bachem, 1 μg/μl (Kask et al. 1998; Jonsson et al. 2002)] the ICV cannula (Alzet Brain Infusion Kit) was implanted and at the same time, its outer end was connected to an Alzet osmotic minipump, that was placed under the skin. The minipump composed of an impermeable layer (inside) and a semipermeable layer (outside) was filled with a solution of the selective

melanocortin antagonist HS024 and PFS used as control. The fluid from the interstitial space passed through the semipermeable layer, then the pressure in the impermeable space became increased. This increased pressure secured a standard slow continuous ICV infusion (1 μg/μl/h HS024 or 1 μl/h PFS) for a period of 7 days. Due to the dead space of the system, the infusion reached the brain of the already awake animal about 8-10 h after the implantations.

At the end of the experiments, the appropriate location of the guide cannula was double-checked. On the one hand, by ICV injection of angiotensin II (Sigma, A9525, 20 ng/5 μl). The subsequent water consumption was measured. The location of the cannula was assumed to be appropriate if at least 5 ml water was consumed within 30 min.

On the other hand, at the termination point of rats following the experiments, animals were euthanized by an overdose of urethane (3g/kg, IP, Reanal). The localization of the cannula in the lateral ventricle was verified by macroscopic observation of the coronal sections of the removed and fixed brains (see in 4.7.1.). Rats with inappropriately located cannula were excluded from the analysis.

4.5. Measurement of food consumption of rats

The orexigenic effects of HS024 (infusion), AgRP (injection) or NPY (injection) and also the anorexigenic effects of alpha-MSH (injection) were measured by an automated FeedScale System (Columbus, OH) in freely moving animals. Two weeks before the tests, rats were transferred individually to chambers of the system. Thus, they were habituated to the environment and to the powdered rat chow, which was provided for rats to prevent hoarding behavior. The system measured the consumed food in grams (weight of the holder filled with powdered chow) every 10 minutes following the injections and every 30 minutes during the 7-day infusion, and a computer recorded the data for the statistical analysis.

In case of cohort of rats for testing *Hypothesis I,* one day before the ICV injection, at 09.00 h food was removed for 24-h. Five minutes before the re-feeding started (at 09.00 h) assigned rat of different age-groups received 5 μg ICV alpha-MSH or PFS to test the inhibitory effect of the peptide on 2-h cumulative FI.

In case of cohort of rats for testing *Hypothesis II*, the following settings of experiments were performed in SHR and NT rats. Spontaneous 12-h FI elicited by the ICV alpha-MSH injection (given at 18.00 h, without previous fasting) was measured during the active night-time period. Upon administration of ICV NPY or AgRP injection (at 09.00 h), cumulative 3-h FI

during the light period or 24-h FI for 4 days were measured, respectively. Effect of ICV HS024 infusion on daily FI was registered during the 7-day course.

4.6. Metabolic and thermoregulatory assessment

Oxygen consumption (ml O_2/kg/min, VO_2 representing metabolic rate) was determined by indirect calorimetry (Oxymax, Equal Flow, Columbus, OH). Simultaneously, core temperature (Tc) and tail skin temperature (Ts, indicating heat loss) were also measured by thermocouples attached to Digi-Sense Benchtop Thermometer (Cole-Parmer). Measurements were performed on semi-restrained rats singly placed in cylindrical wire-mesh confiners in separate metabolic chambers. Animals were previously accustomed to the confiners based on a following protocol: 12-times on separate days (involving 2-times 30-min, a 1-h, a 2-h, and 8-times 4-h sessions) (Füredi et al. 2017) to minimize the restraint stress during *in vivo* measurements.

The experiments were performed between 09.00 h and 15.00 h. During this period, animals did not have access to food and drinking water. The parameters were measured when rats were in semi-restraining cages. This was necessary to avoid that they may reach the thermocouples. The tightly sealed plexiglass metabolic chambers were continuously ventilated with room air. The chambers were immersed into a thermostatically controlled water-bath at a slightly subthermoneutral (25°C) ambient temperature. At this temperature there is a constant skin vasoconstriction without fluctuations in Ts, but vasodilation (an important thermoregulatory reaction to alpha-MSH) can be evoked. This ambient temperature also allows the observation of hyperthermic responses. Four metabolic chambers were used simultaneously. The VO_2 was registered in 10-min intervals for 3 hours following the ICV alpha-MSH and PFS injection.

Rats were equipped with copper-constantan thermocouples for measuring Tc and Ts. The colonic thermocouple was inserted 10 cm beyond the anal sphincter and fixed by tape to the tail, the skin thermocouple was fixed on the dorsal skin of the distal part of the tail. One thermocouple in each chamber recorded the ambient temperature (Ta). Thermocouples and the extensions of the ICV cannula were pulled through a tightly sealed port of the chamber. It allowed us to inject the animals from a distance without causing any acute stress or discomfort.

Temperature data were collected by a Digi-Sense Benchtop Thermometer for electronic processing and evaluation. The rate of heat loss (heat loss index, HLI) was calculated from the measured temperatures: HLI = (Ts-Ta) / (Tc-Ta) (Romanovsky and Blatteis 1996). HLI near 0

(Ts values approaching Ta) indicates vasoconstriction as a heat conserving mechanism, HLI near 1 (Ts values near Tc) suggests vasodilation indicating heat loss activity. From the air flowing through the chamber oxygen consumption (ml O_2/kg/min) and carbon-dioxide production (ml CO_2/kg/min) were determined by indirect calorimetry (Oxymax). This calorimeter measures gas concentrations and flow. Flow is determined by a mass thermal transfer technique that yields data formatted in terms normalized to scientific STPD (*i.e.* standard temperature and pressure, dry: 0˚ Centigrade and 760 mmHg, removal of water vapor by materials with hygroscopic properties that isolate the sample gas from the drying media). Oxygen consumption and CO_2 production values were determined according to the following equations: $VO_2 = (V_iO_{2i}-V_oO_{2o})$/body weight in kg (where Vi = mass of air at chamber input per min; Vo = mass of air at chamber output per min; O_2i = oxygen fraction in Vi; O_2o = oxygen fraction in Vo; $VCO_2 = (V_iCO_{2i}-V_oCO_{2o})$/body weight in kg (where Vi = mass of air at chamber input per min; Vo = mass of air at chamber output per min; CO_2i = carbon dioxide fraction in Vi; CO_2o = carbon dioxide fraction in Vo). The respiratory exchange ratio (VCO_2/VO_2) was also calculated.

4.7. Immunohistochemistry (IHC)

4.7.1. Tissue sampling for immunohistochemistry

To perform immunohistochemistry, rats were deeply anesthetized by an IP overdose of urethane (3–5 g/kg, Reanal). After their breathing slowed down, their chest cavity was opened, and they were transcardially perfused with ice-cold 50 ml of 0.1M phosphate buffered saline (PBS, pH 7.5) followed by 300 ml chilled 4% paraformaldehyde in 0.1M Millonig buffer for 20 min. Consecutively, brains were carefully removed and post fixed in the same fixative for 7 days at 4°C. Coronal sections (30 µm) were cut using a Leica VT1000 S vibratome (Leica, Wetzlar, Germany). For this study, two series of sections were collected from a hypothalamic tissue block between -1.5mm and -2.5mms to the Bregma, each interspaced by 60 µm containing the PVN and ARC. Sections were stored at -20°C in anti-freeze solution until further use (Gaszner 2009).

4.7.2. Double labeling immunofluorescence for alpha-MSH and MC4R

The first series of sections were washed in PBS for 4x15 min, in order to remove anti-freeze solution and fixative. Then, a treatment with 0.5% Triton X-100 (diluted in PBS) for 30 minutes was applied to permeabilize the cell membranes and to enhance antibody penetration.

Subsequently, sections were treated with 2% normal donkey serum (NDS, Jackson Immunoresearch Europe, Suffolk UK) diluted in PBS for 30 minutes, to reduce the background signal. Next, sections were incubated for 2 days in the cocktail of rabbit anti-alpha-MSH antibody diluted to 1:5000 in PBS (Peninsula Laboratories, CA, USA) and in goat anti-MC4R antibody, diluted to 1:100 in PBS (Santa Cruz Biotechnology, Santa Cruz, CA USA) at 4°C. On the third day, samples were rinsed with PBS for 2x15 minutes. Then, samples were incubated for 24 h at 4°C in the mixture of the following secondary antibodies: Cy2 conjugated anti-rabbit (1:250 in PBS) (Jackson), SP-biotin conjugated donkey anti-goat (1:2000 in PBS) (Jackson). After 2x15-min PBS washes samples were incubated for 3 hours at room temperature (RT) with Cy3 conjugated streptavidin (1:1000 in PBS) (Jackson). After PBS washes, sections were mounted to gelatin-coated slides, they were air-dried and covered with glycerol/PBS (1:1) solution.

4.7.3. Single immunofluorescence for AgRP

The second series of sections, as defined above, was used to investigate the AgRP immunoreactivity. Sections, containing PVN and ARC were selected and washed in PBS for 4x15 minutes, then samples were subjected to heat-induced epitope retrieval at 90°C in Na-citrate buffer (pH 6.0) for 10 minutes. After cooling for 20 minutes in the same solution, samples were transferred into 0.5% Triton X-100 for 30 min. Subsequently, sections were treated with 2% NDS diluted in PBS (Jackson) for 30 minutes. The primary antibody (rabbit anti-AgRP; Phoenix Pharmaceuticals, 1:6000) diluted in PBS with 2% NDS was applied for 2 days at 4°C. After washes in PBS, sections were incubated for 24 h at 4°C in SP-biotin conjugated donkey anti-goat serum (Jackson, 1:1500). Subsequently, sections were washed with PBS for 2x15 min and incubated for 3 hours at RT in Cy3 conjugated streptavidin (1:1000 in PBS) (Jackson). Finally, samples were washed in PBS and mounted as described above.

4.7.4. Immunofluorescence for NPY

Further hypothalamic sections containing the ARC and the PVN were selected for NPY labeling. After 4x15 minutes washes in PBS sections were permeabilized in 0.5% Triton X-100 in PBS for 30 minutes. Sections were treated with 2% NDS (Jackson) diluted in PBS for 30 minutes. Then, they were incubated with sheep anti-NPY serum (dilution fold is 1:96.000, FJL #14/3A, generous gift of Prof. István Merchenthaler) for 1 day at RT. Next, samples were

washed with PBS for 2x15 minutes, and incubated for 1 day in SP-biotin conjugated donkey anti-sheep (Jackson, 1:1000) antibody. On the 3rd day, after washes in PBS for 2x15 minutes, samples were incubated in Cy3 conjugated streptavidin for 3 h (Jackson, 1:1500). Subsequently, upon washes mounting was performed as stated above. The light sensitive samples were incubated in a dark box to prevent bleaching of fluorophores in all cases.

4.7.5. Antiserum characterization and immunofluorescence controls

The rabbit alpha-MSH antiserum was generated against whole alpha-MSH. The AgRP antibody (Pheonix Pharmaceuticals.Inc., USA) was produced in rabbit against the agouti-related protein (83-131) amide. MC4R was raised against the C-terminus of MC4R of rat origin. Preadsorption experiments revealed that incubation of final working dilutions of primary antisera with 0.1, 1.0 and 10.0 μg of the respective peptides [*i.e.* alpha-MSH (Bachem AG Switzerland), NPY (Bachem AG Switzerland), AgRP (Phoenix Pharmaceuticals) and MC4R fragment (SC-6880-P, Santa Cruz Biotechnology, Santa Cruz, CA USA)] abolished staining in all specificity controls. The high sensitivity and specificity of our NPY antiserum was also tested earlier on rat brain tissue by Fuzesi et al. (2007). Primary serum omission or replacement by nonimmune goat or rabbit sera at the dilution of the respective primary antiserum completely prevented immunoreaction.

4.7.6. Microscopy and morphometry

Sections were digitalized using a confocal laser scanning microscope (Olympus Fluoview FV1000 (Olympus MicroImaging, Japan). To perform the semi-quantitation of fluorescent signal the photon count mode was preferred with the following settings: confocal aperture: 105 μm, optical sectioning by 5 μm step size, 20x lens with a numeric aperture of 0.75, in a resolution of 1024x1024 pixels with 10 μs excitation time per pixel. Fluorophores (*i.e*. Cy2 and Cy3) were excited by 100% intensity 542 nm and 550 nm laser beams, respectively. Images of both channels were saved and automatically superimposed. Manual cell counting and densitometry was carried out on non-edited images.

The intensity of the immunofluorescence was determined in 10 perikarya per section for alpha-MSH in the ARC, and for MC4R both in the PVN and ARC. The immunosignals on ten nerve fibers per section was measured for alpha-MSH in the PVN. The AgRP fiber density was evaluated both in the PVN and ARC. In case of NPY fiber density ARC was measured. To determine the immunosignal, the Image J software (version 1.37, NIH, Bethesda, MD) was

used. Data were corrected for the background density outside the ARC/PVN, yielding the specific signal density (SSD) per neuron or nerve fiber, which was expressed in arbitrary units (a.u.).

4.8. Quantitative Real-Time Polymerase Chain Reaction (qRT-PCR)
4.8.1. Sampling for qRT-PCR

Rats were removed from their home cages and decapitated within 2 minutes. Brains were instantaneously dissected and quickly frozen in liquid nitrogen and finally stored at -70°C until further use. PVN and ARC samples were punched from 1 mm thick slices (-2 to -3 mms from the Bregma, Paxinos and Watson, 2005) of the brains cut on a brain matrix (Ted Pella, CA, USA) by two razor blades. Sections were placed on an ice-chilled mat. From the mediobasal hypothalamic area a) the PVN and b) ARC were microdissected by a 1mm diameter Harris punching needle (Sigma-Aldrich Budapest, Hungary).

The total amount of RNA was isolated with the Pure Link^{TM} RNA Mini Kit (Life Sciences, Carlsbad CA, USA) according to protocol suggested by the manufacturer. High capacity cDNA kit was applied (Applied Biosystems, Foster City, CA, USA) to perform cDNA synthesis, using 1 μg of total RNA sample according to the official protocol.

SensiFast SYBR Green reagent (BioLine) was used to perform qRT-PCR, for gene expression analysis. Amplifications were run on ABI StepOnePlus system. StepOne software was used to analyze gene expressions, which was normalized to glyceraldehyde 3-phosphate dehydrogenase (GAPDH) housekeeping gene in any qRT-PCR measurements based on our first choice regarding the reference curves (**Table 2**).

β-Actin		**S18**		**GAPDH**	
NT	SHR	NT	SHR	NT	SHR
26.16	18.87	17.17	19.25	21.81	19.99
16.30	18.16	17.96	18.84	18.69	20.01
17.13	17.34	17.85	17.69	19.27	18.81
16.73	16.52	20.22	17.58	19.43	18.72
20.01	19.78	19.10	19.94	20.84	21.16
18.12		18.38		20.41	

Table 2: Ct values of examined housekeeping genes in qRT-PCR analysis. Two-way ANOVA did not find the main effect of strain on the housekeeping gene expression significant. The three examined housekeeping genes did not show any statistically significant differences. Based on the quality of the PCR reference curves the GAPDH was chosen as the reference gene.

The appropriate housekeeping gene was selected based on a pilot comparison of their expression described in **Table 2**. PCR conditions were set as follows: one cycle 95°C for 2 minutes, 40 cycles at 95°C for 5 seconds and 60°C for 30 seconds. The amplification of PCR products were calculated according to the $2^{-\Delta\Delta Ct}$ method. The primer sequences are shown in **Table 3**.

Table 3 **Primer sequences**

Primers	Forward	Reverse
pomc	AAGGTGTACCCCAATGTCGC	GGAAGTGCTCCACCCGATAG
mc4r	GCAACTTTTTGTCTCCCCCG	GACGATGGTTTCTGACCCGT
agrp	TGAAGAAGACAGCAGCAG ACC	AAGGTACCTGTTGTCCCAAGC
β-actin	GTAACCCGTTGAACCCCATT	CCATCCAATCGGTAGTAGCG
18s	TTGCTGATCCACATCTGCTGG	ATTGCCGACAGGATGCAGAA
GAPDH	TGCCATCACTGCCACTCAGA	GTCAGATCCACAACGGATACATTG

Table 3: Primer sequences used in qRT-PCR tests.

4.9. Statistical analysis

Hypothesis I:

Body composition measurements:

The normality of the data was evaluated with the Kolmogorov-Smirnov test. Each variable showed normal distribution, therefore one-way ANOVA tests were used with Tukey's post-hoc analyses (SPSS 15.0 for Windows) to investigate the differences among the animal groups. Correlations of the parameters measured by different methods were analyzed with the Pearson correlation test. Two factor mixed-effects model with type consistency (McGraw and Wong 1996) was used to determine the within-day repeatability of STM and the interclass correlation coefficients (ICCs). Reproducibility of STM measurement was analyzed by two-way random-effect model (Bartlett and Frost 2008). Values are reported as mean ± S.E.M., except in repeatability and reproducibility analysis, where mean ± standard deviation (SD) had to be used. The level of significance was set at $p < 0.05$.

In vivo and *in vitro* experiments:

All results were presented as mean ± standard error of mean (S.E.M.). After confirmation of the normal data distribution, repeated-measures-, two-way- and one-way analysis of variance (ANOVA) were applied followed by Fisher's post hoc analysis. SPSS 11.0 for Windows and Statistica 8.0 for Windows softwares were used. The level of significance was set at $p < 0.05$.

Hypothesis II:

For the statistical analyses, Student's T test, one-way, two-way ANOVA and repeated-measures ANOVA tests were used (SPSS for Windows software). All results are shown as mean ± S.E.M. The level of significance was set at $p < 0.05$.

Statistically significant differences were labelled with symbols (* or #) in every Figure.

5. RESULTS AND DISCUSSION

5.1. Hypothesis I

5.1.1. Body composition (BC) measurements

5.1.1.1. Results of BC analysis

In order to demonstrate middle-aged obesity (increase of fat mass) and aging sarcopenia (loss of weight, especially muscles) in our rat model, we measured BW and assessed BC of Wistar rats of different age-groups. In order to prove our first hypothesis, we attempted to provide evidence on BC changes during ageing by micro-CT, *post mortem* dissection and skinfold based methods. We also aimed to compare these approaches for future *in vivo* studies where the aging-related changes of BC should be quantified. In these experiments we tested different age-groups: 3-, 6-, 12-, 18- and 24-months-old animals, representing young adult, younger and older middle-aged, aging and old age-groups, respectively. Their BW values were the following: 366.5 ± 8.2 g (n = 16), 471.7 ± 37.6 g (n = 17), 490.8 ± 12.0 g (n = 15), 527.9 ± 15.0 g (n = 14) and 487.7 ± 10.7 g (n = 15), respectively.

Evaluation of different methods of body fat assessment with regard to whole-body micro-CT

Fat mass of Wistar rats of different BW values was assessed by whole-body micro-CT, abdominal micro-$CT_{(L1-L3)}$, STM and wet weight of epididymal-, retroperitoneal fat pads determined by PMA calculated for 100 g body weight. In each case, correlation was tested between fat mass values of the same animals determined by whole-body micro-CT (as the most accurate measurement) and another method (**Figure 5**). The strongest correlation was observed between the abdominal and whole-body micro-CT. This relationship was characterized by a coefficient close to 1 ($r = 0.99$, $p < 0.001$, **Figure. 5A**). When comparing fat percentage values of the same animal determined by whole-body or abdominal micro-CT, the latter tended to slightly overestimate fat mass. The more obese the animal was the higher the difference. The mean absolute difference in fat percentages of the tested 31 rats was -1.31 ± 0.48 (individual differences ranging from -9.60 to 2.14). The total skinfold thickness showed a surprisingly close correlation with fat percentage determined by whole-body scan ($r = 0.80$, $p < 0.001$, **Figure 5B**). Fat mass indicators (PMA) showed also significant, but weaker associations with whole-body micro-CT (for wet weight of epididymal fat for 100 g body weight: $r = 0.56$, $p = 0.024$, **Figure 5C**; for wet weight of retroperitoneal fat for 100 g body weight: $r = 0.72$, $p = 0.002$, **Figure 5D**).

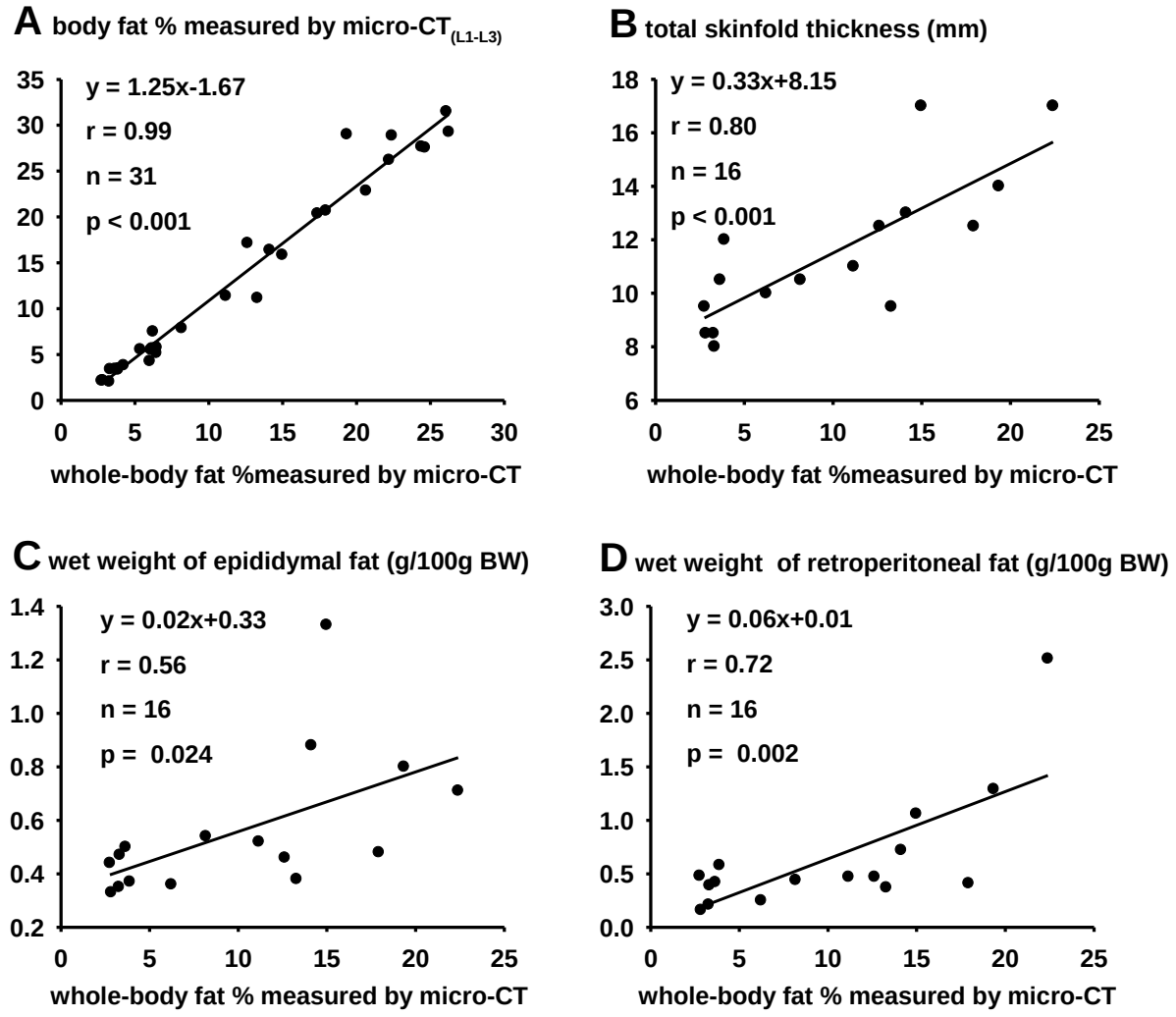

Figure 5: Correlation analysis between the body fat percentage measured by whole-body micro-CT and various other body fat indicators in Wistar rats. **Panel A**: Correlation between fat percent values assessed by abdominal micro-CT$_{(L1-L3)}$ and whole-body micro-CT. **Panel B**: Correlation between total skinfold thickness and fat percent values assessed by whole-body micro-CT. **Panel C**: Correlation between wet weight of epididymal fat for 100 g body weight (BW) and fat percent values assessed by whole-body micro-CT. **Panel D**: Correlation between wet weight of retroperitoneal fat for 100 g BW and fat percent values assessed by whole-body micro-CT.

Comparison of body fat assessment by abdominal micro-CT or skinfold thickness with regard to post mortem body composition analysis

Correlations between fat percentage values based on abdominal micro-CT$_{(L1-L3)}$ and wet weights of epididymal and retroperitoneal fat pads measured by PMA also proved to be significant (for wet weight of epididymal fat for 100 g BW: $r = 0.73$, $p < 0.001$, **Figure 6A**; for wet weight of retroperitoneal fat for 100 g BW: $r = 0.81$, $p < 0.001$, **Figure 6B**). Regarding total

skinfold thickness, correlations were also strong (for wet weight of epididymal fat for 100 g BW: r = 0.76, p < 0.001, **Figure 6C**; for wet weight of retroperitoneal fat for 100 g BW: r = 0.77, p < 0.001, **Figure 6D**).

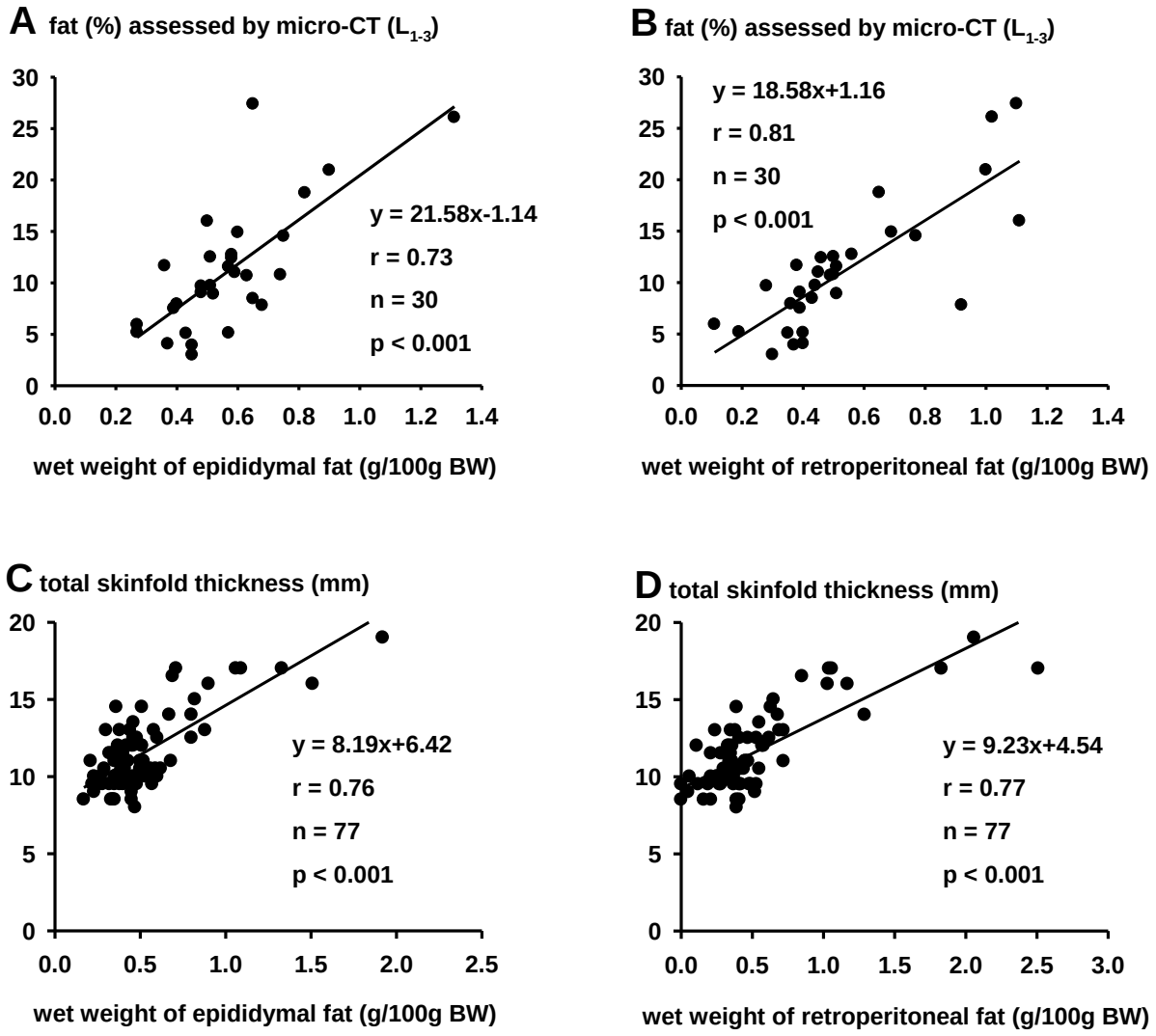

Figure 6: Correlation analysis between post mortem body fat indicators and fat percent values assessed by abdominal micro-$CT_{(L1-L3)}$ or total skinfold thickness in Wistar rats. **Panel A**: Correlation between fat percentage determined by micro-$CT_{(L1-L3)}$ and wet weight of epididymal fat for 100 g body weight (BW). **Panel B**: Correlation between fat percentage determined by micro-$CT_{(L1-L3)}$ and wet weight of retroperitoneal fat for 100 g BW. **Panel C**: Correlation between total skinfold thickness and wet weight of epididymal fat for 100 g BW. **Panel D**: Correlation between total skinfold thickness and wet weight of retroperitoneal fat for 100 g BW.

Assessment of age-related changes in body fat using abdominal micro-CT, post mortem body composition analysis and skinfold thickness

Age-related changes in fat percentages of Wistar rats assessed by abdominal micro-$CT_{(L1-L3)}$ (**Figure 7C**) were remarkably similar to those in retroperitoneal fat pads (for 100 g BW) determined by PMA (**Figure 7B**). Both methods showed significant difference between the 3- and 18-months-old groups ($p = 0.049$ for retroperitoneal fat, $p = 0.039$ for abdominal micro-$CT_{(L1-L3)}$). In addition, according to both methods, fat mass of the oldest rats declined. In contrast, a different age-related pattern emerged in case of wet weight of epididymal fat pads determined by PMA for 100 g BW (**Figure 7A**): compared to the 3-months-old group fat mass of the middle-aged 12-months-old rats proved to be significantly higher ($p = 0.048$) and fat mass declined thereafter. With regard to total skinfold thickness, values of all older age-groups differed significantly from that of the young adult 3-months-old rats (3- versus 6-, 12-, 18-or 24-months-old rats, $p = 0.034$, $p = 0.014$, $p = 0.001$ or $p < 0.001$, respectively). In contrast with age-related patterns shown by the other methods, total skinfold thickness increased during the course of aging without any decline.

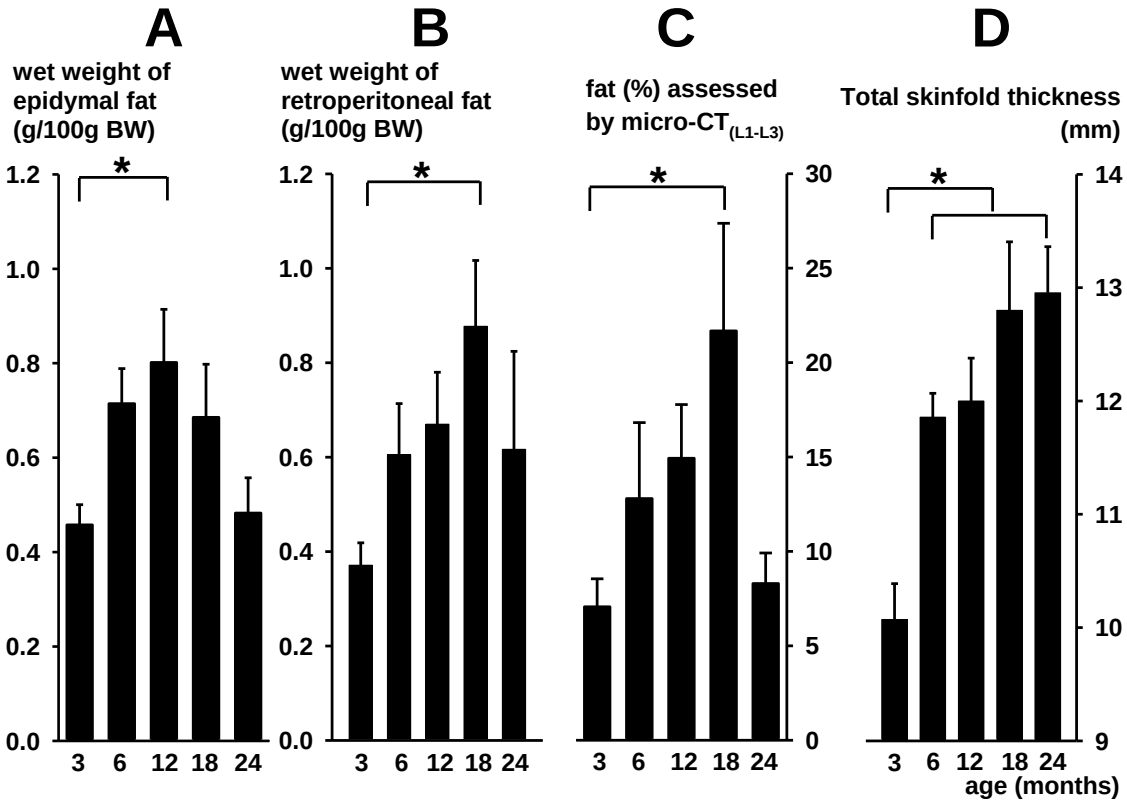

Figure 7: Age-related patterns of changes in body fat assessed by different methods in different age-groups of Wistar rats [3-month-old (n = 16), 6-month-old (n = 17), 12-month-old (n = 15), 18-month-old (n = 14), 24-month-old (n = 15)]. **Panel A**: Wet weight of epididymal fat pads for 100 body weight (BW). **Panel B**: Wet weight of retroperitoneal fat for 100 g BW. **Panel C**: Fat percentage values determined by abdominal micro-$CT_{(L1-L3)}$. **Panel D**: Total skinfold thickness. Asterisks indicate significant differences.

With regard to the differentiation between visceral and subcutaneous fat percentages assessed by abdominal micro-$CT_{(L1-L3)}$ (**Figure 8**), age-related changes in visceral fat percentages (**Figure 8A**) were similar to those in retroperitoneal fat pads (for 100 g BW) determined by PMA (**Figure 7B**) or total fat assessed by micro-$CT_{(L1-L3)}$ (**Figure 7C**). We have observed a significant difference between the 3- and 18-months-old groups ($p = 0.005$) and a slight subsequent decline in the oldest rats. In contrast, the age-related pattern characterizing subcutaneous fat (**Figure 8B**) resembled that of total ST (**Figure 7D**). Our analysis showed significant differences between the young adult 3-months-old rats and the three oldest age-groups (3- versus 12-, 18-or 24-months-old rats, $p = 0.031$, $p = 0.007$ or $p = 0.003$, respectively) without any decline in the oldest rats.

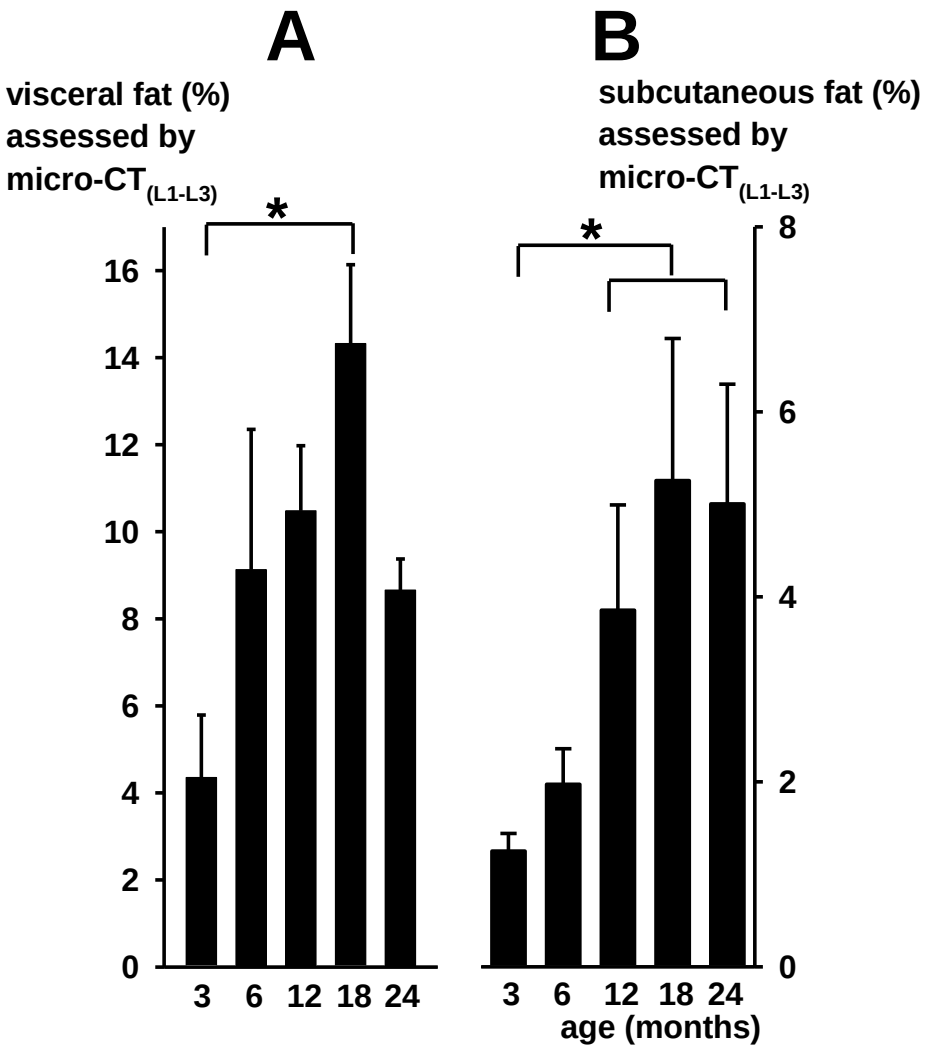

Figure 8: Age-related patterns of changes in visceral (**Panel A**) and subcutaneous (**Panel B**) fat percentage values assessed by abdominal micro-$CT_{(L1-L3)}$ in different age-groups of Wistar rats. Asterisks indicate significant differences. Animal number/age group: 3-month-old (n = 16), 6-month-old (n = 17), 12-month-old (n = 15), 18-month-old (n = 14), 24-month-old (n = 15).

Repeatability and reproducibility of STM

Repeatability analysis showed good relationship between the two within-day measurements of STM. The highest ICCs were found in connection with the repeatability of the right abdominal, the right iliac crest and the total ST (**Table 4**). Similarly, the STM reproducibility between observers showed the highest ICCs concerning the right abdominal, the right iliac crest and the total ST (**Table 5**). Thus, total ST depicted in **Figures 7 and 9** could be regarded as a reliable parameter.

	Repeatability analysis (Observer 1)		**Repeatability analysis (Observer 2)**	
Skinfold thickness	Mean within-day variation (mm)	Interclass correlation coefficient	Mean within-day variation (mm)	Interclass correlation coefficient
Right scapular	0.65 ± 1.00	0.540	0.45 ± 1.07	0.718
Right abdominal	0.25 ± 0.26	0.924	0.20 ± 0.35	0.908
Right triceps	0.15 ± 0.34	0.796	0.15 ± 0.34	0.792
Right leg	0.05 ± 0.50	0.152	0.00 ± 0.33	0.615
Right iliac crest	0.00 ± 0.24	0.987	0.15 ± 0.34	0.969
Total	1.00 ± 1.49	0.921	1.00 ± 1.70	0.897

Table 4: Repeatability analysis of the skinfold thickness-based method using two within-day (morning and afternoon) assessments. Values are means ± SD.

	Reproducibility analysis (Morning STM)		**Reproducibility analysis (Afternoon STM)**	
Skinfold thickness	Mean between-observer variation (mm)	Interclass correlation coefficient	Mean between-observer variation (mm)	Interclass correlation coefficient
Right scapular	0.50 ± 0.71	0.912	0.05 ± 0.28	0.603
Right abdominal	0.05 ± 0.44	0.845	0.05 ± 0.44	0.803
Right triceps	0.25 ± 0.26	0.762	0.05 ± 0.28	0.859
Right leg	0.00 ± 0.41	0.286	0.05 ± 0.44	0.448
Right iliac crest	0.05 ± 0.16	0.994	0.20 ± 0.35	0.966
Total	0.50 ± 0.71	0.986	0.00 ± 0.41	0.922

Table 5: Reproducibility analysis of the skinfold thickness-based method (STM) between observers in the morning and afternoon sessions. Values are means ± SD.

Assessment of age-related changes in muscle mass using post mortem body composition analysis

Age-related changes in muscle mass of Wistar rats was assessed by PMA (**Figure 9**) using a new indicator of muscle mass (i.e. wet weight of m. tibialis anterior, m. soleus, m. extensor hallucis longus, m. extensor digitorum longus calculated for 100 g BW). This method showed significantly lower value in the aging 18-month-old rats than in younger ones (18- versus 3-, 6-, 12-month-old rats, $p = 0.006$, $p = 0.049$, $p = 0.011$, respectively). The muscle indicator showed a further decline in the oldest group: compared to the younger animals this loss of muscle was

more pronounced in the 24-month-old animals (24- versus 3-, 6-, 12-month-old rats, $p < 0.001$, $p = 0.002$, $p < 0.001$, respectively), but the values of two oldest age-groups did not differ significantly. These results suggest the appearance of sarcopenia in the aging and old groups, otherwise all other values were similar.

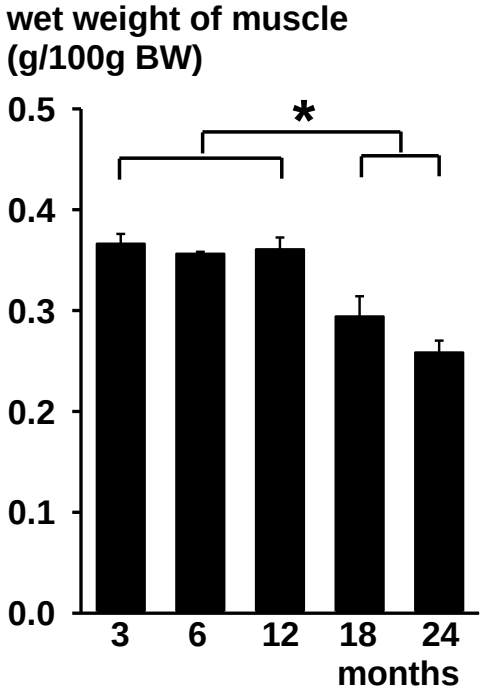

Figure 9: Age-related patterns of changes in muscle mass indicator assessed by PMA in different age-groups of Wistar rats. Wet weight of muscle calculated for 100g body weight (BW). Asterisk indicates significant differences. Number of rats in different aged-group: 3-month-old (n = 16), 6-month-old (n = 17), 12-month-old (n = 15), 18-month-old (n = 14), 24-month-old (n = 15).

5.1.1.2. Discussion of the results of the BC analysis

We demonstrated here the efficacy of different methods in the assessment of body fat in rats of different age-groups.

Regarding the abdominal micro-$CT_{(L1\text{-}L3),}$ we have hypothesized that scanning this previously untested abdominal region in rats (with advantageously short scanning time) could be an equally useful tool as whole-body micro-CT. Indeed, our results revealed an exceptionally strong correlation ($r = 0.99$) with whole-body micro-CT regarding body fat percentage assessment. However, there is a small difference between values of the same animal determined by the two methods. This difference is bigger in obese rats and negligible in lean ones. Our results are in accordance with earlier reports claiming that scanning the abdomen with micro-

CT between vertebrae L1-L6, L1-L5 or L4-L5 (Hillebrand et al. 2010; Judex et al. 2010; Lubura et al. 2012) may provide sufficient basis to estimate total body fat in mice as judged by comparison with whole-body micro-CT. It has been reported that there was no loss in relative information by restricting the region of interest to the abdominal volume (Judex et al. 2010). In rats, the potential importance of abdominal micro-CT (L1-L6, L1-L5, L4-L5) has also been suggested (Hillebrand et al. 2010). Our present findings indicate that fat percentage determined by abdominal micro-CT focusing on yet another region (L1-L3) is a sufficiently precise indicator of abdominal visceral fat also in rats. Therefore, scanning an entire rat (that takes at least 1.5-2 hours depending on the size of the animal) may not be necessary to obtain data on total body fat. Reducing the size of the scanned region decreased the duration of the scan and that of the necessary anesthesia markedly. It is especially important in old (450-510 g) rats that show especially high mortality risk during anesthesia. Another problem is presented by obese rats (600-700 g) requiring especially long whole body scan time.

The value of total skinfold thickness lies in the fact that it is simple, quick cost-effective and non-invasive, moreover it can be carried out repeatedly without deep anesthesia. This method is an accepted technique in various animal species (e.g. dairy ewes, British Angora rabbit or Galapagos sea lion) (Caroprese et al. 2006; Dhungel et al. 2009; Brock et al. 2013). It is also a useful technique in humans to assess adiposity, longitudinal effects of anti-obesity drug therapy or efficiency of long-term physical training (Wang et al. 2000; Vasheghani-Farahani et al. 2013; Horan et al. 2015). However, it requires technical training and only measures subcutaneous fat. Although, Marshall and coworkers (1969) showed that skinfold thickness significantly correlated with fat mass measured with chemical carcass analysis in different animal groups (age, sex and strain), in rats the method has not been sufficiently validated. Most researchers believe that instrumental methods are more precise than simple body measurements (Yamakage et al. 2014). In our present study we hypothesized that STM may also be suitable to detect differences and follow changes in fat mass in rats. According to our data, total skinfold thickness (measured in five locations) also correlates strongly with fat percentage assessed by whole-body micro-CT and to a lesser extent with retroperitoneal and epididymal fat ratios based on PMA. Even the repeatability and reproducibility of STM emphasized the outstanding value of total ST along with those of the right abdominal and the right iliac crest skinfolds.

We have tested these methods on age-related differences in body fat. Our result confirmed our hypothesis that visceral fat assessed separately by micro-$CT_{(L1-L3)}$ and retroperitoneal fat determined by *post mortem* measurement show similar age-related differences: both methods indicated a gradual increase from 3- to 18 months of age, followed

by a slight decline in the oldest rats. They also show close correlation with each other. In contrast, although total skinfold thickness also correlated with fat pads measured *post mortem*, it showed a monotonous age-related increase without any late decline. Therefore, loss of fat in previously more obese animals may not be followed by this latter method especially in very old rats characterized by age-related accumulation of connective tissue. These conclusions are further supported by our separate assessment of age-related changes in subcutaneous fat percentage determined by micro-$CT_{(L1-L3)}$ also showing the above described pattern.

Concerning *post mortem* body fat indicators, Luu and coworkers (2009) found that perigonadal and subcutaneous fat pads highly correlated body fat with whole-body micro-CT. In other studies there was a significant relationship between four adipose tissue depots (inguinal subcutaneous, epididymal, retroperitoneal, and mesenteric) and micro CT-derived adipose tissue mass in mice (Hildebrandt et al. 2002). In our study Pearson correlation showed significant relationship between the wet weights of retroperitoneal or epididymal fat pads calculated for 100 g BW and fat percentage assessed by whole body as well as abdominal micro-$CT_{(L1-L3)}$. However, some differences emerge between the two *post mortem* body fat indicators. For retroperitoneal fat the correlations with micro-CT methods were stronger. In contrast to age-related pattern in retroperitoneal fat pads, that showed a gradual increase from 3- to 18 months of age, followed by a slight decline in the oldest rats, the *post mortem* method based on epididymal fat pad indicated the peak earlier, already at 12 months of age. In addition, the age-related pattern obtained by abdominal micro-$CT_{(L1-L3)}$ was in accord with that based on the retroperitoneal fat measurement. These findings support our hypothesis, that *post mortem* retroperitoneal fat measurement reflects age-related differences in body fat better than measurement of epididymal fat.

Obesity presents a progressively growing public health problem therefore the analysis of body composition is of great clinical relevance. There are numerous possibilities to treat obesity with lifestyle interventions (physical exercises, diets), bariatric surgery and anti-obesity drugs (Jones and Bloom 2015). For determining the weight loss or weight gain, the development of proper animal models is important (Lutz and Woods 2012; Osto and Lutz 2015). More non-invasive methods for the assessment of body fat would be essential to test the efficacy of long-term interventions in animals. Micro-CT-$L_{1,3}$ appears to be a useful method for repeated body fat assessment in rats with reduced scanning time. Our STM may also be a useful, cost-effective, non-invasive and simple *in vivo* technique to follow changes in body fat, although it requires some technical training.

Body fat indicators assessed by PMA and mean BWs of different age groups were in accord with those observed in our previous studies (Pétervári et al. 2010; Balaskó et al. 2013; Tenk et al. 2017). In our earlier studies, the wet weight of the anterior tibial muscle (expressed as percentage of the actual BW) as muscle mass indicator suggested the appearance of sarcopenia only in the oldest (24-month-old) group. In our recent study we used a new muscle mass indicator complemented with measurement of *m. soleus, m. extensor hallucis longus* and *m. extensor digitorum longus*, which represents larger proportion of the muscle mass. Age-related loss of the extensor digitorum longus muscle and the soleus muscle in male Fischer 344 rats has also been shown by other research groups (Payne et al. 2003). Our new assessment of muscle mass indicated the appearance of age-related muscle loss already in aging 18-month-old animals with the highest BW and body fat. These data are in accord with human observations: muscle mass declines at a greater rate with age than body mass, reducing muscle strength leading to disability and loss of independence (Keller et al. 2014).

5.1.2. Age-related changes in the hypothalamic MC system: in *vivo* investigation of catabolic responsiveness to exogenous melanocortin in Wistar rats

5.1.2.1. Results of *in vivo* experiments

In our *in vivo* study using two separate cohorts of rats, acute thermoregulatory and anorexigenic effects of ICV injected alpha-MSH were investigated in different age-groups of rats. The number of rats was in the metabolic/thermoregulatory cohort as follows: n = 8, 6, 9, 8, 6 and 16 in 2-, 3-, 6-, 12-, 18- and 24-month-old rats, respectively. In the cohort used for food intake assessment, the number of animals was as follows: n = 8, 6, 8, 6 and 16 in 3-, 6-, 12-, 18- and 24-month-old rats, respectively. The thermoregulatory tests were carried out in a slightly subthermoneutral environment (25 °C). At this Ta, rats of all adult age-groups (from 3 to 24 months) showed similar resting Tc values around 37.5 °C (means for alpha-MSH treated vs. control rats aged 3-, 6-, 12 or 24 months: 37.7±0.3 vs. 37.5±0.2 °C, 37.5±0.2 vs. 37.4±0.1 °C, 37.3±0.1 vs. 37.5±0.1 °C or 37.4±0.1 vs. 37.3±0.2 °C, respectively). Juvenile rats, however, exhibited higher resting Tc (38.3±0.2 °C vs. 38.6±0.2 °C). At higher Ta, reaching the reported thermoneutral zone for Wistar rats (Székely and Szelényi 1979; Romanovsky et al. 2000), similar rats of different age-groups did not show any significant change of resting Tc, although heat loss mechanisms were activated. At 25 °C Ta, resting VO_2 was also similar in all adult rats (21.7 ± 1.2, 21.4 ± 1.7, 23.5 ± 1.7 and 19.1 ± 1.9 ml/kg/min for 3-, 6-, 12- and 24-month-old groups, respectively), while the juvenile group was characterized by a higher VO_2 at rest (24.8 ± 1.3 ml/kg/min). In this setting, under control conditions, continuous tail skin vasoconstriction was shown by the low values of HLI in all animals.

The juvenile age-group showed a significant alpha-MSH-induced increase in metabolic rate as indicated by VO_2 [$F(1,9) = 11.331$, $p = 0.008$ for MSH-treated vs. control animals between 10 to 90 min. following ICV injections], and a consequent rise in Tc [$F(1,10) = 15.249$, $p = 0.003$ for MSH-treated vs. control animals between 10 to 120 min.]. Vasodilation developed immediately [as shown by a rise in HLI, $F(1,10) = 19.371$, $p = 0.001$ for MSH-treated vs. control animals between 10 to 90 min.]. In young adult rats, the elevations in VO2 [$F(1,11) = 13.686$, $p = 0.004$ for MSH-treated vs. control groups between 10 to 70 min.] and Tc [$F(1,19) = 23.064$, $p < 0.001$ for MSH-treated vs. control animals between 10 to 120 min.] were more pronounced. Vasodilation developed with a 20-min delay [$F(1,19) = 15.661$, $p = 0.001$ for MSH-treated vs. control animals between 20 to 70 min.] and prevented further rise in Tc. At 6 months of age, the rises in VO_2 [$F(1,26) = 5.659$, $p = 0.025$ for MSH-treated vs. control animals between 10 to 30 min.], Tc [$F(1,26) = 7.569$, $p = 0.011$ for MSH-treated vs. control animals between 10 to

120 min.], and HLI [F(1,15) = 5.110, p = 0.039 for MSH-treated vs. control animals between 10 to 50 min.] were significant, however less pronounced than in the previous age-groups. In contrast, in older middle-aged rats (aged 12 months) neither VO_2 nor Tc values showed significant changes. No vasodilation was observed, either. Interestingly, in old rats, the significant increase in VO_2 [F(1,20) = 8.835, p = 0.008 for MSH-treated vs. control animals between 10 to 70 min.] was associated with a significant rise in Tc again [F(1,12) = 5.883, p = 0.032 for MSH-treated vs. control animals between 10 to 120 min.], despite the strong vasodilation [for HLI F(1,10) = 79.489, p < 0.001 for MSH-treated vs. control animals between 10 to 120 min.].

Accordingly, the maximal effects of alpha-MSH on Tc varied with aging, as shown by two-way ANOVA [F(4,79) = 3.552, p = 0.010]. The rises in Tc were highest in young adult rats, more modest in juvenile and younger middle-aged, non-significant in older middle-aged rats but became significant again in old animals (**Figure 10**).

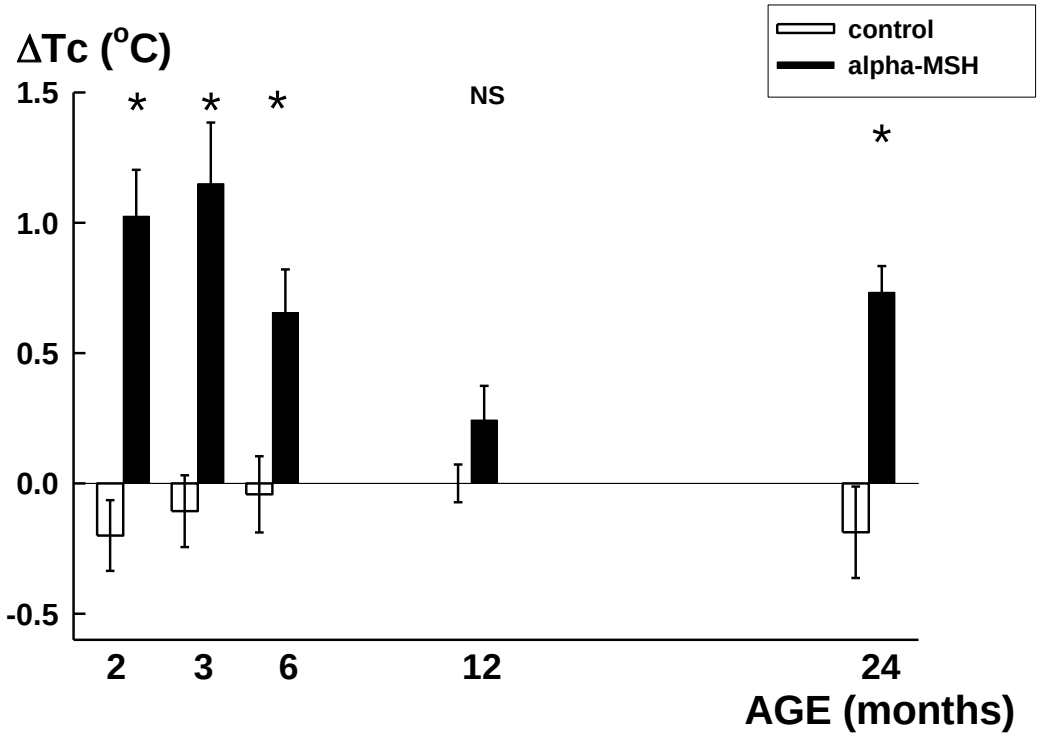

Figure 10: Alpha-MSH-induced hyperthermia in different age-groups of Wistar rats. Full columns represent changes in core temperature (ΔTc) at 120 min. following an ICV alpha-MSH injection (5 μg/5μl), empty columns indicate similar values of controls, following administration of ICV pyrogen-free saline (PFS, 5 μl). Values are expressed as mean ± S.E.M.. One-way ANOVA showed significant differences between treated vs. corresponding control rats (indicated by asterisks, p < 0.01) in all age-groups except for 12-months-old animals.

Regarding maximal changes in HLI (**Figure 11**), a similar age-related pattern can be observed [two-way ANOVA: $F(4,79) = 7.804$, $p < 0.001$]. A steady decline of responsiveness was observed up to 12 months of age, followed by a great enhancement in the oldest age-group.

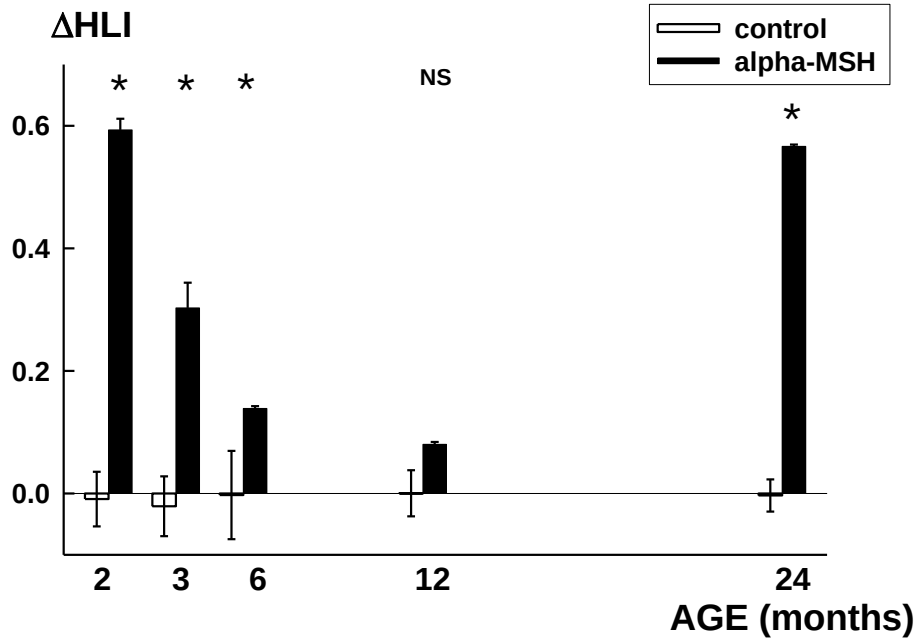

Figure 11: Alpha-MSH-induced effects on heat loss in different age-groups of Wistar rats. Full columns represent maximal changes in heat loss index (HLI) following an ICV alpha-MSH injection (5 μg/5μl), empty columns indicate similar values of controls, following administration of ICV pyrogen-free saline (PFS, 5μl). Values are expressed as mean ± S.E.M.. One-way ANOVA showed significant differences between treated vs. corresponding control rats (indicated by asterisks, $p < 0.01$) in all age-groups except for 12-months-old animals.

The maximal effects of alpha-MSH on VO_2 varied similarly with aging [two-way ANOVA: $F(4,79) = 4.274$, $p = 0.004$]. Baseline respiratory exchange ratio did not change with aging (mean around 0.85) and it also failed to be influenced significantly by acute ICV alpha-MSH administration. We analyzed these changes in hypermetabolic effect along with the anorexigenic effect of the peptide in five adult age-groups of rats (complementing our experiments with data of 18-month-old animals) with special regard to the BW development curve of our Wistar strain (**Figure 12**).

The BW development of male Wistar rats of our colony shows a marked continuous age-related rise until 18 months of age: a period of rapid growth to 6 months is followed by a more moderately rising slope reaching the peak of the growth curve (**Figure 12A**). Thereafter a pronounced decline is observed (**Figure 12A**). Both hypermetabolic and anorexigenic

components of the catabolic effects of ICV alpha-MSH-injection show similar characteristic age-related changes. The hypermetabolic effect (based on VO_2) remained significant in all age-groups (as compared with their age-matched controls treated with PFS without any hypermetabolism, not shown) except for older middle-aged (12-month) rats. Accordingly, this effect reached its nadir in the 12-month-old group followed by an increase in older animals (**Figure 12B**). Similarly, the anorexigenic effect (based on suppression of fasting-induced refeeding) was also significant in all age-groups (as compared with their age-matched controls, not shown) except for older 12-month-old rats. Accordingly, this effect of the peptide also reached its minimum in the 12-month-old group followed by an increased efficacy in older animals (**Figure 12C**). Thus, the age-related drop in the hypermetabolic and anorexigenic responsiveness to alpha-MSH occurs (12-month) before the marked weight gain (and the highest visceral fat percentage, s. also **Figures 7 and 8**) observed by 18 months of age, whereas the strong catabolic responsiveness of the 18-month-old group precedes the appearance of weight loss and sarcopenia by 24 months of age (cp. **Figure 9**). These results suggest that decreased catabolic efficacy of alpha-MSH precedes middle-aged weight gain and obesity, and later on an increased efficacy precedes weight/muscle loss in old rats. The observed age-related shifts in catabolic alpha-MSH-effects may contribute to the development of middle-aged obesity and later to that of weight loss of old age.

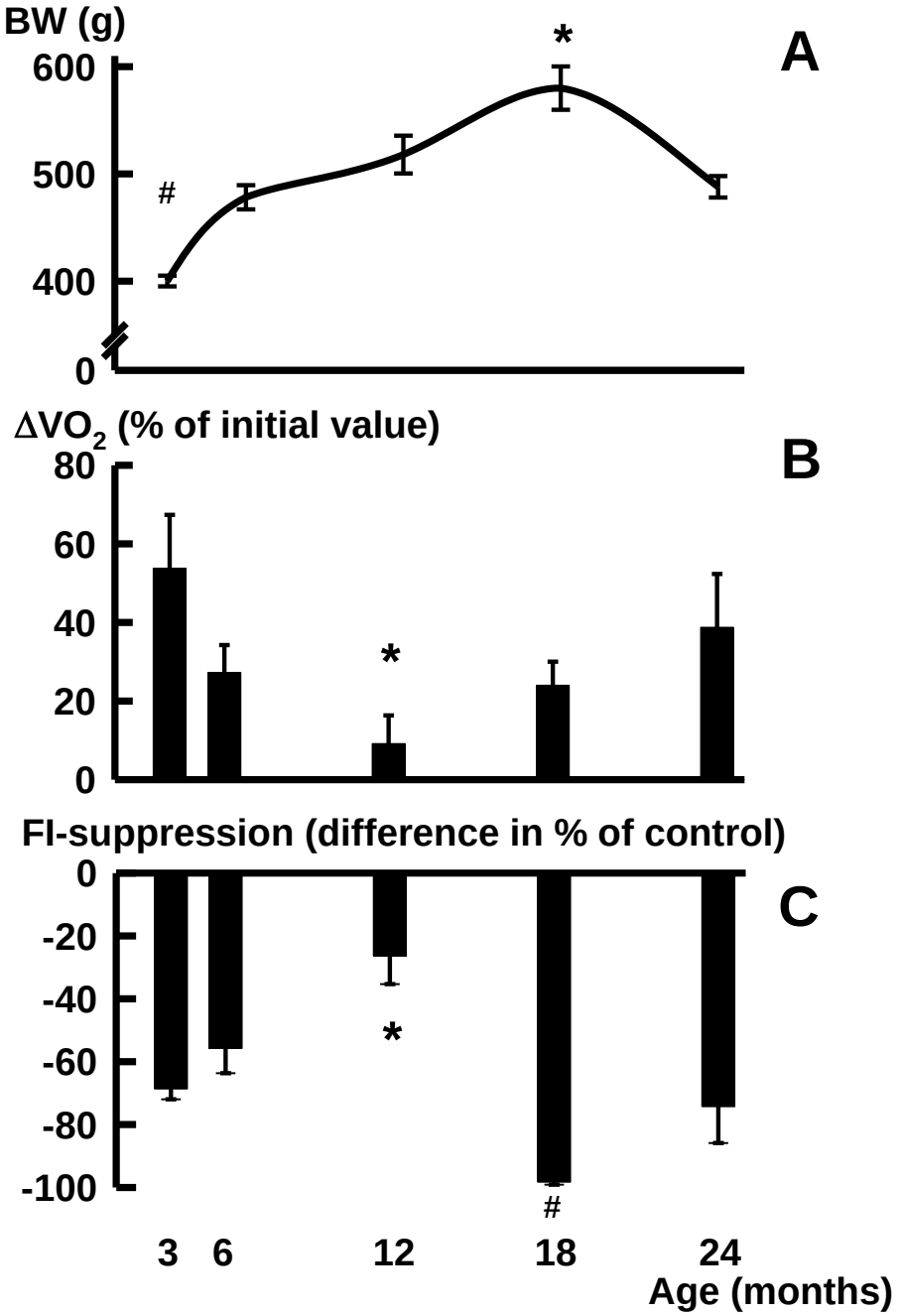

Figure 12: Age-related changes in body weight (BW) (**Panel A**) of male Wistar rats, and their hypermetabolic (**Panel B**) and anorexigenic (**Panel C**) responsiveness to ICV injected alpha-melanocyte-stimulating-hormone (alpha-MSH, 5 μg/5μl). **Panel A:** BW development curve constructed from mean ± S.E.M. values of 3-, 6-, 12-, 18- and 24-month-old male Wistar rats. #: $p < 0.001$ 3-month vs. all other age-groups, *: $p < 0.001$ 18-month vs. all other age-groups. **Panel B**: Alpha-MSH-induced increase in oxygen consumption (ΔVO_2, expressed in % of the initial value) at 20 min following alpha-MSH injection in different age-groups of rats. The initial VO_2-values did not differ (21.7 ± 1.2, 21.4 ± 1.7, 23.5 ± 1.7, 22.0 ± 1.5 and 19.1 ± 1.9 ml/kg/min for 3-, 6-, 12-, 18- and 24-month-old groups, respectively).*: $p < 0.05$ concerning the difference between 12-month-old and 3- or 24-month-old groups. **Panel C**: Alpha-MSH-

induced suppression of 2-h cumulative refeeding food intake (FI) following 24-h fasting in various age-groups of rats. Anorexigenic responsiveness is represented by the difference between cumulative FI values of the treated and the age-matched control groups (injected ICV with physiological saline) expressed as a % of the control cumulative values (control refeeding FI values: 21.7 ± 1.2, 21.4 ± 1.7, 23.5 ± 1.7, 22.0 ± 1.5 and 19.1 ± 1.9 g for 3-, 6-, 12-, 18- and 24-month-old groups, respectively). *: $p < 0.001$ 12-month vs. other age-groups; #: $p < 0.02$ 18-month vs. younger age-groups. All data (A-C) are expressed as mean ± S.E.M. and were analyzed by one-way analysis of variance (ANOVA) with Fisher's *post hoc* test.

5.1.2.2. Discussion of *in vivo* experiments

In the present study age-related alterations of the acute central complex catabolic (thermoregulatory and anorexigenic) effects of melanocortin agonist alpha-MSH were investigated using different age-groups of rats.

Our study confirms earlier observations that described an alpha-MSH-induced rise in metabolic rate upon acute ICV injection that results in a rise in Tc despite a parallel activation of heat loss in young adult rats (Fan et al. 2005, Balaskó et al. 2010). This peptide induces a progressive increase in Tc despite a transient increase in VO_2, because heat loss mechanisms, as indicated by HLI, become activated only for a very short time coinciding with the initial rise in Tc, and HLI decreases rapidly afterwards. The effects of such a short-term vasodilation are very limited. In addition, alpha-MSH has been shown to induce activation of the sympathetic nervous system, that in turn, elicits (via $beta_3$-adrenergic receptors) uncoupling of terminal oxidation and ATP production in brown-fat mitochondria, resulting in enhanced heat production that does not require further increases in VO_2 (Richard et al. 2012).

Concerning age-related alterations, our study shows that alpha-MSH induced the highest acute increase in Tc in young adult rats due to a rise in VO_2. Tail skin vasodilation limiting hyperthermia developed with a short delay. In comparison, the rises in Tc and VO_2 were similar in juvenile animals, starting from higher initial values, and slightly diminished in the younger middle-aged group. Thermoregulatory changes induced by alpha-MSH were suppressed in the older middle-aged rats and they became significant again in old animals. This latter observation demonstrates that old rats still maintain their capacity to raise their metabolic rate and body temperature substantially, at least for a short period of time. It is possible that in old rats such hypermetabolism cannot be sustained for longer periods. Moreover, in our earlier experiments (Pétervári et al. 2011) a 7-day ICV infusion of alpha-MSH elicited significant hyperthermia in old rats, albeit for a shorter duration than in younger groups.

Thermoregulatory responsiveness to an acute ICV alpha-MSH injection shows similar age-related pattern to that observed in connection with acute central anorexigenic melanocortin effects (Pétervári et al. 2010). The latter observation was confirmed in our recent FI-related tests. These findings appear to be somewhat surprising as previous reports indicated that different components of the catabolic effects of alpha-MSH (the anorexigenic and hypermetabolic ones) may diverge. Balthasar and coworkers (2005) demonstrated in genetically modified mouse strains that MC4Rs in the paraventricular nucleus of the hypothalamus and/or the amygdala are responsible for the control of food intake, while other central MC4Rs appear to control energy expenditure. Age-related alterations in MC4R receptor density have not been properly investigated in earlier studies. Therefore, some parallel age-related changes in the level of MC4Rs in different nuclei of the brain responsible for both acute anorexigenic and hypermetabolic melanocortin actions, may explain our observation.

Previously, we have demonstrated that these components of the catabolic effects of a chronic central melanocortin infusion change in a disparate way during aging (Pétervári et al. 2011). The anorexigenic component that was strong in the juvenile and young adult age-groups proved to be non-significant in the middle-aged and became very strong again in the old one. The hypermetabolic component, on the other hand, shows a distinctly different pattern in the chronic study: it appeared to be strong in middle-aged and was maintained at a high level in the oldest rats (Pétervári et al. 2011).

Such a difference in the acute and chronic hypermetabolic responsiveness may be explained by several factors. The ICV infusion technique used in the chronic study did not allow collection of convincing data on the 1st day of infusion due to the simultaneously appearing acute effects of the surgical intervention, i.e. implantation of the ICV cannula of the Brain Kit and that of the Alzet osmotic minipump (Pétervári et al. 2011, 2014). Thus, our present results may indicate that the onset of the hyperthemic response in the middle-aged group (seen in chronic experiments) is delayed. Moreover, the semi-restrained (acute study) vs. freely moving state (chronic observation) of the rats may also contribute to the differences.

We analyzed these complex acute catabolic (hypermetabolic and anorexigenic) effects of alpha-MSH in five age-groups of male Wistar rats from young adult to old age with special regard to the BW development curve. Both the decreased catabolic responsiveness of middle-aged animals and the enhanced responsiveness of aging rats appeared before characteristic alterations in the slope of the BW development curve. These dynamics suggest a regulatory role of the MC system in age-related changes of BW. These BW changes imply disadvantageous consequences regarding body composition, which were demonstrated also as a part of this PhD

thesis (chapter 5.1.1.): weight gain in middle-aged rats is usually a result of visceral fat accumulation (obesity), while weight loss in old animals affects mainly muscles (sarcopenia) (Pétervári et al. 2010, Wolden-Hanson 2006). Therefore, investigation of their mechanisms using *in vitro* techniques are of major importance.

In conclusion: Age influences significantly the acute hyperthermic, hypermetabolic effects of ICV applied alpha-MSH. The age-related shifts in the hyperthermic responses appear to be similar to those of the anorexigenic effects of the peptide. Our results may also contribute to the explanation of the development of middle-aged obesity and aging cachexia.

5.1.3. Age-related changes in the hypothalamic MC system: i*n vitro* analysis of the endogenous activity in Wistar rats

5.1.3.1. Results of i*n vitro* analysis

To test our *Hypothesis I*, we investigated changes in the endogenous activity of the hypothalamic MC system during the course of aging. We aimed to clarify the endogenous mechanisms of the above discussed in vivo phenomena at the level of hypothalamic gene expression and protein content in all five adult age-groups.

Alpha-MSH immunoreactivity in the ARC and PVN declines in middle-aged and increases together with POMC gene expression in aging rats

To assess the age dependence of the main factors of the endogenous MC system at mRNA level in the ARC and PVN, qRT-PCR measurements were conducted (**Figure 13**). Regarding protein levels, immunofluorescence method was applied (**Figures 14 and 15**).

The relative expression of POMC mRNA in the ARC was a function of age (**Figure 13A**, ANOVA: $F=5.097$; $p<0.005$). Based on the *post hoc* comparison, gene expression increased until 18 months of age with a transient non-significant 30 % decline between 6 and 12 months. In the oldest (24-month-old) rats the gene expression became low again.

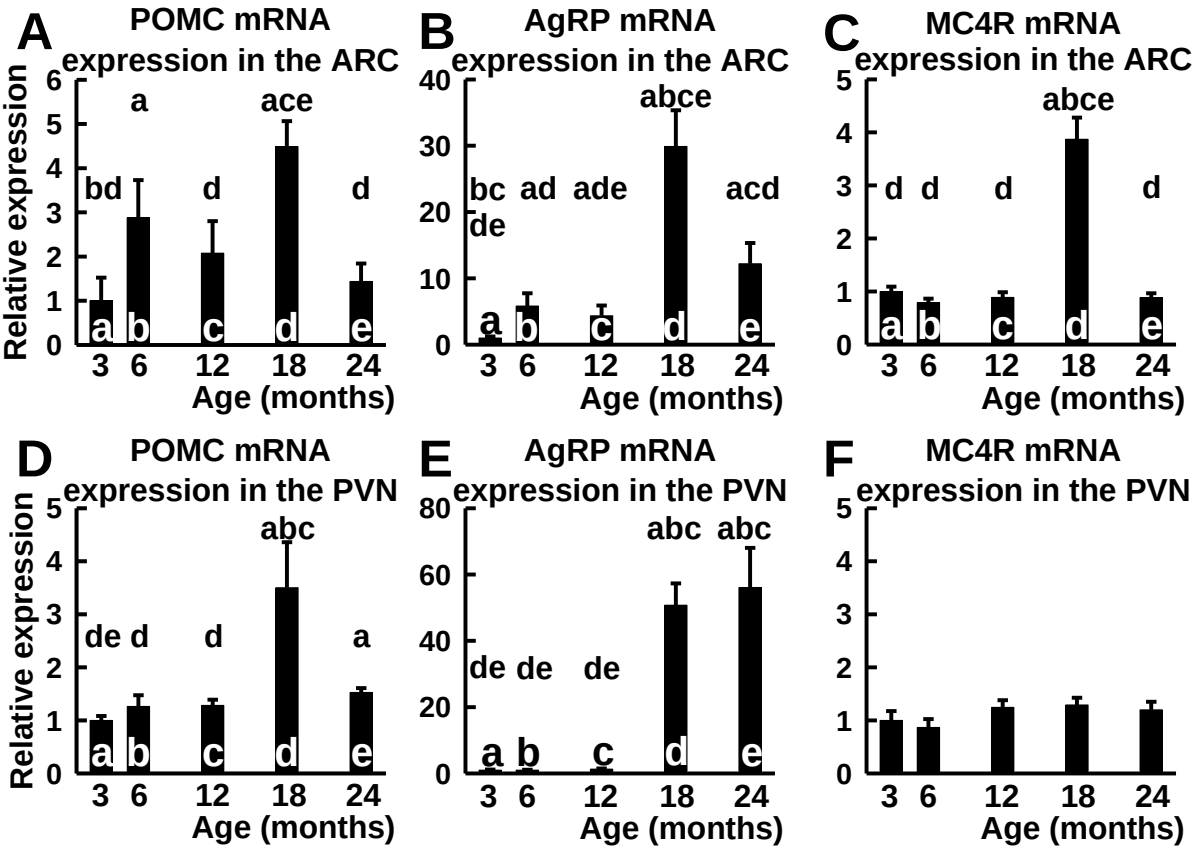

Figure 13: Relative mRNA expression of POMC, AgRP and MC4R in the ARC (**A-C**) and in the PVN (**D-F**) of 3-, 6-, 12-, 18-, and 24-month-old male Wistar rats (n = 6, 6, 5, 9 and 6, respectively). All data (**A-F**) are expressed as mean± S.E.M. Lettering on top of the columns represents significant differences between pairs of age groups according to Fisher's post hoc test ($p<0.05$).

Regarding immunohistochemical results, we found clearly recognizable neuronal cell bodies labeled by alpha-MSH antibodies in the ARC using alpha-MSH-MC4R double labeling (**Figures 14A-C**). The SSD measurement of alpha-MSH immunoreactivity (**Figure 14G**) revealed that the peptide content of ARC alpha-MSH neurons was also a function of age (ANOVA: $F = 3.761$; $p<0.02$). Here, resembling the results concerning the POMC gene expression (cp. **Figure 13A**), a somewhat similar age-related pattern emerged: compared with the similarly high SSD values of 3-month-old and middle-aged 6-month-old rats, the 12-month-old animals showed a significant decline followed by a marked increase, in the aging 18-month-old rats. In the oldest group (24-month-old) the SSD dropped significantly. Thus, the peak was found once again in the 18-month-old group (**Figure 14G**).

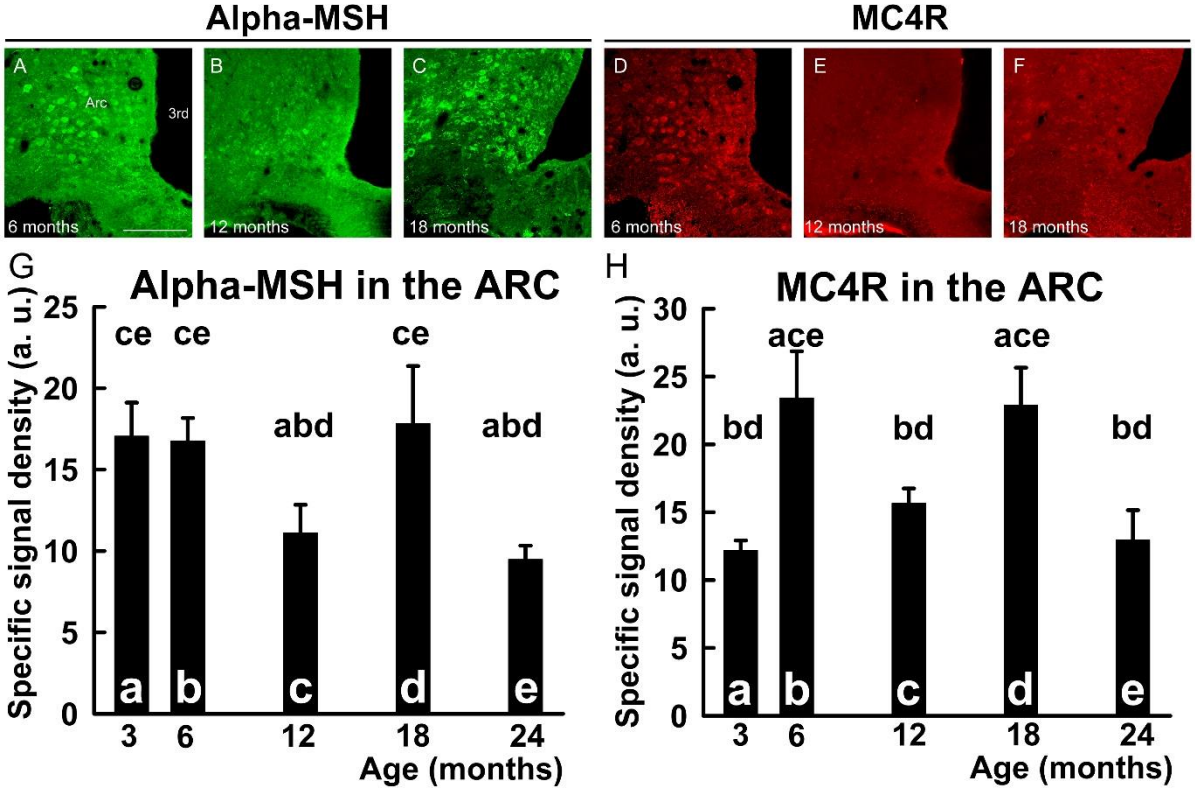

Figure 14: Immunohistochemical detection of alpha-MSH and MC4R in the arcuate nucleus (ARC) of male Wistar rats revealed age-related differences using alpha-MSH-MC4R double labeling. Representative confocal immunofluorescent images show alpha-MSH (red, **Panels A, B** and **C**) and MC4R (green, **Panels D, E** and **F**) immunoreactive neuronal cell bodies in 6-, 12- and 18-month-old male Wistar rats, respectively. Immunoreactivity in the middle-aged 12-month-old group is decreased as compared with the younger or older age-group. Scale bar: 100 µm. Specific signal density (in arbitrary units, a.u.) of alpha-MSH (**Panel G**) and MC4R (**Panel H**) of 3-, 6-, 12-, 18- and 24-month-old male Wistar rats demonstrates a characteristic age-related pattern (n = 5, 6, 8, 5 and 5, respectively). All data (**Panels G-H**) are expressed as mean ± S.E.M. Lettering on top of the columns indicates significant differences between pairs of age-groups according to Fisher's post hoc test ($p < 0.05$).

At the site of release of alpha-MSH (*i.e.* in the PVN), relatively low POMC expression was found in all age-groups with the exception of the aging, 18-month-old rats (**Figure 13D**, ANOVA: $F=6.062$; $p<0.002$). Their high value was followed by a non-significant decline in 24-month-old rats ($p = 0.19$). Interestingly, the relative POMC expression of the oldest rats was still higher than that of the 3-month-old group ($p < 0.001$).

At the PVN, we saw a dense network of alpha-MSH immunoreactive nerve fibers (**Figures 15A-C**). No alpha-MSH immunoreactive cell bodies were found here. Statistical analysis revealed an overall effect of age on alpha-MSH peptide immunosignal (**Figure 15G**, $F=4.804$, $p<0.01$). The age-related pattern was similar to that seen in the ARC (cp. **Figure**

14G): 12-month-old animals showed a significant decline compared to the SSD values of 6-month-old rats, followed by a marked increase in the aging,18-month-old group. The decline in the oldest animals did not reach statistical significance ($p = 0.06$; **Figure 15G**).

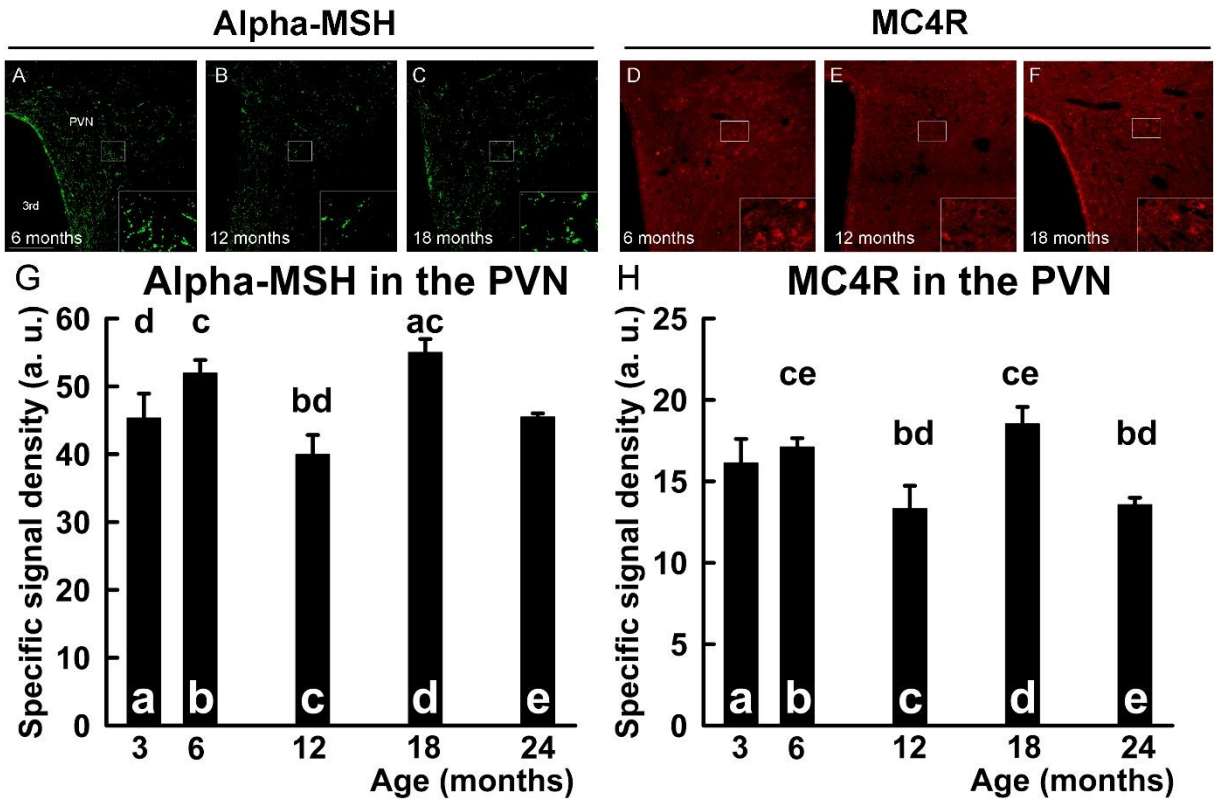

Figure 15: Immunohistochemical detection of alpha-MSH and MC4R in the PVN of male Wistar rats revealed age-related differences using alpha-MSH-MC4R double labeling. Representative confocal immunofluorescent images show alpha-MSH (red; **A–C**) immunoreactive nerve fibers and MC4R (green; **D–F**) immunoreactive neuronal cell bodies in 6-, 12-, and 18-month-old male Wistar rats, respectively. Immunoreactivity in the middle-aged 12-month-old group is decreased as compared with the younger or older age group. Areas marked by white boxes are also depicted as higher magnification insets in the right bottom corner of the respective panel. Scale bar: 100 μm. Specific signal density (in arbitrary units, a.u.) of alpha-MSH (**G**) and MC4R (**H**) of 3-, 6-, 12-, 18-, and 24-month-old male Wistar rats demonstrates a characteristic age-related pattern (n = 5, 6, 8, 5 and 5, respectively). All data (**G** and **H**) are expressed as mean ± S.E.M. Lettering on top of the columns indicates significant differences between pairs of age groups according to Fisher's post hoc test ($p < 0.05$).

AgRP gene expression, but not its immunoreactivity increases in the ARC and PVN of aging rats

AgRP produced in the ARC also binds to MC4R as an endogenous inverse agonist in the PVN. Results of the quantitation of AgRP mRNA expression (**Figure 13B and 13E**) were somewhat surprising since relative mRNA expression values exceeded those of POMC or

MC4R (cp. **Figure 13A, 13C, 13D and 13F**). In the ARC, the AgRP mRNA expression changed with aging (**Figure 13B,** ANOVA: $F=22.324$; $p < 0.001$). It was low in 3-, 6- and 12-month-old rat groups followed by a dramatic increase in 18-month-old animals (a 30-fold increase was observed compared to the 3-month-old rats). In the oldest animals AgRP mRNA expression decreased again. In the PVN, a similar age-related pattern of AgRP mRNA expression was seen (**Figure 13E**, ANOVA: $F=122.890$; $p < 0.001$): uniformly low values in 3-, 6- and 12-month-old groups were followed by a highly significant 50-fold rise in the 18- and 24-month-old rat groups. In contrast with the ARC (cp. **Figure 13B**), the two oldest groups here did not differ significantly (**Figure 13E**).

The AgRP staining was performed both in the ARC and PVN. In both locations the signal was clear in nerve fibers. In contrast to AgRP mRNA expression, the high level of nerve fiber SSD for AgRP failed to show any age-dependence either in the ARC or in the PVN (**Figure 16A-B**; for ARC: $F=1.103$, $p=0.380$, for PVN: $F=0.801$, $p=0.539$).

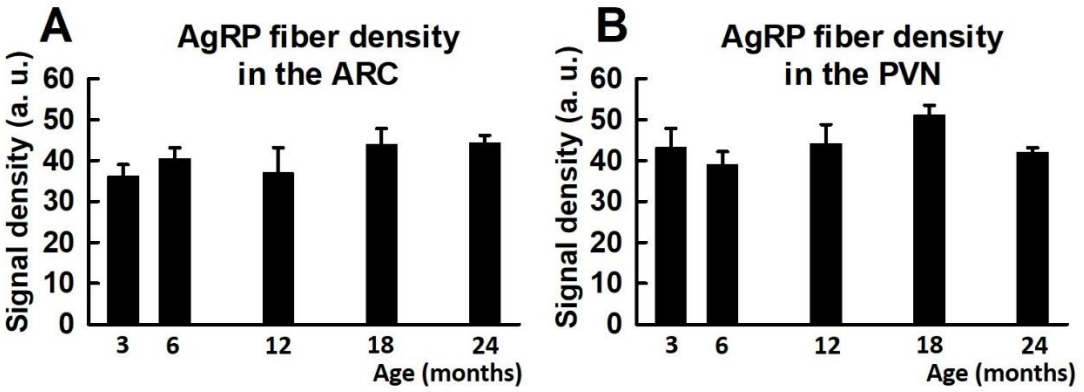

Figure 16: Agouti-related peptide (AgRP) immunosignal (in arbitrary units, a.u.) in nerve fibers of the arcuate nucleus (ARC, **Panel A**) and the paraventricular nucleus (PVN, **Panel B**) of 3-, 6-, 12-, 18- and 24-month-old male Wistar rats (n = 5, 6, 8, 5 and 5, respectively) does not show any difference. All data are expressed as mean ± S.E.M.

MC4R immunoreactivity in the ARC and PVN declines in middle-aged and increases in aging rats whereas gene expression increases only in the ARC of aging rats

The presence of MC4Rs was detected not only in the PVN but also in the ARC. The qRT-PCR measurements of MC4R mRNA in the ARC (**Figure 13C)** showed that 18-month-old rats expressed approximately four times more MC4R transcripts than other age-groups (ANOVA: $F=50.560$, $p < 0.0001$).

Regarding immunohistochemical findings, alpha-MSH-MC4R double labeling revealed that alpha-MSH neurons in the ARC co-express MC4R (**Figure 17/C**).

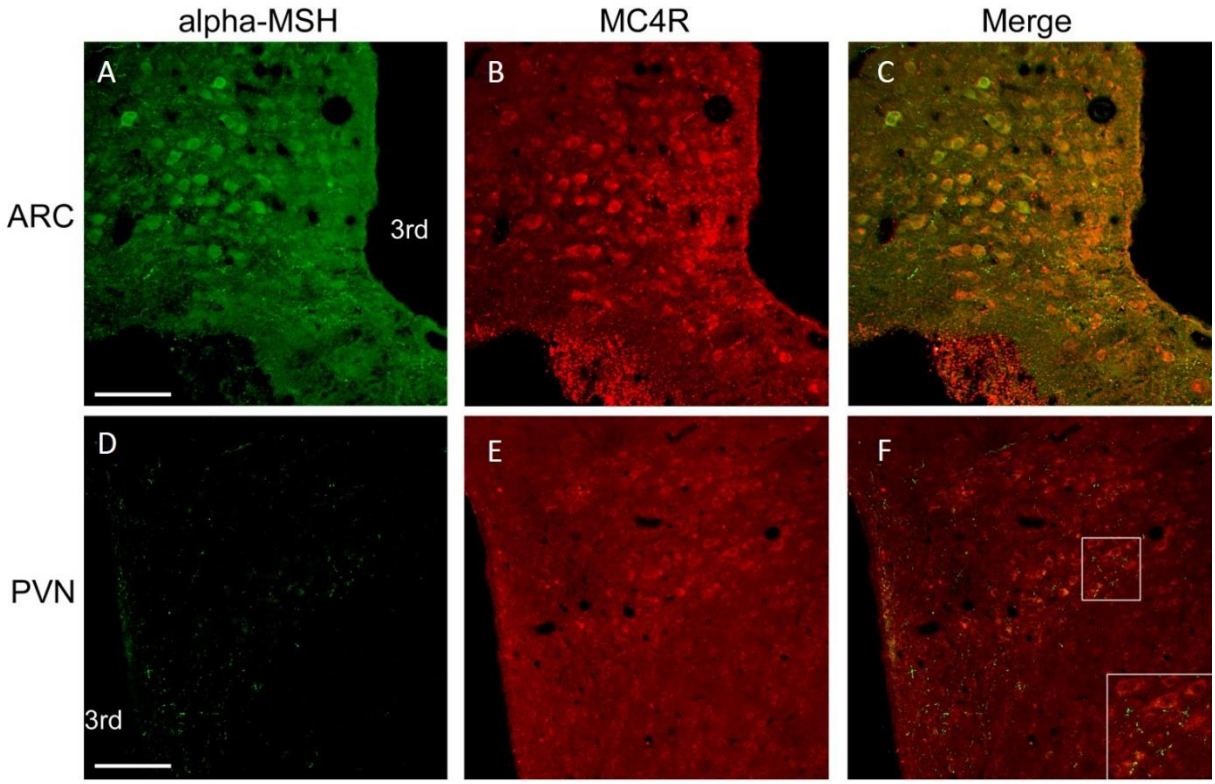

Figure 17: Representative confocal immunofluorescent images in the arcuate (ARC) and paraventricular nuclei (PVN) of the hypothalamus. Alpha-MSH immunoreactive nerve cell bodies were found in the ARC (**A**). In contrast, in the PVN (**D**), alpha-MSH nerve fibers (**D**) were seen. **Panel B** and **E** show MC4R positive immunoreactive perikarya in the ARC and PVN, respectively. The co-localization of alpha-MSH (green) and MC4R (red) immunoreactivities is also demonstrated by the merged images in **panels C** and **F**. Note that most alpha-MSH immunoreactive perikarya (green) co-express MC4R (red) also (**C**) in the ARC. **Panel F** represents the alpha-MSH (green) immunoreactive nerve fibers juxtaposed to MC4R immunoreactive (red) perikarya in PVN. Areas marked with white boxes in image **F** is also depicted as higher magnification insets in the right bottom corner of the respective panel. 3rd: third ventricle. Scale bar: 100 μm.

The SSD of MC4R in the ARC showed age-dependence (**Figure 14H,** ANOVA: $F=5.447$, $p<0.005$). *Post hoc* comparison revealed that MC4R immunosignal in 6- and 18-month-old groups was approximately 90% higher than that of 3-, 12 or 24-month-old rats. This age-related pattern showed similarities with that of alpha-MSH SSD in the ARC (cp. **Figure 14G**): the decline in the 12-month-old animals was followed by an increase in the aging group (18-month-old) and then again a decrease was observed in the oldest (24-month-old) rats. The

rise in the aging rats and the drop in the oldest ones were in accord with the mRNA expression data in the ARC (cp. **Figure 13C**).

In the PVN, there was no difference in MC4R mRNA expression between the age-groups (**Figure 13F**, ANOVA: F=1.625, p=0.199). However, the age-related pattern of MC4R SSD values (immunofluorescence, **Figures 15D-F** and **15H**) resembled those of alpha-MSH SSD in the ARC and PVN (cp. **Figures 14A-C, 14G** and **15A-C, 15G**). This general pattern involves a decline in the middle-aged followed by a rise in aging 18-month-old rats and a final drop in the oldest animals. These data suggest corresponding age-related fluctuations in the activity of the endogenous MC system. On the other hand, these shifts in MC4R in the PVN may contribute to the explanation of the changes in the responsiveness to exogenously administered alpha-MSH (**Figure 12B-C**).

5.1.3.2. Discussion of *in vitro* results in view of our *in vivo* observations

The MC system plays a pivotal role in the control of energy homeostasis, with deep impact on BW and body composition (Lee and Wardlaw 2007; Mountjoy 2015). Based on earlier observations (Zhang et al. 2004; Pétervári et al. 2010; 2011;) we hypothesized that age-related changes in the intrinsic activity of the hypothalamic MC system contribute to the development of middle-aged obesity and aging anorexia/cachexia seen in humans and in rodents. To test this hypothesis, we investigated changes in the reactivity and also in the endogenous activity of the hypothalamic MC system during the course of aging. Thus, on the one hand, we analyzed complex acute catabolic (hypermetabolic and anorexigenic) effects of an exogenous MC agonist in five age-groups of male Wistar rats from young adult to old age with special regard to the BW development curve (discussed above). On the other hand, we also aimed to clarify the endogenous mechanisms of these *in vivo* phenomena at the level of hypothalamic gene expression and protein content in all five age-groups. Our in *vivo* and i*n vitro* results support our hypothesis as discussed below.

Our results regarding immunofluorescent labeling of alpha-MSH neurons were in accord with earlier studies reporting alpha-MSH-immunopositive perikarya (Dubé et al. 1978) in the ARC and alpha-MSH-immunoreactive nerve fibers projecting from the ARC into the PVN (Knigge and Joseph 1982). Our alpha-MSH-MC4R double labeling did not only confirm the presence of MC4R in the PVN but also on alpha-MSH-immunopositive perikarya of the ARC (Mountjoy et al. 1994; Kishi et al. 2003; Gelez et al. 2010). Detection of MC4R in the ARC has proven to be elusive so far, only a handful of studies reported its low density in addition to the

moderate density of MC3R (Mountjoy et al. 1994; Harrold et al. 1999; Liu et al. 2003). The significance of MC4R expression in alpha-MSH immunopositive neurons was recently assessed in elegant studies by groups of Smith (Smith et al. 2007) *in vitro* and do Carmo (do Carmo et al. 2013) *in vivo*. These authors suggested a self-up-regulatory action of alpha-MSH on POMC neurons via their own MC4R that could amplify MC peptide release. In contrast to alpha-MSH, AgRP binding to MC4R of POMC neurons in the ARC would inhibit the above mentioned positive feedback loop, through inverse agonism. Our immunofluorescent labeling of AgRP showed clearly positive nerve fibers both in the ARC and PVN (site of activation of second order neurons) indicating active interactions with other neurons described earlier in both nuclei (Légrádi and Lechan 1999; Garfield et al. 2015). We could not detect AgRP perikarya in the ARC, since the visualization of AgRP neurons by immunohistochemistry would have absolutely required a high-dose colchicine pretreatment (Légrádi and Lechan 1999), which would have biased the results in this experimental setup.

With regard to gene expressions, our RT-PCR results revealed the presence of not only MC4R mRNA, but also that of POMC and AgRP in both nuclei. A discrepancy appears between the relatively high alpha-MSH and AgRP immunoreactivity and the low POMC and AgRP mRNA expression in the ARC of the 3-month-old group. This phenomenon awaits further studies. One could speculate that the gene transcription and the peptide release is slower in this age-group which leads to a relative accumulation of the immunoreactivity.

Concerning age-related alterations, we analyzed our *in vitro* findings (depicted in a schematic way in **Figure 18**) in view of our *in vivo* observations. As compared with the responsiveness of 3-month-old animals the decline in efficacy of alpha-MSH reached statistical significance by 12 months of age (**Fig. 12B** and **C**). This decline may be explained by the drop in MC4R immunoreactivity that we found in the PVN and even in the ARC of 12-month-old rats (**Figure 18**). Interestingly, this drop was not associated with a parallel decrease in MC4R gene expression suggesting an increased receptor turnover or decreased efficacy of synthesis. Moreover, the drop of MC4R immunoreactivity in the ARC could lead to a diminished positive feedback affecting POMC neurons that manifested in parallel drop of alpha-MSH immunoreactivity in the ARC and PVN suggesting a suppressed endogenous activity of alpha-MSH (peptide content). Again, POMC gene expression was maintained in both nuclei, therefore the decreased alpha-MSH peptide content could be explained by decreased efficacy of synthesis or increased elimination. At the same time, neither AgRP gene expression nor immunoreactivity decreased until 12-month-old, implying a maintained negative feedback affecting POMC neurons in the ARC and inverse agonist action in second order neurons of the PVN.

Accordingly, in 12-month-old rats a relative AgRP dominance over alpha-MSH would explain the observed tendency for weight gain that precedes the appearance of BW peak by 18-month-old animals (**Figure 12A**). This group (aged 18-month) with the maximal BW [associated with the peak visceral fat mass (**Figures 7 and 8**) (Pétervári et al. 2010)] shows a marked change of the MC system in the opposite direction. As compared with of 12-month-old animals the responsiveness rises once again in 18-month-old rats (**Figure 12B** and **C**). This rise may be explained by the significant increase in MC4R immunoreactivity that we found in the PVN and even in the ARC of the 18-month-old group (**Figure 18**). Interestingly, the rise in the ARC but not in the PVN was associated with a parallel increase in MC4R gene expression suggesting an increased synthesis of the receptor. In the PVN a more efficient synthesis or decreased turnover could explain the higher MC4R immunoreactivity. Moreover, the activation of positive feedback affecting the POMC neurons of the ARC is indicated by the parallel rise of POMC gene expression and alpha-MSH immunoreactivity. In the PVN similar increases were detectable. Interestingly, AgRP gene expression increased in the same age-group without any change in AgRP immunoreactivity in either nucleus. Accordingly, in the 18-month-old group a relative MC dominance over AgRP could explain the observed tendency for weight loss occurring between 18- and 24-month-old rat groups (**Figure 12A**). These especially synchronous age-related changes may represent an adaptive reaction upon reaching a critical BW or adiposity. In the oldest animals the synchronous decline in MC4R and alpha-MSH immunoreactivity characterizing both nuclei with parallel suppression of gene expression in the ARC suggest a coordinated decline in the endogenous activity of the MC system. (AgRP immunoreactivity did not change at this age, while gene expression declined only in the ARC.) These 24-month-old animals appear to react to the previously occurring marked weight loss (leading to sarcopenia, **Figure 9**) with an adaptive counter-regulatory reaction also suggested previously by other authors (Rigamonti et al. 2006).

In summary, our *in vitro* findings revealed potential mechanisms of the age-related in vivo trends in BW regulation in male Wistar rats. In middle-aged rats peptide contents of alpha-MSH and MC4R decreased both in the ARC and PVN (without matching changes in gene expression), while in aging animals the increase in alpha-MSH and MC4R peptide contents were associated with parallel increases in POMC and MC4R mRNA expressions. Although AgRP mRNA expression in both nuclei showed some increase in aging animals, its protein content remained unchanged across all age-groups.

In addition to the MC system, other hypothalamic mediators may also contribute to the explanation of the age-related trends in BW regulation. Orexigenic neuropeptide Y (NPY), the

other major regulator of the ARC has been reported to decline with aging (Kmiec et al. 2013). Thus it may also contribute to aging anorexia, but not to middle-aged obesity. However, to date no detailed analysis involving more than three age-groups has been carried out. Thus, future studies are needed to clarify the role of NPY sufficiently.

Our study is the first to analyze age-related shifts in the endogenous tone of the hypothalamic MC system across five age-groups with parallel analysis of gene expression and immunohistochemistry. Previous studies have usually compared POMC and/or AgRP gene expressions of only a young and an old group (Zhang et al. 2004; Kappeler 2003; Nelson et al. 1988; Arens et al. 2003; Rigamonti et al. 2006), only a few of them included a third (middle-aged) group in the comparison (Gruenewald et al. 1991; Wolden-Hanson et al. 2004; McShane et al. 1999; Lloyd et al. 1991). They showed controversial results: some studies reported an age-related decline (Gruenewald and Matsumoto 1991; Kappeler et al. 2003; Nelson et al. 1988; Arens et al. 2003; Lloyd et al. 1991; Rigamonti et al. 2006), while others found unchanged MC activity in old rodents (McSane et al. 1999; Wolden-Hanson et al. 2004; Zhang et al. 2004). The use of different rat and mouse strains, gender differences or diverse methodologies (RT-PCR, *in situ* hybridization, analysis of the whole hypothalamus or that of the ARC) may explain these contradictory findings. Our experimental setting allowed the detailed follow up of age-related shifts within the hypothalamic MC system that could provide explanation for the long-term changes in BW development and BC.

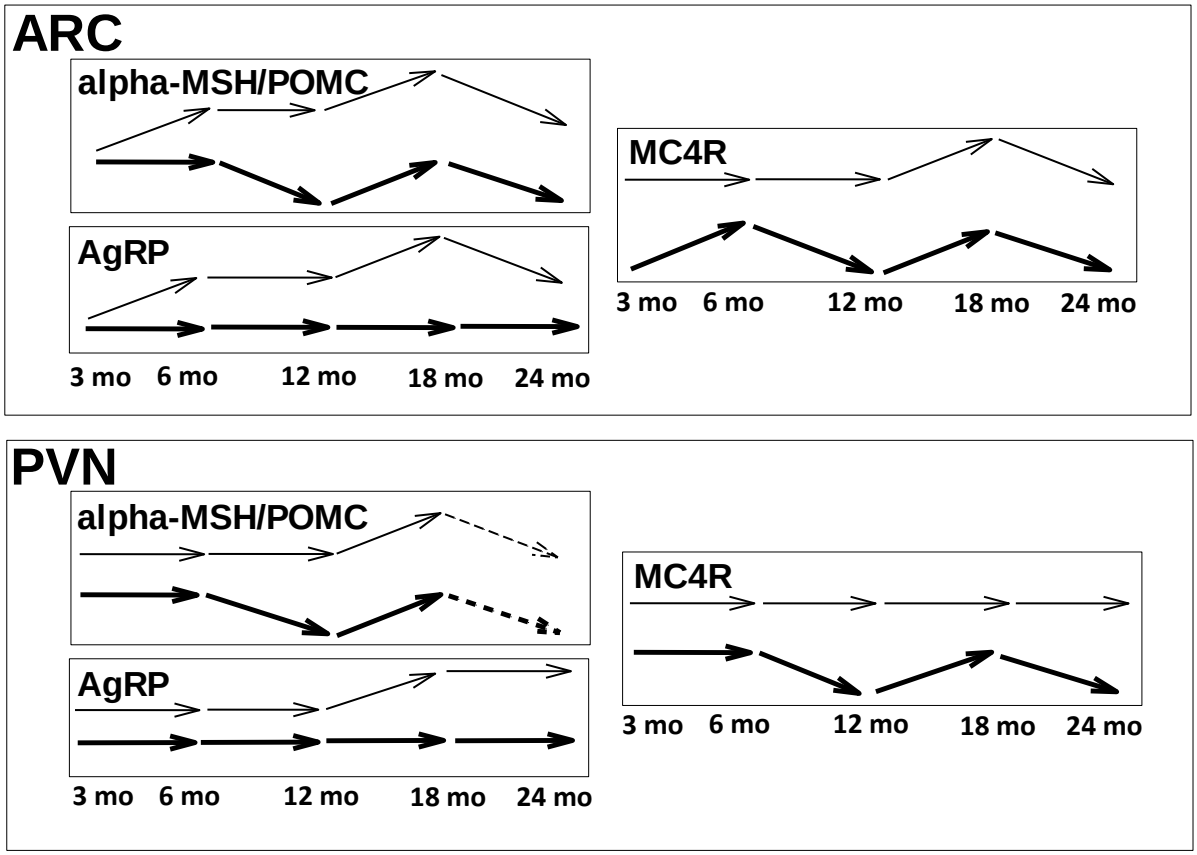

Figure 18: Schematic representation of the directions of age-related changes in relative mRNS expressions of POMC, AgRP and MC4R and in immunosignals of alpha-MSH, AgRP and MC4R in the arcuate (ARC) and paraventricular nuclei (PVN) of the hypothalamus. Thin arrows represent directions of trends in mRNS expression between age groups following one another. Bold arrows demonstrate similar directions of trends in immunosignals. Dashed arrows indicate nonsignificant trends. The age of the animal groups are given in months (mo) under the corresponding boxes.

To the best of our knowledge this study is the first describing an age-related fluctuation of alpha-MSH immunoreactivity both in the ARC and PVN across five age-groups. Our results prove that the alpha-MSH and MC4R peptide immunoreactivity along with the POMC and MC4R mRNA expression are affected by age in a way that may contribute to the explanation of aging anorexia. Moreover, the earlier occurring decline in alpha-MSH and MC4R peptide immunoreactivity may contribute to the explanation of the weight gain and obesity of middle-aged animals. Finally, our results suggest that reaching a critical BW or fat mass may provide the trigger for the activation of the MC system, that in turn aggravates aging anorexia.

Further studies are required to uncover why mRNA and protein expressions of the MC system do not overlap in certain age-groups at certain sites. We predict the existence of age-related changes in the translation efficacy of mRNA or fluctuations in the protein turnover. Other

studies are to be conducted to identify the significance of AgRP mRNA upregulation in aging rats.

5.2. Hypothesis II

5.2.1. Dysregulation in SHR rats

In this study our aim was to analyze the dysregulation of energy homeostasis in SHR rats and to investigate the potential role of major anorexigenic (MC system; *i.e.* alpha-MSH) and orexigenic (NPY and AgRP) peptides in the dysregulation of feeding and body weight of this rat strain. Effects of selective MC system antagonist (HS024) were also tested.

5.2.1.1. Results of *in vivo* and *in vitro* experiments

Concerning resting blood pressure (BP), there was a significant difference between the SHR and NT groups. At age 3 months, average systolic BP of SHR rats was 169 ± 2 mmHg, while the NT rats had normal BP of 121 ± 2 mmHg (n = 20 in both groups, one-way ANOVA, $p < 0.001$).

Our results (obtained in our SHR colony) confirmed earlier observations of the literature (Oliveira et al. 2009). BW development (**Figure 19**) and daily FI values of SHR rats were significantly lower than those of the age-matched NT rats (BW = 360.4 ± 5.3 vs. 483.3 ± 12.5 g; FI = 21.8 ± 0.5 vs. 25.7 ± 0.8 g at 6 months of age, n = 21 vs. 12, respectively, $p < 0.001$ in both cases, one-way ANOVA).

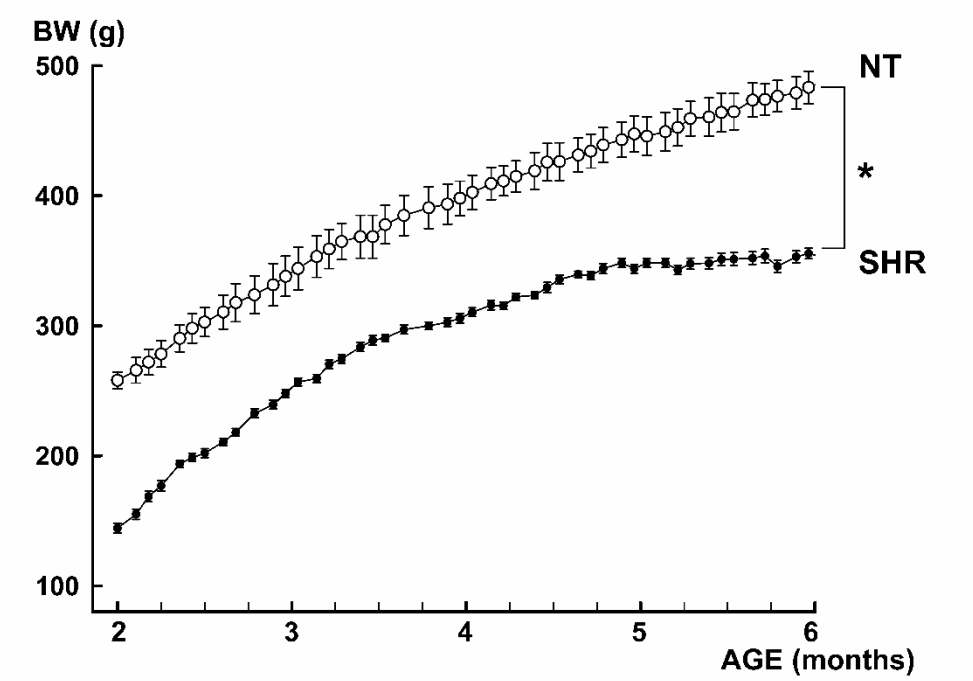

Figure 19: Body weight development of SHR and NT rats from 2 to 6 months of age ($p<0.01$, repeated measures ANOVA)

The ICV alpha-MSH injection reduced the cumulative spontaneous night-time 12-h FI in both groups ($p < 0.001$ in both cases, one-way ANOVA) (**Figure 20/A**). The rate of reduction in the 12-h FI induced by alpha-MSH (given in percentage of the corresponding control value) was significantly stronger in SHR than in NT animals ($p = 0.001$, one-way ANOVA) (**Figure 20/B**).

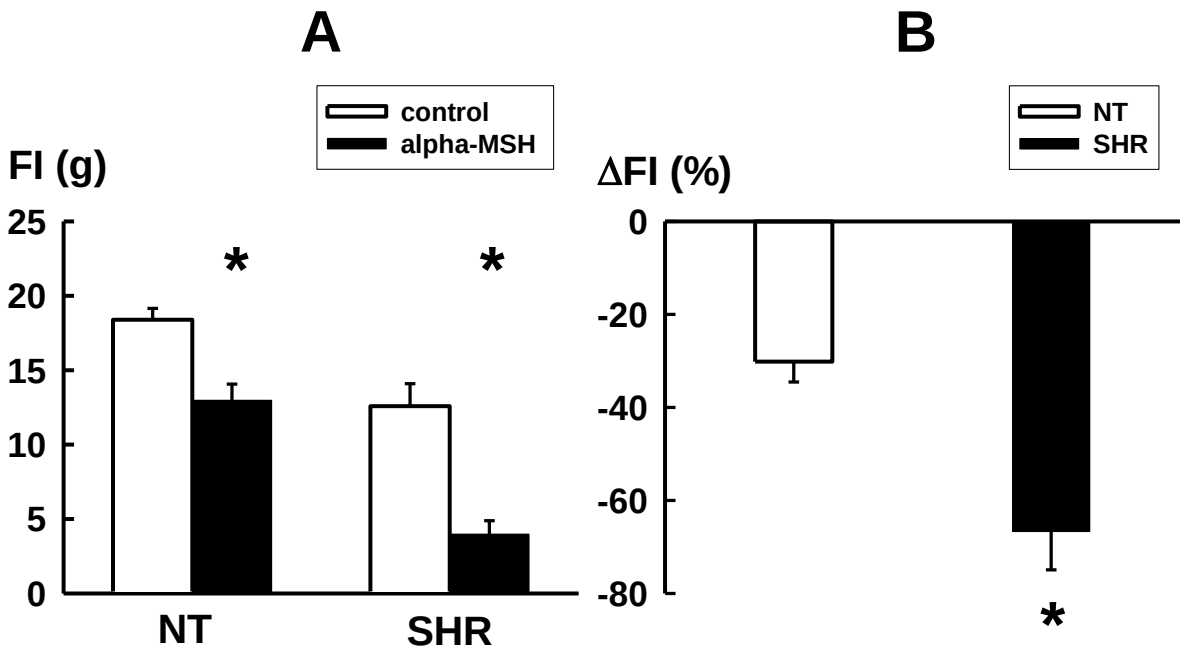

Figure 20: **Panel A**: Effect of an ICV injection of alpha-MSH (alpha-melanocyte-stimulating hormone, 5 μg/5μl) or PFS (pyrogen-free saline, control, 5μl) on spontaneous cumulative night-time (18:00-6:00 h) food intake (FI) in SHR (spontaneously hypertensive rats, n = 6) and in NT (normotensive, n = 8) rats. Asterisks indicate significant differences between treated and control groups. **Panel B**: Rate of inhibition in the cumulative 12-h FI elicited by the alpha-MSH injection (given in percentage of the corresponding control value) in SHR and NT groups. Asterisk indicates significant difference in the rate of suppression between the SHR and NT groups.

The single ICV injection of AgRP significantly increased 24-h FI by the 4th day (NT: from 19.5 ± 0.6 g to 24.4 ± 1.3 g, $p = 0.003$; SHR: from 18.1 ± 0.4 g to 21.4 ± 0.3 g, $p < 0.001$). There was no difference in the rate of increase between SHR vs. NT rats (one-way ANOVA).

The selective MC4R antagonist HS024 increased daily FI in the NT group already from the 2nd day of the ICV infusion, while its orexigenic effect in SHR rats started with a delay, just from the 4th day: the cumulative FI increased significantly during the first 3 days of the infusion in NT rats ($p = 0.049$), but not in the SHR group (**Figure 21/A**). Concerning the whole 7-day duration of the infusion, HS024 was effective and induced significant increase of cumulative 7-day FI in both groups (NT: $p = 0.005$; SHR: $p = 0.02$, **Figure 21/A**, one-way ANOVA).

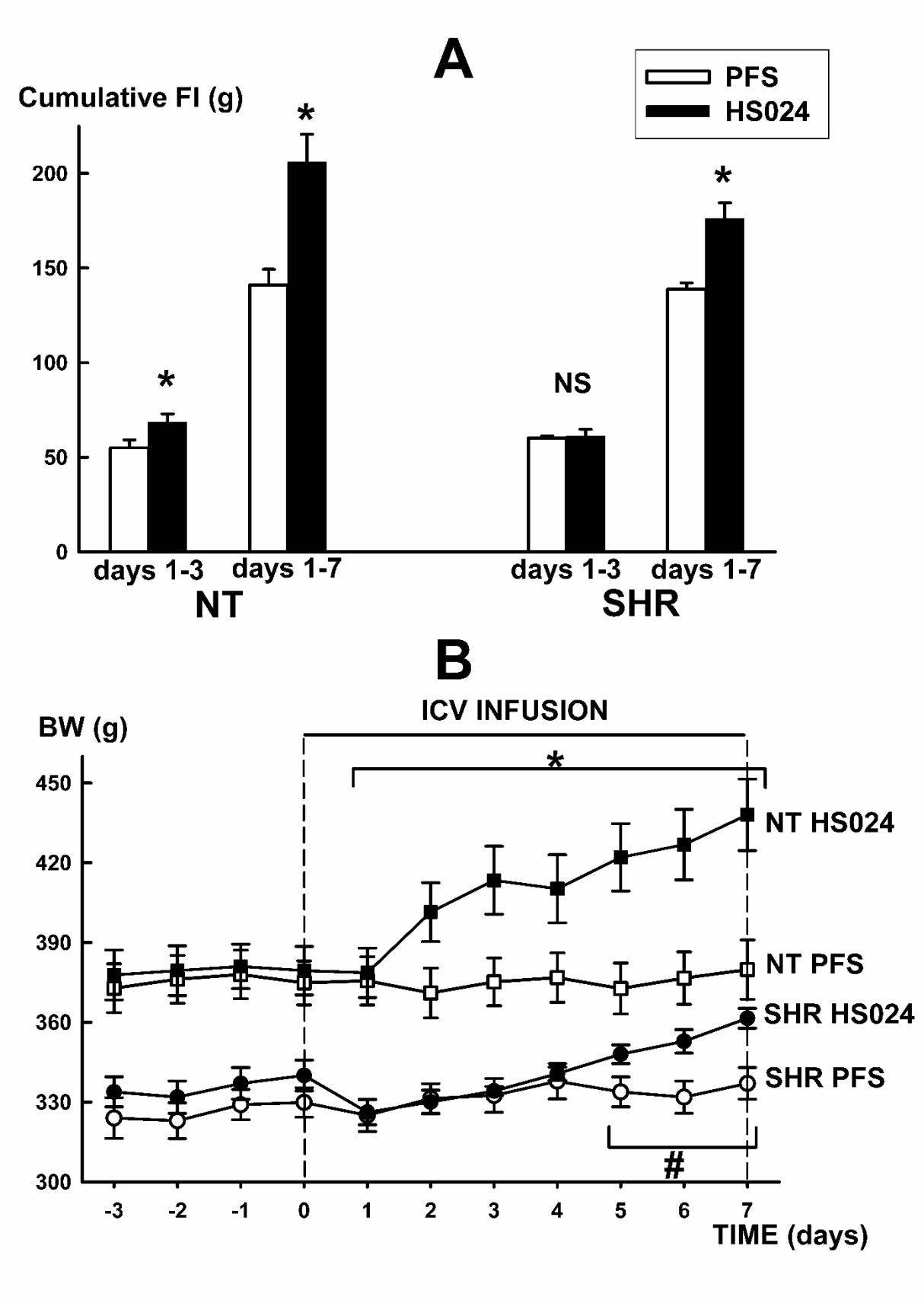

Figure 21: **Panel A**: Effect of intracerebroventricularly applied HS024 (1μg/1μl/1h) - or PFS-infusion (pyrogen-free saline, 1μl/1h) on cumulative food intake (FI) values during the first 3 days and for the first 7 days in SHR (spontaneously hypertensive rats) and in NT (normotensive)

animals (n = 6 in each experimental group). Asterisk indicates significant difference between HS024- and PFS-treated NT animals. NS: non-significant. **Panel B**: Effect of intracerebroventricularly (ICV) applied HS024- or PFS-infusion on body weight (BW) during the 7 days course in SHR and in NT rats. Asterisk indicates significant difference between BW courses of the HS024- vs. PFS-treated NT groups, number sign (#) indicates significant difference between BW courses of the HS024- vs. PFS-treated SHR groups.

As a consequence of increased FI, the BW in both HS024-treated groups also increased but with a different time course. The BW of the NT group started to increase already from the 2nd day of the HS024 infusion [$F(1,10) = 5.977$, $p = 0.04$, repeated-measures ANOVA for days 1-7 of the infusion], but that of SHR animals started to rise only from the 5th day of the infusion [$F(1,10) = 8.227$, $p = 0.017$, repeated-measures ANOVA for days 5-7 of the infusion] (**Figure 21/B**).

With regard to the investigation of NPY-induced responsiveness of SHR, the orexigenic peptide was given in the early phase (9:00 AM) of the inactive day-time period and the 3-h FI induction was registered. An injection of PFS does not induce any FI in the inactive day-time period irrespective of age or BW, therefore it cannot serve as control. Thus, the NPY-induced FI was expressed as % of the corresponding spontaneous cumulative 24-h FI of each group (SHR: 24-h FI = 16.2 ± 1.2 g, BW = 247.3±5.3 g; NT: 24-h FI = 20.9 ± 0.5 g, BW = 338.8±10.4 g). The NPY-induced cumulative 1-, 2- and 3-h FI, in percentage of daily FI, was significantly lower in SHR than in the age-matched NF group ($p < 0.001$, $p = 0.002$ and $p = 0.030$, respectively, one-way ANOVA, **Figure 22**).

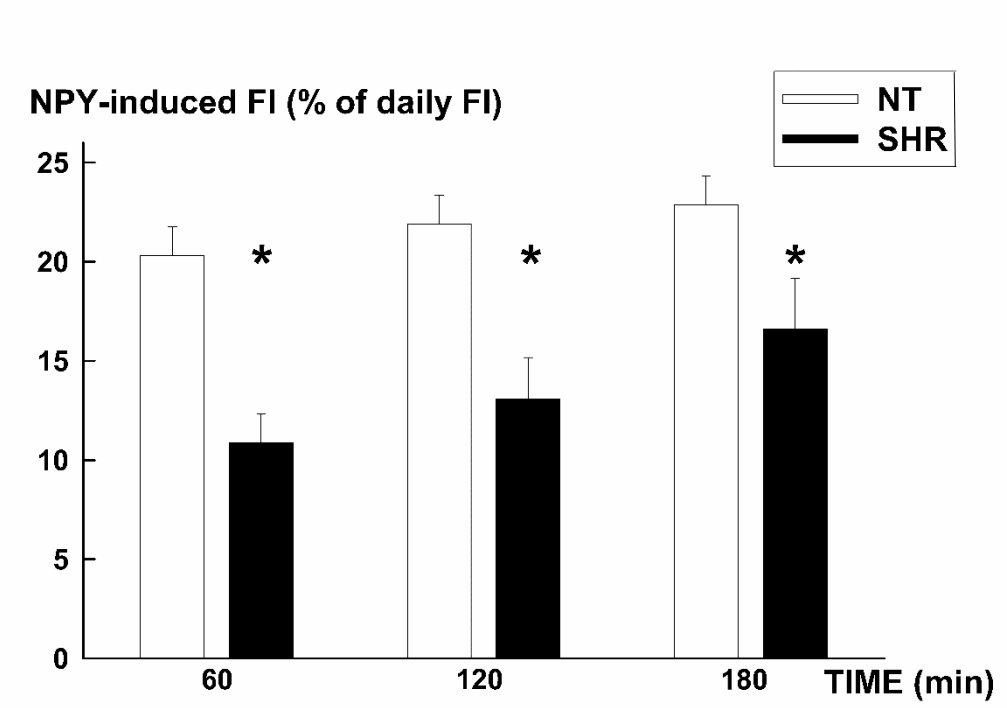

Figure 22: Effect of ICV applied neuropeptide Y (NPY) injection (5 μg/5μl) on the day-time food intake (FI) in the 1st, 2nd and 3rd hour in percentage of daily FI in SHR (spontaneously hypertensive rats, n = 8) and in NT (normotensive, n = 6) rats. Asterisks indicate significant differences between corresponding values of SHR and NT rats.

To further support our functional data, functional-morphological tools were also applied to compare the functioning of alpha-MSH, AgRP and NPY systems in the ARC and PVN of SHR and NT rats. Our immunofluorescent labeling proved the presence of alpha-MSH neurons in the ARC of both NT and SHR rats (**Figure 23**). Cell counting revealed that there is no statistically significant difference between SHR and NT rats in the number alpha-MSH immunoreactive neurons in the ARC **(Figure 23b**). In contrast, assessment of fluorescent light intensity revealed that SHR had 28 % higher alpha-MSH SSD in the ARC then NT rats. This difference proved to statistically significant ($p = 0.006$, Student's t test, **Figure 23a**).

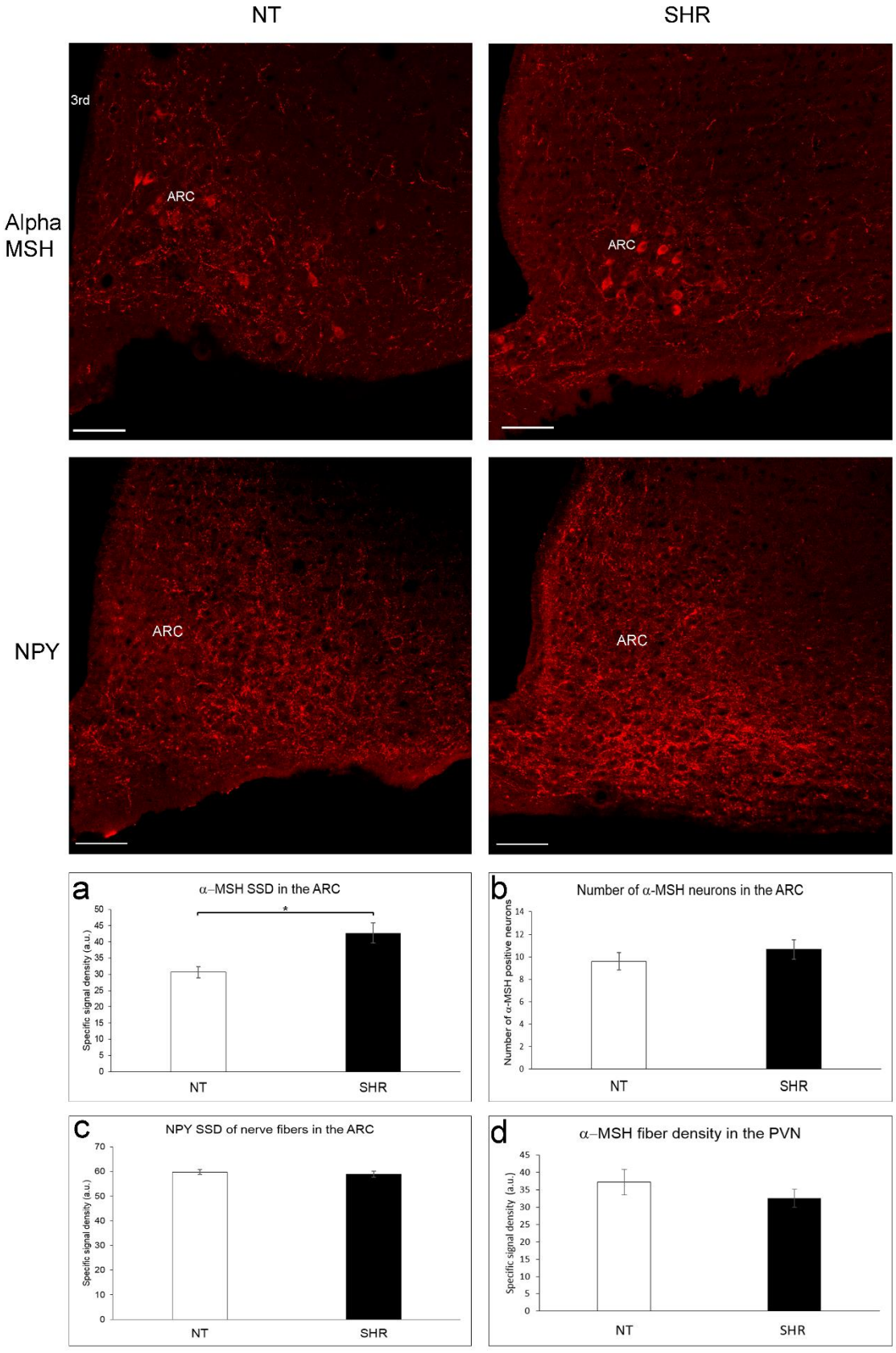
NT
SHR
Alpha MSH
NPY
3rd
ARC
a
α–MSH SSD in the ARC
Specific signal density (a.u.)
b
Number of α-MSH neurons in the ARC
Number of α-MSH positive neurons
c
NPY SSD of nerve fibers in the ARC
d
α–MSH fiber density in the PVN

Figure 23. Representative photos of alpha-MSH (upper images) and NPY (lower images) immunofluorescence in the arcuate nucleus (ARC) of spontaneously hypertensive (SHR, n = 6) and normotensive (NT, n = 6) rats. Images were grayscaled and inverted for publication purposes. **Panel A** shows comparison of cellular alpha-MSH SSD (specific signal strength density) between NT control (open bar) and SHR groups (closed bar) expressed in arbitrary units (a.u.). **Panel A** represents number of alpha-MSH producing cells in NT vs. SHR rats. **Panel C**: comparison of SSD in NPY immunoreactive nerve fibers between SHR and NT rats. **Panel D** represents the comparison of alpha-MSH SSD in the paraventricular nucleus of NT vs. SHR rats. Asterisk in **panel A** represents statistically significant difference. 3rd: third ventricle, bars: 100 μm.

Our immunolabeling with NPY antiserum revealed that there is a dense network of NPY immunoreactive nerve fibers in the ARC both in SHR and NT rats. Our antibody did not mark NPY and AgRP containing perikarya in the ARC. In this experimental setup we could not apply colchicine treatment to enhance immunosignal in cell bodies due to its severe side effects on several physiological aspects including FI and energy homeostasis. Therefore, here we decided to quantify the SSD of NPY nerve fibers and found that there is no significant difference between SHR vs. NT groups in the NPY immunoreactivity in the ARC (**Figure 21c**).

As ARC-derived alpha-MSH, NPY and AgRP immunoreactive nerve fibers innervate the PVN, the density of the respective immunosignals was measured also in the PVN. Although these neuropeptides were seen to provide dense fiber network in the PVN, when NT and SHR rats were compared, no statistical difference was found in the SSD of respective immunosignals in alpha-MSH, NPY and AgRP immunopositive terminals in the PVN (Student's T test: $p > 0.05$, respectively). **Figure 23d** demonstrates alpha-MSH immunoreactive nerve fiber density in the PVN of SHR vs. NT.

Our qRT-PCR measurements revealed that the POMC mRNA content of the ARC in SHR is 18.51-times higher (Student's t test, $p < 0.01$) than that of NT rats (**Figure 24**).

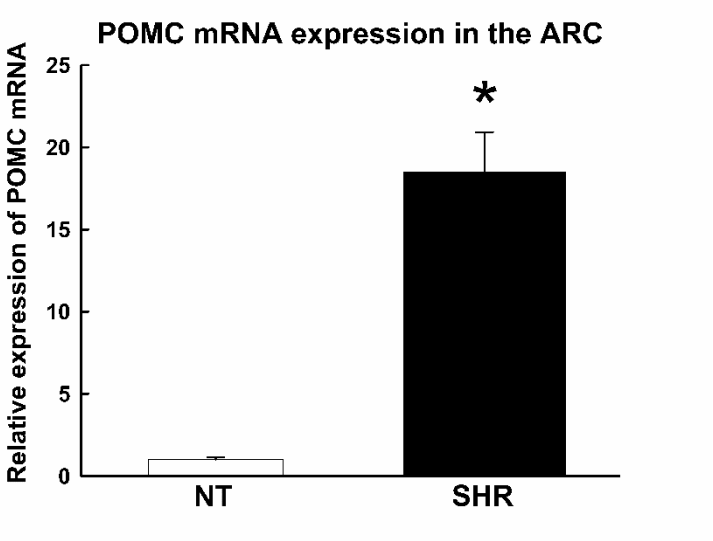

Figure 24: Relative POMC (pro-opiomelanocortin) mRNA expression in Wistar (n = 6) and SHR (n = 5). Data were evaluated by the delta delta Ct method for qRT-PCR analysis. POMC mRNA expression was normalized to the GAPDH expression. Data were presented as fold difference compared to POMC mRNA in Wistar rats with the reference value of 1. Asterisk indicates significant difference.

5.2.1.2. Discussion of *in vivo* and *in vitro* experiments

In the present study we aimed to investigate the dysregulation of energy homeostasis of SHR animals. Previous data showed lower BW and lower caloric intake in this rat strain as compared with NT controls (Woo et al. 1993; Sato et al. 1995; Oliveira et al. 2009). An increased activity of the catabolic neuropeptides, e.g. an enhanced activity of the MC system may be assumed in the background (da Silva et al. 2008) that may be associated with their enhanced sympathetic activity (Judy et al. 1976). Yin and coworkers (1997) detected higher amount of POMC mRNA in the ARC of SHR rats. Autelitano and van den Buuse (1997) also showed that adult SHR animals express POMC mRNA in the neurointermediate lobe of the pituitary at approximately 2-4 times higher level than seen in NT Wistar-Kyoto controls. In contrast, in older 32 weeks old animals Felder and Garland (1989) found significantly reduced POMC biosynthesis in the SHR, that may indicate an inverse correlation between systolic blood pressure and pituitary POMC biosynthesis, because POMC biosynthesis in neurointermediate lobe increased with normalization of blood pressure in the SHR. Based on these observations,

the decreased pituitary POMC biosynthesis in SHR may be a consequence rather than a cause of the elevated blood pressure in SHR. Other observations described disrupted diurnal rhythm of feeding behavior along with altered expression patterns of regulatory peptides in the mediobasal hypothalamus of SHR (Cui et al. 2011): lack of NPY expression peak before the onset of the active dark period (consequently suppressed night-time FI) and lack of day-time rise in POMC expression (consequently somewhat enhanced day-time FI, not sufficient to restore overall daily intake).

Hypothalamic NPY as a major orexigenic peptide has a crucial role in the regulation of energy balance through the induction of FI (Morley et al. 1987). Earlier studies detected increased NPY level and gene expression in the ARC of SHR by 15-20 weeks of age as compared with NT controls (Clark et al. 1991; McLean et al. 1996). In contrast, other observations described a lack of difference in NPY-like immunoreactivity in the hypothalamus of young SHR vs. NT controls (Pavia and Morris 1994) or a decrease in cerebral NPY gene expression (cerebral cortex, midbrain, pons, medulla oblongata) in SHR from 17-20 weeks of age (Higuchi et al. 1993).

Based on these controversial data of the literature, we aimed to investigate the possible role of the MC system and that of NPY in the regulatory disorder of energy balance in SHR.

Our results show that an acute ICV alpha-MSH-injection reduced the FI of SHR rats more efficiently (66.7% reduction instead of 30.1%) than in the NT group. The selective MC4R antagonist, HS024 started to increase FI and consequently BW earlier, already from the 2nd day of the central infusion in the NT group, while in SHR animals the hyperphagia started only from the 4th day. Nevertheless, this antagonist was capable of inducing significant hyperphagia and weight gain in SHR, albeit with a delay reaching somewhat diminished values. Using immunohistochemistry, we found significantly higher alpha-MSH SSD in the ARC of SHR vs. NT rats but there was no significant difference concerning the number of alpha-MSH immunoreactive cells. On the other hand, POMC gene expression in the ARC of SHR was 18-times increased as compared with values of NT animals (as shown by quantitative RT-PCR). These findings suggest an enhanced endogenous alpha-MSH production in SHR. In contrast, we did not find any difference in AgRP immunosignal between NT and SHR rats in this study. Based on our *in vitro* results, we propose that the findings of our *in vivo* experiments may be explained at least in part by increased alpha-MSH action via MC4Rs.

The orexigenic effect of NPY was smaller in SHR rats than in the NT animals. No difference was found concerning NPY immunoreactivity in the ARC of SHR vs. NT groups, either. In the background of the impaired NPY responsiveness but unaltered NPY

immunoreactivity seen in young SHR, one may speculate about altered trafficking or production/release ratio of NPY in the ARC, or about modified receptorial effectivity at the PVN. In older SHR the elevated NPY production of the ARC described by other studies (Clark et al. 1991, McLean et al. 1996) still appeared to be insufficient to normalize BW development. However, this awaits further studies.

Our findings concerning the MC system, however, raise complex questions. In the beginning of our study, we have assumed that an increased melanocortin tone in general would be associated with an increased orexigenic effect of the antagonist. And indeed, in previous observations, concerning the abnormally high blood pressure of SHR, administration of a MC3R/MC4R antagonist (SHU9119) was able to decrease blood pressure efficiently (daSilva et al. 2008), whereas normal blood pressure of control rats of that study was not affected. However, concerning food intake of SHR, the same study using the same MC3R/MC4R antagonist, reported diminished orexigenic effect in SHR, as compared with that of controls. In our present study, the administration of a high dose of a specific MC4R antagonist (HS024) also elicited a significant but delayed orexigenic effect in SHR. As our applied dose of HS024 was 8 times higher than that used by previous studies (Jonsson et al. 2002) and it was also close to the toxic value derived from the literature (Kask et al. 1998), the diminished orexigenic effect can not be explained on the basis of insufficient dose. Moreover it also proved to be efficient (and non-toxic) in the NT group.

As an explanation for this delay of orexigenic action we propose some hypotheses. Our antagonist HS024 was shown to bind to MC4Rs without inducing any effect on intracellular signal transduction and without decreasing the basal activity of the receptor (Sánchez et al. 2009). The delay of the onset of the orexigenic effect may be explained by an increased amount of endogenous alpha-MSH, the suppression of which, requires a higher amount of competitive antagonist delivered by a longer administration.

Regarding the diminished extent of the orexigenic effect of HS024 infusion in SHR, we propose that the orexigenic arm of the complex anorexigenic/orexigenic regulatory balance (as shown by the weaker neuropeptide Y responsiveness in SHR) fails to increase food intake as high as in controls once the long-term melanocortin-induced suppression has finally been removed.

Other potential mechanisms may also have to be taken into consideration. The attenuated HS024 effect could also be due to a decreased release of biologically active alpha-MSH, altered processing of POMC and alpha-MSH *e.g.* due to decreased acetylation of alpha-MSH, or due to an increased release of the melanocortin antagonist AgRP. Regarding the assessment of the

release of biologically active alpha-MSH (from neurons originating from the ARC through nerve fibers innervating the PVN), our results showed that no statistical difference was found in the SSD of respective immunosignals in alpha-MSH immunopositive terminals in the PVN. As perikarya of the alpha-MSH producing neurons in the ARC contain stronger alpha-MSH SSD in SHR vs. control rats, we may assume that the alpha-MSH production is higher. This idea was further supported by our qRT-PCR assessment as POMC expression that was 18-times higher in SHR vs. NT rats.

Concerning the possibility of increased release of AgRP, our results do not support this hypothesis. No statistical difference was found in the SSD of immunosignals in AgRP immunopositive terminals in the PVN, and the orexigenic efficacy of AgRP did not differ in SHR and control rats (in contrast with the orexigenic effects of NPY, which proved to be weaker in SHR).

Based on our results, we propose that the characteristic phenotype of SHR may be partly explained by enhanced responsiveness to the MC agonist and by the diminished orexigenic responsiveness to NPY found in young adult animals. Both our immunohistochemical and qRT-PCR findings provide further support for the role of the enhanced activity of the central MC system in the regulation of energy balance in SHR. Delayed and diminished orexigenic effects of the MC4R antagonist infusion are still compatible with the concept of increased endogenous melanocortin tone, but the underlying mechanisms require further investigations including, among other factors, the development of innervation of second order nuclei in SHR.

6. SUMMARY OF MAIN FINDINGS

The summary and the main finding of my PhD thesis:

Hypothesis I.:

Activity of the MC system shows characteristic age-related pattern: decreased activity of the hypothalamic melanocortin system contributes to the development of middle-aged obesity, but later the MC activity increases leading to anorexia and weight loss in old age.

- Micro-CT-L $_{1\text{-}3}$ is a good and useful method for repeated body fat assessment in rats.
- The skin thickness measurement (STM) is also useful to follow the body fat changes *in vivo* in rats
- The acute catabolic effects of intracerebroventricularly applied alpha-MSH show characteristic age-dependent changes in male Wistar rats: decreased catabolic efficacy of alpha-MSH precedes middle-aged weight gain, and later on an increased efficacy precedes weight loss in old rats. The observed age-related shifts in catabolic alpha-MSH-effects may contribute to the development of middle-aged obesity and later to that of weight loss of old age.
- Our *in vitro* findings revealed potential mechanisms of these age-related *in vivo* trends in BW regulation. In middle-aged rats peptide contents of alpha-MSH and MC4R decreased both in the ARC and PVN (without matching changes in gene expression), while in aging animals the increase in alpha-MSH and MC4R peptide contents were associated with parallel increases in POMC and MC4R mRNA expressions. Although AgRP mRNA expression in both nuclei showed some increase in aging animals, its protein content remained unchanged across all age-groups.

Hypothesis II.:

We assumed, that enhanced activity of hypothalamic anorexigenic melanocortins and diminished tone of orexigenic NPY may contribute to the BW dysregulation of SHR strain.

- Our results suggest that a higher melanocortin-production/responsiveness and lower NPY-responsiveness may contribute to the BW dysregulation of SHR.

7. CONCLUSIONS

The main aim of this PhD program was to investigate the hypothalamic melanocortin system in the regulation of energy homeostasis.

The first main hypothesis of this research program was that the aging-related dynamics of body weight and body composition is underlined by characteristic fluctuation of the hypothalamic melanocortin system: decreased activity of the melanocortins contributes to the development of middle-aged obesity, but later the melanocortin activity increases leading to anorexia and subsequently weight loss in old age.

To support this scientific assumption, we first performed a methodological study — applying methods suitable for long-term *in vivo* monitoring of body composition — in order to demonstrate middle-aged obesity and aging sarcopenia in our Wistar rat model and in order to prove the efficacy of skinfold thickness measurement as well as abdominal computer tomography restricted to the area lumbar 1 to lumbar 3. The comparison with *post mortem* body composition analysis as well as with whole body computer tomography revealed that the skinfold thickness measurement as well as computer tomography restricted to L1-L3 are valid, useful and re-evaluable tools to assess the dynamics of body composition in the course of aging.

In the second step, to investigate the age dependency in the melanocortin system, catabolic responsiveness of five age-groups of Wistar rats to central alpha-MSH administration were compared. Supporting our hypothesis, here we found that the magnitude of alpha-MSH-induced reduction in food intake and increase in metabolic rate (indicated by oxygen consumption) was the lowest in middle-aged 12-months old rats, while the peptide exerted a higher efficacy in young and again in old age.

When the endogenous melanocortin system was studied in the same age-groups, the semi-quantitative assessment of MC4R and POMC mRNA as well as MC4R protein and alpha-MSH peptide content of the ARC and PVN revealed that there is indeed a characteristic age-dependent dynamics in these variables contributing to the weight gain and obesity in middle-aged rats and to the anorexia in old animals.

The second main hypothesis of this research program was that the absence of middle-aged obesity of spontaneously hypertensive rats may be related to an increased hypothalamic melanocortin activity which is concomitant with reduced NPY expression in the hypothalamus.

Our results revealed that spontaneously hypertensive rats were more sensitive to the anorexigenic effect of centrally administered alpha-MSH. When the MC4R antagonist was tested, although the efficacy was maintained in spontaneously hypertensive rats, the effect was delayed and blunted in its magnitude. In line with this, POMC/alpha-MSH mRNA/peptide expression was increased in spontaneously hypertensive rats. Though, the orexigenic efficacy of central NPY treatment was found to be lower in spontaneously hypertensive rats, we did not see altered peptide expression in the hypothalamus. Nevertheless, based on these results one cannot exclude altered NPY trafficking, release and/or changes at the level of NPY receptorial action and signal transduction.

In summary, this PhD program fulfilled the aims to show that age-dependent alterations in the sensitivity and activity of hypothalamic melanocortin system contribute to the dynamics of body weight and body composition in the course of aging. The spontaneously hypertensive rat model further supported the hypothesis that the hypothalamic melanocortin system substantially contributes to the body weight control. However, several questions remained to be answered, our studies increased the methodological repertoire also to perform follow-up studies in rats in order to understand how the ageing-related fluctuation in body weight occurs. Our findings may also have great translational significance taking the deep impact of increased body weight and altered body composition in human health and disease in consideration. Our results presented in this PhD thesis add to our knowledge in the central regulation of body weight and body composition. Deeper understanding of the hypothalamic control of energy homeostasis may ultimately help to identify new therapeutic strategies in the fight against obesity in middle-age and anorexia in senescence.

8. ACKNOWLEDGEMENT

All the work presented in this thesis could not have been carried out without the enormous help from numerous people, to whom I owe a great debt of gratitude. First of all I would like to thank my supervisors *Dr. Erika Pétervári* and Dr. *Balázs Gaszner* for their support, guidance and help in summarizing my thesis. Special thanks must be paid to Dr. *Márta Balaskó* and Prof. *Miklós Székely*. I would like to thank the possibility to perform the qRT-PCR measurements for Prof. *Judit Pongrácz*, and the help of *Diána Feller*. I am also thankful for Prof. *Zsuzsanna Helyes* for the blood pressure measurements and the help during the CT analyses. I also thank the help of *dr. Éva Tékus* to perform the body composition measurements. I thank the assistants of the Research Group for the Regulation Energy Homeostasis and Experimental Gerontology of the Institute for Translational Medicine and I am very thankful to *Izabella Orbán* for her technical support during my work. Special thanks must be paid to my *friends* and my *family* for supporting and encouraging me through all these years.

Financial supports:

GINOP-2.3.2-15-2016-00050 "PEPSYS",

EFOP-3.6.2-16-2017-00008 „The role of neuro-inflammation in neurodegeneration: from molecules to clinics"

9. ABBREVIATIONS

a.u.: arbitrary unit

A: anterior

ACTH: adrenocorticotrop- hormone

AgRP: agouti-related peptide

alpha-MSH: alpha-melanocyte stimulating hormone

ARC: arcuate nucleus

BBB: blood-brain barrier

BNST: bed nucleus of stria terminalis

BC: body composition

BP: blood pressure

BW: body weight

cAMP: cyclic adenosine monophosphate

CART: calcitonin gene-related peptide

CART: cocaine- and amphetamine-regulated transcript

CLIP: corticotropin-like intermediate-lobe proteine

CNS: central nervous system

DMH: dorsomedial hypothalamus

DMN: dorsal motor nucleus

EP: endogen pyrogen

FI: food intake

GABA: gamma-aminobutyric acid

GAPDH: glyceraldehyde 3-phosphate dehydrogenase

GFP: green fluorescent protein

GPCR: G-protein coupled receptor

g: gramm

HL: heat loss

HLI: heat loss index

HR: heart rate

IP: intraperitoneal

L: lateral

LEPR: leptin receptor

LH: lateral hypothalamic area

LPB: lateral parabrachial nucleus

m.: *musculus*

MAP: mean arterial pressure

MC: melanocortin

MCR: melanocortin receptor

microCT: micro-computed tomography

MR: metabolic rat

NDS: normal donkey serum

NPY: neuropeptide Y

NT: normotensive

NTS: *nucleus tractus solitarii*

O2i: oxygen fraction

OXR: orexin receptor

PACAP: pituitary adenylate cyclase-activating polypeptide

PAG: periaqueductal gray

PBS: phosphate-buffered saline

PC1/2: proteinase prohormone convertase 1/2 .

PFS: pyrogen-free saline

PMA: *post mortem* body composition analysis

POMC/pomc: pro-opimelanocortin

PVN/PVH: paraventricular nucleus

PYY: peptide YY

RT: room temperature

SD: standard deviation

SEM: standard error of mean

SHR: spontaneously hypertensive rat

SNS: sympathetic nervous system

SSD: specific signal density

STM: skinfold thickness-based method

STPD: standard temperature and pressure

Ta: ambient temperature

Tc: core temperature

Tc: core temperature

Ts: tail skin temperature

V: ventral

Vi: mass of air at chamber input/min

VMH: ventromedial hypothalamus

Vo: mass of air at chamber output/min

VO2: oxygen consumption

WKY: Wistar-Kyoto rat

Y1 R: neuropeptide Y 1 receptor

10. REFERENCES

Adan RA, Tiesjema B, Hillebrand JJ, la Fleur SE, Kas MJ, de Krom M. The MC4 receptor and control of appetite. *Br J Pharmacol*. 2006;149(7):815-27.

Akimoto S, Miyasaka K. Age-associated changes of appetite-regulating peptides. *Geriatr Gerontol Int.* 2010;Suppl 1:S107-19.

Akimoto-Takano S, Sakurai C, Kanai S, Hosoya H, Ohta M, Miyasaka K. Differences in the appetite-stimulating effect of orexin, neuropeptide Y and ghrelin among young, adult and old rats. *Neuroendocrinology*. 2005;82(5-6):256-263.

An JJ, Rhee Y, Kim SH, Kim DM, Han DH, Hwang JH, Jin YJ, Cha BS, Baik JH, Lee WT, Lim SK. Peripheral effect of alpha-melanocyte-stimulating hormone on fatty acid oxidation in skeletal muscle. *J. Biol. Chem*. 2007;282(5):2862-2870.

Aponte Y, Atasoy D, Sternson SM. AGRP neurons are sufficient to orchestrate feeding behavior rapidly and without training. *Nat Neurosci.* 2011;14(3):351-355.

Arens J, Moar KM, Eiden S et al. Age-dependent hypothalamic expression of neuropeptides in wild-type and melanocortin-4 receptor-deficient mice. *Physiol Genomics.* 2003;16(1):38-46.

Arime Y, Kubo Y, Sora I. Animal models of attention-deficit/hyperactivity disorder. *Biol Pharm Bull.* 2011;34(9):1373-6.

Autelitano DJ, van den Buuse M. Concomitant up-regulation of proopiomelanocortin and dopamine D2-receptor gene expression in the pituitary intermediate lobe of the spontaneously hypertensive rat. *J Neuroendocrinol.* 1997;9:255–262.

Bagnol D, Lu XY, Kaelin CB, Day HE, Ollmann M, Gantz I, Akil H, Barsh GS, Watson SJ. Anatomy of an endogenous antagonist: relationship between Agouti-related protein and proopiomelanocortin in brain. *J Neurosci.* 1999;19(18):RC26.

Balaskó M, Garami A, Soós S, Koncsecskó-Gáspár M, Székely M, Pétervári E. Central alpha-MSH, energy balance, thermal balance, and antipyresis. *J Therm Biol.* 2010;35: 211-217.

Balaskó M, Rostás I, Füredi N, Mikó A, Tenk J, Cseplő P, Koncsecskó-Gáspár M, Soós Sz, Székely M, Pétervári E. Age and nutritional state influence the effects of cholecystokinin on energy balance. *Exp Gerontol*. 2013;48(11):1180-1188.

Balaskó M, Soós S, Székely M, Pétervári E. Leptin and aging: Review and questions with particular emphasis on its role in the central regulation of energy balance. *J Chem Neuroanat*. 2014;61-62:248-255.

Baltatzi M, Hatzitolios A, Tziomalos K, Iliadis F, Zamboulis Ch. Neuropeptide Y and alpha-melanocyte-stimulating hormone: interaction in obesity and possible role in the development of hypertension. *Int J Clin Pract*. 2008;62(9):1432-1440.

Balthasar N, Dalgaard LT, Lee CE, Yu J, Funahashi H, Williams T, Ferreira M, Tang V, McGovern RA, Kenny CD, Christiansen LM, Edelstein E, Choi B, Boss O, Aschkenasi C,

Zhang CY, Mountjoy K, Kishi T, Elmquist JK, Lowell BB. Divergence of melanocortin pathways in the control of food intake and energy expenditure. *Cell*. 2005;123(3):493-505.

Ballyuzek MF, Mashkova MV, Stepanov BP. [CACHEXIA AS A COMPLEX METABOLIC SYNDROME AND OTHER CAUSES OF WEIGHT LOSS IN ELDERLY]. *Adv Gerontol*. 2015;28(2):344-353.

Baranowska B, Bik W, Baranowska-Bik A, Wolinska-Witort E, Szybinska A, Martynska L, Chmielowska M. Neuroendocrine control of metabolic homeostasis in Polish centenarians. *J Physiol Pharmacol*. 2006;57 Suppl 6:55-61.

Barsh GS, Schwartz MW. Genetic approaches to studying energy balance: perception and integration. *Nat Rev Genet*. 2002;3(8):589-600.

Bartlett JW, Frost C. Reliability, repeatability and reproducibility: Analysis of measurement errors in continuous variables. *Ultrasound Obstet Gynecol*. 2008;31:466–475.

Barzel B, Lim K, Davern PJ, Burke SL, Armitage JA, Head GA. Central proopiomelanocortin but not neuropeptide Y mediates sympathoexcitation and hypertension in fat fed conscious rabbits. *J Hypertens*. 2016;34(3):464-473.

Benjannet S, Rondeau N, Day R, Chrétien M, Seidah NG. PC1 and PC2 are proprotein convertases capable of cleaving proopiomelanocortin at distinct pairs of basic residues. *Proc Natl Acad Sci U S A.* 1991;88(9):3564-3568.

Bertagna X. Proopiomelanocortin-derived peptides. *Endocrinol Metab Clin North Am*. 1994;23(3):467-485. Review.

Betley JN, Cao ZF, Ritola KD, Sternson SM. Parallel, redundant circuit organization for homeostatic control of feeding behavior. *Cell.* 2013;155(6):1337-1350.

Bhardwaj RS, Schwarz A, Becher E, Mahnke K, Aragane Y, Schwarz T, Luger TA. Pro-opiomelanocortin-derived peptides induce IL-10 production in human monocytes 1. *Journal of Immunology*. 1996;156(7):2517–2521.

Blackwell BN, Bucci TJ, Hart RW, Turturro A. Longevity, body weight, and neoplasia in ad libitum-fed and diet-restricted C57BL6 mice fed NIH-31 open formula diet. *Toxicol Pathol*. 1995;23(5):570-582.

Blanton CA, Horwitz BA, Blevins JE, Hamilton JS, Hernandez EJ, McDonald RB. Reduced feeding response to neuropeptide Y in senescent Fischer 344 rats. *Am J Physiol Regul Integr Comp Physiol*. 2001;280(4):R1052-R1060.

Blondet A, Doghman M, Rached M, Durand P, Bégeot M, Naville D. Characterization of cell lines stably expressing human normal or mutated EGFP-tagged MC4R. *J of Biochem*. 2004;135(4):541–546.

Bodo M, Thuróczy G, Pánczél G, Sipos K, Iliás L, Szonyi P, Bodó M Jr, Nebella T, Bányász A, Nagy Z. Prevalence of stroke/cardiovascular risk factors in rural Hungary--a cross-sectional descriptive study. *Ideggyogy Sz*. 2008;61(3-4):87-96.

Boston BA, Cone RD. Characterization of melanocortin receptor subtype expression in murine adipose tissues and in the 3T3-L1 cell line. *Endocrinology.* 1996;137:2043–2050.

Boston BA. The role of melanocortins in adipocyte function. *Ann NY Acad Sci.* 1999;885:75–84.

Botelho M, Cavadas C. Neuropeptide Y: An Anti-Aging Player? *Trends Neuro*sci. 2015;38(11):701-711.

Brock PM, Hall AJ, Goodman SJ, Cruz M, Acevedo-Whitehouse K. Immune Activity, Body Condition and Human-Associated Environmental Impacts in a Wild Marine Mammal. *PLoS One* 2013;8(6):e67132.

Bronstein DM, Schafer MK, Watson SJ, Akil H. Evidence that beta-endorphin is synthesized in cells in the nucleus tractus solitarius: detection of POMC mRNA. *Brain Res.* 1992;587(2):269-275.

Bruijnzeel AW. Neuropeptide systems and new treatments for nicotine addiction. *Psychopharmacology (Berl).* 2017;234(9-10):1419-1437.

Brzoska T, Luger TA, Maaser C, Abels C, Böhm M. Alpha-melanocyte-stimulating hormone and related tripeptides: biochemistry, antiinflammatory and protective effects in vitro and in vivo, and future perspectives for the treatment of immune-mediated inflammatory diseases. *Endocr Rev.* 2008;29(5):581-602.

Buggy JJ. Binding of alpha-melanocyte-stimulating hormone to its G-protein-coupled receptor on B-lymphocytes activates the Jak/STAT pathway. *Biochem J.* 1998; 331(Pt 1):211–216.

Butler AA, Kesterson RA, Khong K, Cullen MJ, Pelleymounter MA, Dekoning J, Baetscher M, Cone RD. A unique metabolic syndrome causes obesity in the melanocortin-3 receptor-deficient mouse. *Endocrinology* 2000; 141:3518–3521.

Butler AA. The melanocortin system and energy balance. *Peptides.* 2006;27(2):281-290.

Cameron AJ, Welborn TA, Zimmet PZ, Dunstan DW, Owen N, Salmon J, Dalton M, Jolley D, Shaw JE. Overweight and obesity in Australia: the 1999-2000 Australian Diabetes, Obesity and Lifestyle Study (AusDiab). *Med J Aust.* 2003;178:427–432.

Caroprese M, Albenzio M, Muscio A, Sevi A. Relationship between welfare and udder health indicators in dairy ewes. *Vet Res Commun.* 2006;30:83–94.

Caruso C, Lio D, Cavallone L, Franceschi C. Aging, longevity, inflammation, and cancer. *Ann N Y Acad Sci*. 2004;1028:1-13. Review

Castro MG, Morrison E. Post-translational processing of proopiomelanocortin in the pituitary and in the brain. *Crit Rev Neurobiol*. 1997;11(1):35–57.

Catania A, Airaghi L, Colombo G, Lipton JM. Alpha-melanocyte-stimulating hormone in normal human physiology and disease states. *Trends Endocrinol Metab.* 2000;11(8):304-308. Review.

Catania A, Gatti S, Colombo G, Lipton JM. Targeting melanocortin receptors as a novel strategy to control inflammation. *Pharmacol Rev.* 2004;56:1–29.

Catania A, Lonati C, Sordi A, Carlin A, Leonardi P, Gatti S. The melanocortin system in control of inflammation. *Sci World J.* 2010;10:1840–1853.

Chai BX, Neubig RR, Millhauser GL, Thompson DA, Jackson PJ, Barsh GS, Dickinson CJ, Li JY, Lai YM, Gantz I. Inverse agonist activity of agouti and agouti-related protein. Peptides. 2003;24(4):603-609.

Chapman IM, MacIntosh CG, Morley JE, Horowitz M: The anorexia of ageing. *Biogerontology* 2002;3:67–71.

Chen W, Kelly MA, Opitz-Araya X, Thomas RE, Low MJ, Cone RD. Exocrine gland dysfunction in MC5-R-deficient mice: evidence for coordinated regulation of exocrine gland function by melanocortin peptides. *Cell*. 1997;91(6):789–798.

Chen YY, Pelletier G. Demonstration of contacts between proopiomelanocortin neurons in the rat hypothalamus. *Neurosci Lett.* 1983;43:271-276.

Cho KJ, Shim JH, Cho MC, Choe YK, Hong JT, Moon DC, Kim JW, Yoon DY. Signaling pathways implicated in alphamelanocyte stimulating hormone-induced lipolysis in 3T3-L1 adipocytes. *J Cell Biochem*. 2005;96:869–878.

Chretien M, Mbikay M. 60 YEARS OF POMC: From the prohormone theory to proopiomelanocortin and to proprotein convertases (PCSK1 to PCSK9). *J Mol Endocrinol.* 2016;56(4):T49-T62.

Chung TT, Webb TR, Chan LF, Cooray SN, Metherell LA, King PJ, Chapple JP, Clark AJ. The majority of adrenocorticotropin receptor (melanocortin 2 receptor) mutations found in familial glucocorticoid deficiency type 1 lead to defective traf- ficking of the receptor to the cell surface. *J Clin Endocrinol Metab*. 2008;93:4948–4954.

Civelli O, Birnberg N, Herbert E. Detection and quantitation of pro-opiomelanocortin mRNA in pituitary and brain tissue from different species. *J of Biol Chem*. 1982; 257:6783– 6787.

Clark AJ, Weber A. Adrenocorticotropin insensitivity syndromes. *Endocr Rev*. 1998;19:828–843.

Clark JT, Sahu A, Mrotek JJ, Kalra SP. Sexual function and neuropeptide Y levels in selected brain regions in male spontaneously hypertensive rats. *Am J Physiol* 1991;261:R1234–R1241.

Cone RD. Studies on the physiological functions of the melanocortin system. *Endocr*. 2006(7):736-749. Review

Cowley MA, Cone R, Enriori P, Louiselle I, Williams SM, Evans AE. Electrophysiological actions of peripheral hormones on melanocortin neurons. *Ann N Y Acad Sci*. 2003;994:175-186.

Crine P, Gossard F, Seidah NG, Blanchette L, Lis M, Chretien M. Concomitant synthesis of betaendorphin and alpha-melanotropin from two forms of pro-opiomelanocortin in the rat pars intermedia. *Proc Natl Acad Sci U S A.* 1979;76:5085–5089.

Crnkovic S, Egemnazarov B, Jain P, Seay U, Gattinger N, Marsh LM, Bálint Z, Kovacs G, Ghanim B, Klepetko W, Schermuly RT, Weissmann N, Olschewski A, Kwapiszewska G. NPY/Y_1 receptor-mediated vasoconstrictory and proliferative effects in pulmonary hypertension. *Br J Pharmacol*. 2014;171(16):3895-3907.

Cui H, Kohsaka A,Waki H, Bhuiyan ME, Gouraud SS, Maeda M. Metabolic cycles are linked to the cardiovascular diurnal rhythm in rats with essential hypertension. *PLoS One* 2011;6:e17339.

Da Silva AA, do Carmo JM, Kanyicska B, Dubinion J, Brandon E, Hall JE. Endogenous melanocortin system activity contributes to the elevated arterial pressure in spontaneously hypertensive rats. Hypertension. 2008;51:884–890.

DeBoer MD, Marks DL. Therapy insight: Use of melanocortin antagonists in the treatment of cachexia in chronic disease. *Nat Clin Pract Endocrinol Meta*b. 2006;2(8):459-466. Review.

Dhungel S, Sinha R, Sinha M, Paudel BH, Bhattacharya N, Mandal MB. High fat diet induces obesity in British Angora Rabbit: A model for experimental obesity. *Indian J Physiol Pharmacol* 2009;53:55–60.

Di Francesco V, Zamboni M, Dioli A, Zoico E, Mazzali G, Omizzolo F, Bissoli L, Solerte SB, Benini L, Bosello O: Delayed postprandial gastric emptying and impaired gallbladder contraction together with elevated cholecystokinin and peptide YY serum levels sustain satiety and inhibit hunger in healthy elderly persons. *J. Gerontol. A Biol. Sci. Med. Sci*. 2005;60(12): 1581–1585.

do Carmo JM, da Silva AA, Rushing JS, Pace B, Hall JE. Differential control of metabolic and cardiovascular functions by melanocortin-4 receptors in proopiomelanocortin neurons. *Am J Physiol Regul Integr Comp Physiol*. 2013;305:R359–R368.

Dolinsky VW, Morton JS, Oka T, Robillard-Frayne I, Bagdan M, Lopaschuk GD, Des Rosiers C, Walsh K, Davidge ST, Dyck JR. Calorie restriction prevents hypertension and cardiac hypertrophy in the Spontaneously Hypertensive Rat. *Hypertension* 2010;56:412–421.

Dores RM, Baron AJ. Evolution of POMC: origin, phylogeny, posttranslational processing, and the melanocortins. *Ann N Y Acad Sci*. 2011;1220:34-48.

Dubé D, Lissitzky JC, Leclerc R, Pelletier G. Localization of alpha-melanocyte-stimulating hormone in rat brain and pituitary. *Endocrinology.* 1978;102(4):1283-1291.

Dunbar JC, Lu H. Leptin-induced increase in sympathetic nervous and cardiovascular tone is mediated by proopiomelanocortin (POMC) products. *Brain Res Bull*. 1999;50(3):215-221.

Ellacott KL, Cone RD. The central melanocortin system and the integration of short- and long-term regulators of energy homeostasis. *Recent Prog Horm Res*. 2004;59:395-408. Review.

Enriori PJ, Chen W, Garcia-Rudaz MC, Grayson BE, Evans AE, Comstock SM, Gebhardt U, Müller HL, Reinehr T, Henry BA, Brown RD, Bruce CR, Simonds SE, Litwak SA, McGee SL, Luquet S, Martinez S, Jastroch M, Tschöp MH, Watt MJ, Clarke IJ, Roth CL, Grove KL, Cowley MA. α-Melanocyte stimulating hormone promotes muscle glucose uptake via melanocortin 5 receptors. *Mol Metab*. 2016;5(10):807-822.

Escobar CM, Krajewski SJ, Sandoval-Guzma´n T, Voytko ML & Rance NE. Neuropeptide Y expression is increased in the hypothalamus of older women. *The J of Clin Endocrinol and Metab.* 2004;89(5):2338–2343.

Eskay RL, Giraud P, Oliver C, Brown-Stein MJ. Distribution of α-melanocyte-stimulating hormone in the rat brain: evidence that α-MSH-containing cells in the arcuate region send projections to extrahypothalamic areas. *Brain Res.* 1979;178:55-67.

FanW, Voss-Andreae A, CaoWH, Morrison SF. Regulation of thermogenesis by the central melanocortin system. *Peptides* 2005;10:1800–1813.

Farooqi IS, Keogh JM, Yeo GS, Lank EJ, Cheetham T, O'Rahilly S. Clinical spectrum of obesity and mutations in the melanocortin 4 receptor gene. *N Engl J Med.* 2003;348(12):1085-1095.

Felder RA,Garland DS. POMC biosynthesis in the intermediate lobe of the spontaneously hypertensive rat. *Am J Hypertens*. 1989;2:618–624.

Feng N, Young SF, Aguilera G, Puricelli E, Adler-Wailes DC, Sebring NG, Yanovski JA. Co-occurrence of two partially inactivating polymorphisms of MC3R is associated with pediatric-onset obesity. *Diabetes* 2005;54:2663–2667.

Fong TM, Mao C, MacNeil T, Kalyani R, Smith T, Weinberg D, Tota MR, Van der Ploeg LH. ART (protein product of agouti-related transcript) as an antagonist of MC-3 and MC-4 receptors. *Biochem Biophys Res Commun*. 1997;237(3):629-631.

Fuxe K, Agnati LF, Härfstrand A, Zoli M, von Euler G, Grimaldi R, Merlo Pich E, Bjelke B, Eneroth P, Benfenati F, et al. On the role of neuropeptide Y in information handling in the central nervous system in normal and physiopathological states. Focus on volume transmission and neuropeptide Y/alpha 2 receptor interactions. *Ann N Y Acad Sci*. 1990;579:28-67. Review.

Fuxe K, von Euler G, van der Ploeg I, Fredholm BB, Agnati LF. Pertussis toxin treatment counteracts the cardiovascular effects of neuropeptide Y and clonidine in the awake unrestrained rat. *Neurosci Lett.* 1989;101:337–341.

Fuzesi T, Wittmann G, Liposits Z, Lechan RM, Fekete C. Contribution of noradrenergic and adrenergic cell groups of the brainstem and agouti-related protein-synthesizing neurons of the arcuate nucleus to neuropeptide-y innervation of corticotropinreleasing hormone neurons in hypothalamicparaventricular nucleus of the rat. *Endocrinology*. 2007;148:5442–5450.

Füredi N, Nagy Á, Mikó A, Berta G, Kozicz T, Pétervári E, Balaskó M, Gaszner B. Melanocortin 4 receptor ligands modulate energy homeostasis through urocortin 1 neurons of the centrally projecting Edinger-Westphal nucleus. *Neuropharmacology.* 2017;118:26-37.

Gantz I, Konda Y, Tashiro T, Shimoto Y, Miwa H, Munzert G, Watson SJ, DelValle J, Yamada T. Molecular cloning of a novel melanocortin receptor. *J Biol Chem*. 1993;268(11):8246-8250.

Gantz I. Fong TM. The melanocortin system. *Am J Physiol Endocrinol Metab*. 2003;284(3):E468-E474. Review.

Garfield AS, Lam DD, Marston OJ, Przydzial MJ, Heisler LK. Role of central melanocortin pathways in energy homeostasis. *Trends Endocrinol Metab*. 2009;20(5):203-215.

Garfield AS, Li C, Madara JC, Shah BP, Webber E, Steger JS, Campbell JN, Gavrilova O, Lee CE, Olson DP, Elmquist JK, Tannous BA, Krashes MJ, Lowell BB. A neural basis for melanocortin-4 receptor-regulated appetite. *Nat Neurosci.* 2015;18(6):863-871.

Gaszner B, Van Wijk DC, Korosi A, Józsa R, Roubos EW, Kozicz T. Diurnal expression of period 2 and urocortin 1 in neurones of the non-preganglionic Edinger-Westphal nucleus in the rat. *Stress.* 2009;12(2):115-124.

Gautron L, Lee C, Funahashi H, Friedman J, Lee S, Elmquist J. Melanocortin-4 receptor expression in a vago-vagal circuitry involved in postprandial functions. *J Comp Neurol*. 2010;518(1):6-24.

Gelez H, Poirier S, Facchinetti P, Allers KA, Wayman C, Bernabé J, Alexandre L, Giuliano F. Neuroanatomical distribution of the melanocortin-4 receptors in male and female rodent brain. *J Chem Neuroanat.* 2010;40(4):310-324.

Getting, SJ, Perretti M. MC3-R as a novel target for antiinflammatory therapy. *Drug News Perspect*. 2000(1):19–27.

Giuliani D, Neri L, Canalini F, Calevro A, Ottani A, Vandini E, Sena P, Zaffe D, Guarini S. NDP-α-MSH induces intense neurogenesis and cognitive recovery in Alzheimer transgenic mice through activation of melanocortin MC4 receptors. *Mol Cell Neurosci.* 2015;67:13-21.

Giuliani D, Ottani A, Neri L, Zaffe D, Grieco P, Jochem J, Cavallini GM, Catania A, Guarini S. Multiple beneficial effects of melanocortin MC₄ receptor agonists in experimental neurodegenerative disorders: Therapeutic perspectives. *Prog Neurobiol*. 2017;148:40-56. Review

Graham A, Wakamatsu K, Hunt G, Ito S, Thody AJ. Agouti protein inhibits the production of eumelanin and phaeomelanin in the presence and absence of alpha-melanocyte stimulating hormone. *Pigment Cell Res*. 1997;10(5):298-303.

Gruenewald DA, Marck BT, Matsumoto AM. Fasting-induced increases in food intake and neuropeptide Y gene expression are attenuated in aging male brown Norway rats. *Endocrinology*. 1996;137(10):4460-4467.

Gruenewald DA, Matsumoto AM. Age-related decrease in proopiomelanocortin gene expression in the arcuate nucleus of the male rat brain. *Neurobiol Aging*. 1991;12(2):113-121.

Harrold JA, Widdowson PS, Williams G. Altered energy balance causes selective changes in melanocortin-4(MC4-R), but not melanocortin-3 (MC3-R), receptors in specific hypothalamic regions: further evidence that activation of MC4-R is a physiological inhibitor of feeding. *Diabetes.* 1999;48(2):267-271.

Hartl J, Dietrich P, Moleda L, Müller-Schilling M, Wiest R. Neuropeptide Y restores non-receptor-mediated vasoconstrictive action in superior mesenteric arteries in portal hypertension. *Liver Int.* 2015;35(12):2556-2563.

Haskell-Luevano C, Monck EK. Agouti-related protein functions as an inverse agonist at a constitutively active brain melanocortin-4 receptor. *Regul Pept.* 2001;99(1):1-7.

Hazell TJ, Sawula L, Edgett BA, Walsh JJ, Gurd BJ. Regulation of plasma agouti-related protein and its relationship with hunger in lean and obese men. *Appetite.* 2016;107:166-170.

Hellard REA, Impastato RA, Gilpin NW. Intra-cerebral and intra-nasal melanocortin-4 receptor antagonist blocks withdrawal hyperalgesia in alcohol-dependent rats. *Addict Biol*. 2017;22(3):692-701.

Henry R, Casto R, Printz MP. Diurnal cardiovascular patterns in spontaneously hypertensive and Wistar-Kyoto rats. *Hypertension*. 1990;16(4):422-428.

Higuchi H, Nakano K, Iwasa A Decrease in prepro-neuropeptide Y gene expression in the adrenal gland and cerebral cortex of spontaneously hypertensive rats. *Neuropeptides.* 1993;25(6):343-349.

Hildebrandt AL, Kelly-Sullivan DM, Black SC. Validation of a high-resolution X ray computed tomography system to measure murine adipose tissue depot mass in situ and longitudinally. *J Pharmacol Toxicol Methods* 2002;47:99–106.

Hill C, Dunbar JC. The effects of acute and chronic alpha melanocyte stimulating hormone (alphaMSH) on cardiovascular dynamics in conscious rats. *Peptides* 2002;23(9):1625–1630.

Hillebrand JJ, Langhans W, Geary N. Validation of computed tomographic estimates of intra-abdominal and subcutaneous adipose tissue in rats and mice. *Obesity (Silver Spring)*. 2010;18:848-853.

Honda T, Wada E, Battey JF, Wank SA. Differential Gene Expression of CCK(A) and CCK(B) Receptors in the Rat Brain. *Mol Cell Neurosci*. 1993;4(2):143-154.

Horan M, Gibney E, Molloy E, McAuliffe F. Methodologies to assess paediatric adiposity. *Ir J Med Sci*. 2015;184:53-68.

Hsieh YL, Yang CC. Age-series characteristics of locomotor activities in spontaneously hypertensive rats: a comparison with the Wistar-Kyoto strain. *Physiol Behav*. 2008;93(4-5):777-782.

Huszar D, Lynch CA, Fairchild-Huntress V, Dunmore JH, Fang Q, Berkemeier LR, Gu W, Kesterson RA, Boston BA, Cone RD, Smith FJ, Campfield LA, Burn P, Lee F. Targeted disruption of the melanocortin-4 receptor results in obesity in mice. *Cell*. 1997; 88:131–141.

Ichiyama T, Sakai T, Catania A, Barsh GS, Furukawa S, Lipton JM. Systemically administered alpha-melanocyte-stimulating peptides inhibit NF-kappaB activation in experimental brain inflammation. *Brain Res.* 1999;836(1-2):31-37.

Ito N, Ito T, Kromminga A, Bettermann A, Takigawa M, Kees F, Straub RH, Paus R. Human hair follicles display a functional equivalent of the hypothalamic-pituitary-adrenal axis and synthesize cortisol. *FASEB J*. 2005;19(10):1332-1334.

Jégou S, Cone RD, Eberlé AN, Vaudry H: Handbook of Biologically Active Peptides: Chapter 111. 2013. Edited by: Abba J. Kastin.

Jones BJ, Bloom SR. The New Era of Drug Therapy for Obesity: The Evidence and the Expectations. *Drugs* 2015;75: 935–945.

Jonsson L, Skarphedinsson JO, Skuladottir GV, Watanobe H, Schiöth HB. Food conversion is transiently affected during 4-week chronic administration of melanocortin agonist and antagonist in rats. *J Endocrinol*. 2002;173(3):517-523.

Joseph SA, Pilcher WH, Bennett-Clarke C. Immunocytochemical localization of ACTH perikarya in nucleus tractus solitarius: evidence for a second opiocortin neuronal system. *Neurosci Lett.* 1983;38(3):221-225.

Judex S, Luu YK, Ozcivici E, Adler B, Lublinsky S, Rubin CT. Quantification of adiposity in small rodents using micro-CT. M*ethods* 2010;50:14-19.

JudyWV, Watanabe AM, Henry DP, Besch HR Jr, Murphy WR, Hockel GM. Sympathetic nerve activity: role in regulation of blood pressure in the spontaneously hypertensive rat. *Circ Res* 1976;38:21–29.

Jun DJ, Na KY, Kim W, Kwak D, Kwon EJ, Yoon JH, Yea K, Lee H, Kim J, Suh PG, Ryu SH, Kim KT. Melanocortins induce interleukin 6 gene expression and secretion through melanocortin receptors 2 and 5 in 3T3-L1 adipocytes. *J Mol Endocrinol*. 2010;44:225–236.

Kappeler L, Gourdji D, Zizzari P, Bluet-Pajot MT, Epelbaum J. Age-associated changes in hypothalamic and pituitary neuroendocrine gene expression in the rat. *J Neuroendocrinol.* 2003;15(6):592-601.

Kask A, Mutulis F, Muceniece R, Pähkla R,Mutule I,Wikberg JE, Rägo L, Schiöth HB. Discovery of a novel superpotent and selective melanocortin-4 receptor antagonist (HS024): evaluation in vitro and in vivo. *Endocrinology* 1998;139(12):5006–5014.

Kawabe T, Kawabe K, Sapru HN. Cardiovascular responses to chemical stimulation of the hypothalamic arcuate nucleus in the rat: role of the hypothalamic paraventricular nucleus. *PLoS One.* 2012;7(9):e45180.

Keller K, Engelhardt M. Strength and muscle mass loss with aging process. Age and strength loss. *Muscles Ligaments Tendons J.* 2014;3(4):346-350.

Khoury M, Manlhiot C, Gibson D, Chahal N, Stearne K, Dobbin S, McCrindle BW. Universal screening for cardiovascular disease risk factors in adolescents to identify high-risk families: a population-based cross-sectional study. *BMC Pediatr*. 2016;16:11.

Kim MS, Rossi M, Abbott CR, AlAhmed SH, Smith DM, Bloom SR. Sustained orexigenic effect of Agouti related protein may be not mediated by the melanocortin 4 receptor. *Peptides* 2002;23(6):1069-1076.

Kirk EP, Klein S. Pathogenesis and pathophysiology of the cardiometabolic syndrome. *J Clin Hypertens (Greenwich).* 2009;11(12):761-765.

Kishi T, Aschkenasi CJ, Lee CE, Mountjoy KG, Saper CB, Elmquist JK. Expression of melanocortin 4 receptor mRNA in the central nervous system of the rat. *J Comp Neurol.* 2003;457(3):213-235.

Kiss JZ, Williams TH. ACTH-immunoreactive boutons form synaptic contacts in the hypothalamic arcuate nucleus of rat: evidence for local opiocortin connections. *Brain Res.* 1983;263:142-146.

Kmiec Z, Pétervári E, Balaskó M, Székely M. Anorexia of Aging. Vitamins & Hormones - Advances in research and applications 2013;92:319-355.

Knigge KM, Joseph SA. Relationship of the central ACTH-immunoreactive opiocortin system to the supraoptic and paraventricular nuclei of the hypothalamus of the rat. *Brain Res.* 1982;239(2):655-658.

Koch M, Varela L, Kim JG, Kim JD, Hernández-Nuño F, Simonds SE, Castorena CM, Vianna CR, Elmquist JK, Morozov YM, Rakic P, Bechmann I, Cowley MA, Szigeti-Buck K, Dietrich MO, Gao XB, Diano S, Horvath TL. Hypothalamic POMC neurons promote cannabinoid-induced feeding. *Nature*. 2015;519(7541):45-50.

Konda Y, Gantz I, DelValle J, Shimoto Y, Miwa H, Yamada T. Interaction of dual intracellular signaling pathways activated by the melanocortin-3 receptor. *J of Biol Chem*. 1994;269(18):13162–13166.

Kowalski C, Micheau J, Corder R, Gaillard R, Conte-Devolx B. Age-related changes in cortico-releasing factor, somatostatin, neuropeptide Y, methionine enkephalin and beta-endorphin in specific rat brain areas. *Brain Res*. 1992;582(1):38-46.

Krashes MJ, Lowell BB, Garfield AS. Melanocortin-4 receptor-regulated energy homeostasis. *Nat Neurosci*. 2016;19(2):206-219.

Krude H, Biebermann H, Luck W, Horn R, Brabant G, Grüters A. Severe early-onset obesity, adrenal insufficiency and red hair pigmentation caused by POMC mutations in humans. *Nat Genet*. 1998:19(2):155-157.

Landi F, Calvani R, Tosato M, et al. Anorexia of Aging. Risk Factors, Consequences, and potential Treatments. *Nutrients.* 2016;8(2):69.

Lechan RM, Fekete C. The TRH neuron: a hypothalamic integrator of energy metabolism. *Prog Brain Res*. 2006;153:209-235.

Lee DJ, Taylor AW. Following EAU recovery there is an associated MC5r-dependent APC induction of regulatory immunity in the spleen. *Invest Ophthalmol Vis Sci*. 2011;52:8862–8867.

Lee M, Wardlaw SL. The central melanocortin system and the regulation of energy balance. *Front Biosci.* 2007;12:3994-4010.

Lee MJ, Pramyothin P, Karastergiou K, Fried SK. Deconstructing the roles of glucocorticoids in adipose tissue biology and the development of central obesity. *Biochim Biophys Acta*. 2014;1842(3):473-481.

Légrádi G, Lechan RM. Agouti-related protein containing nerve terminals innervate thyrotropin-releasing hormone neurons in the hypothalamic paraventricular nucleus. *Endocrinology*. 1999;140(8):3643-3652.

Leinninger GM. Location, location, location: the CNS sites of leptin action dictate its regulation of homeostatic and hedonic pathways. *Int J Obes (Lond).* 2009;33 Suppl 2:S14-7.

Leoni G, Patel HB, Sampaio AL, Gavins FN Murray JF, Grieco P, Getting SJ, Perretti M. Inflamed phenotype of the mesenteric microcirculation of melanocortin type 3 receptor-null mice after ischemiareperfusion. *FASEB J.* 2008(12): 4228–4238.

Li P, Cui BP, Zhang LL, Sun HJ, Liu TY, Zhu GQ. Melanocortin 3/4 receptors in paraventricular nucleus modulate sympathetic outflow and bloodpressure. Exp Physiol. 2013;98(2):435-443.

Lindsay WR, Wapstra E, Silverin B, Olsson M. Corticosterone: a costly mediator of signal honesty in sand lizards. *Ecol Evol*. 2016;6(20):7451-7461.

Liu H, Kishi T, Roseberry AG, Cai X, Lee CE, Montez JM, Friedman JM, Elmquist JK. Transgenic mice expressing green fluorescent protein under the control of the melanocortin-4 receptor promoter. *J Neurosci*. 2003;23(18):7143-7154.

Lloyd JM, Scarbrough K, Weiland NG, Wise PM. Age-related changes in proopiomelanocortin (POMC) gene expression in the periarcuate region of ovariectomized rats. *Endocrinology*. 1991;129(4):1896-1902.

Loh YP. Immunological evidence for two common precursors to corticotropins, endorphins, and melanotropin in the neurointermediate lobe of the toad pituitary. *Proc Natl Acad Sci U S A.* 1979;76:796–800.

Loos RJ, Lindgren CM, Li S, Wheeler E, Zhao JH, Prokopenko I, Inouye M, Freathy RM, Attwood AP, Beckmann JS, Berndt SI et al. Common variants near MC4R are associated with fat mass, weight and risk of obesity. *Nat Genet.* 2008;40(6):768-775.

Loos RJ. The genetic epidemiology of melanocortin 4 receptor variants. *Eur J Pharmacol* 2011;660:156–164.

Lubura M, Hesse D, Neumann N, Scherneck S, Wiedmer P, Schürmann A. Non invasive quantification of white and brown adipose tissues and liver fat content by computed tomography in mice. *PLoS One* 2012;7(5):e37026.

Lutz TA, Woods SC. Overview of animal models of obesity. *Curr Protoc Pharmacol*. 2012;Chapter 5:Unit5.61.

Luu YK, Lublinsky S, Ozcivici E, Capilla E, Pessin JE, Rubin CT, Judex S. In vivo quantification of subcutaneous and visceral adiposity by micro-computed tomography in a small animal model. *Med Eng Phys.* 2009;31:34–41.

Maaser C, Kannengiesser K, Kucharzik T. Role of the melanocortin system in inflammation. *Ann N Y Acad Sci*. 2006;1072:123-34. Review

MacIntosh CG, Morley JE, Wishart J, Morris H, Jansen JB, Horowitz M, Chapman IM: Effect of exogenous cholecystokinin (CCK)-8 on food intake and plasma CCK, leptin, and insulin concentrations in older and young adults: evidence for increased CCK activity as a cause of the anorexia of aging. *J. Clin. Endocrinol. Metab*. 2001;86:5830–5837.

MacNeil DJ, Howard AD, Guan X, Fong TM, Nargund RP, Bednarek MA, Goulet MT, Weinberg DH, Strack AM, Marsh DJ, Chen HY, Shen CP, Chen AS, Rosenblum CI, MacNeil T, Tota M, MacIntyre ED, Van der Ploeg LH. The role of melanocortins in body weight

regulation: opportunities for the treatment of obesity. *Eur J Pharmacol.* 2002;450(1):93-109. Review.

Mains RE, Eipper BA. Synthesis and secretion of corticotropins, melanotropins, and endorphins by rat intermediate pituitary cells. *J Biol Chem*. 1979;254:7885–7894.

Malik IA, Triebel J, Posselt J, Khan S, Ramadori P, Raddatz D, Ramadori G. Melanocortin receptors in rat liver cells: change of gene expression and intracellular localization during acute-phase response. *Histochem Cell Biol.* 2012;137(3):279-291.

Manna SK, Aggarwal BB. *α*-melanocyte-stimulating hormone inhibits the nuclear transcription factor NF-*κ*B activation induced by various inflammatory agents. *J of Immun*. 1998;161(6):2873–2880.

Marshall MW, Smith BP, Munson AW, Lehmann RP. Prediction of carcass fat from body measurements made on live rats differing in age, sex and strain. *Br. J. Nutr*. 1969;2:353-369.

Martin WJ, MacIntyre DE. Melanocortin receptors and erectile function. *Eur Urol*. 2004;45(6):706-713.

Martinez M, Hernanz A, Go´mez-Cerezo J, Pena JM, Vazquez J J, & Arnalich F. Alterations in plasma and cerebrospinal fluid levels of neuropeptides in idiopathic senile anorexia. *Regulatory Peptides.* 1993;49(2):109–117.

Matsumoto AM, Marck BT, Gruenewald DA, Wolden-Hanson T, Naai MA. Aging and the neuroendocrine regulation of reproduction and body weight. *Exp Gerontol*. 2000;35(9-10):1251-1265.

Matsumura K, Tsuchihashi T, Abe I, Iida M. Central alpha-melanocyte-stimulating hormone acts at melanocortin-4 receptor to activate sympathetic nervous system in conscious rabbits. *Brain Res*. 2002;948(1–2):145–148.

McGraw KO, Wong SP. Forming inferences about some intraclass correlations coefficients. *Psychol Metho*ds 1996;1:30–46.

McLean KJ, Jarrott B, Lawrence AJ. Neuropeptide Y gene expression and receptor autoradiography in hypertensive and normotensive rat brain. *Brain Res Mol Brain Res*. 1996;35(1-2):249-259.

McShane TM, Wilson ME, Wise PM. Effects of lifelong moderate caloric restriction on levels of neuropeptide Y, proopiomelanocortin, and galanin mRNA. *J Gerontol A Biol Sci Med Sci.* 1999;54(1):B14-B21.

Mencarelli M, Dubern B, Alili R, Maestrini S, Benajiba L, Tagliaferri M, Galan P, Rinaldi M, Simon C, Tounian P, Hercberg S, Liuzzi A, Di Blasio AM, Clement K. Rare melanocortin-3 receptor mutations with in vitro functional consequences are associated with human obesity. *Hum Mol Genet*. 2011; 20:392–399.

Meneses A, Perez-Garcia G, Ponce-Lopez T, Tellez R, Gallegos-Cari A, Castillo C. Spontaneously hypertensive rat (SHR) as an animal model for ADHD: a short overview. *Rev Neurosci.* 2011;22(3):365-371.

Miesel A, Müller H, Thermann M, Heidbreder M, Dominiak P, Raasch W. Overfeeding-induced obesity in spontaneously hypertensive rats: an animal model of the human metabolic syndrome. *Ann Nutr Metab*. 2010;56(2):127-142.

Moehlecke M, Canani LH, Silva LO, Trindade MR, Friedman R, Leitão CB. Determinants of body weight regulation in humans. *Arch Endocrinol Metab.* 2016;60(2):152-162.

Møller CL, Raun K, Jacobsen ML, Pedersen T, Holst B, CondeFrieboes KW, Wulff BS. Characterization of murine melanocortin receptors mediating adipocyte lipolysis and examination of signalling pathways involved. *Mol Cell Endocrinol.* 2011;341:9–17.

Morley JE, Hernandez EN, Flood JF. Neuropeptide Y increases food intake in mice. *Am J Physiol*. 1987;253(3 Pt 2):R516-R522.

Morley JE. Anorexia, sarcopenia, and aging. *Nutrition.* 2001;17(7-8):660–663.

Morton GJ, Cummings DE, Baskin DG, Barsh GS, Schwartz MW. Central nervous system control of food intake and body weight. *Nature.* 2006; 443:289–295.

Mountjoy KG, Mortrud MT, Low MJ, Simerly RB, Cone RD. Localization of the melanocortin-4 receptor (MC4-R) in neuroendocrine and autonomic control circuits in the brain. *Mol Endocrinol*. 1994;8:1298-1308.

Mountjoy KG, Robbins LS, Mortrud MT, Cone RD. The cloning of a family of genes that encode the melanocortin receptors. *Science*. 1992;257(5074):1248-1251.

Mountjoy KG, Wu CS, Cornish J, Callon KE. alpha-MSH and desacetyl-alpha-MSH signaling through melanocortin receptors. *Ann N Y Acad Sci*. 2003;994:58-65. Review.

Mountjoy KG. Functions for pro-opiomelanocortin-derived peptides in obesity and diabetes. *Biochem J.* 2010;428(3):305-324.

Mountjoy KG. POMC neurons, POMC-derived peptides, melanocortin receptors and obesity: How understanding of this system has changed over the last decade. *J Neuroendocrinol.* 2015;27(6):406-418.

Myers B, McKlveen JM, Herman JP. Glucocorticoid actions on synapses, circuits, and behavior: Implications for the energetics of stress. *Front Neuroendocrinol*. 2014;35(2):180-196.

Nelson JF, Bender M, Schachter BS. Age-related changes in proopiomelanocortin messenger ribonucleic acid levels in hypothalamus and pituitary of female C57BL/6J mice. *Endocrinology*. 1988;123(1):340-344.

Ni XP, Bhargava A, Pearce D, Humphreys MH. Modulation by dietary sodium intake of melanocortin 3 receptor mRNA and protein abundance in the rat kidney. *Am. J. Physiol. Regul. Integr. Comp. Physiol.* 2006;290(3):R560–R567.

Ni XP, Butler AA, Cone RD. Humphreys MH. Central receptors mediating the cardiovascular actions of melanocyte stimulating hormones. *J. Hypertens*. 2006;24(11):2239–2246.

Nicholson JR, Kohler G, Schaerer F, Senn C, Weyermann P, Hofbauer KG. Peripheral administration of a melanocortin 4-receptor inverse agonist prevents loss of lean body mass in tumor-bearing mice. *J Pharmacol Exp Ther*. 2006;317(2):771-777.

Nijenhuis WA, Oosterom J, Adan RA. AgRP(83-132) acts as an inverse agonist on the human-melanocortin-4 receptor. *Mol Endocrinol*. 2001;15(1):164-171.

Norman D, Isidori AM, Frajese V, Caprio M, Chew SL, Grossman AB, Clark AJ, Michael Besser G, Fabbri A. ACTH and alpha-MSH inhibit leptin expression and secretion in 3T3-L1 adipocytes: model for a central-peripheral melanocortin-leptin pathway. *Mol Cell Endocrinol.* 2003; 200:99–109.

Ohta M, Tanaka Y, Masuda M, Miyasaka K, Funakoshi A: Impaired release of cholecystokinin (CCK) from synaptosomes in old rats. *Neurosci. Lett*. 1995;198, 161–164.

Oliveira SA Jr, Okoshi K, Lima-Leopoldo AP, Leopoldo AS, Campos DH, Martinez PF, Okoshi MP, Padovani CR, Pai-Silva MD, Cicogna AC. Nutritional and cardiovascular profiles of normotensive and hypertensive rats kept on a high fat diet. *Arq Bras Cardiol* 2009;93:526–533.

Ollmann MM, Wilson BD, Yang YK, Kerns JA, Chen Y, Gantz I, Barsh GS. Antagonism of central melanocortin receptors in vitro and in vivo by agouti-related protein. *Science* 1997; 278:135–138.

Osto M, Lutz T. Translational value of animal models of obesity—Focus on dogs and cats. *Eur J Pharmacol*. 2015;759:240–252.

Padilla SL, Reef D, Zeltser LM. Defining POMC neurons using transgenic reagents: impact of transient Pomc expression in diverse immature neuronal populations. *Endocrinology*. 2012;153(3):1219-31.

Pan XC, Song YT, Liu C, Xiang HB, Lu CJ. Melanocortin-4 receptor expression in the rostral ventromedial medulla involved in modulation of nociception in transgenic mice. *J Huazhong Univ Sci Technolog Med Sci*. 2013;33(2):195-198.

Pavia JM, Morris MJ. Age-related changes in neuropeptide Y content in brain and peripheral tissues of spontaneously hypertensive rats. *Clin Exp Pharmacol Physiol*. 1994;21(4):335-338.

Pavia JM, Schioth HB, Morris MJ. Role of MC4 receptors in the depressor and bradycardic effects of alpha-MSH in the nucleus tractus solitarii of the rat. *Neuroreport* 2003;14(5)703–707.

Paxinos G, Watson C. The rat brain in stereotaxic coordinates. 2005;5th edn. Academic, San Diego

Payne AM, Dodd SL, Leeuwenburgh C. Life-long calorie restriction in Fischer 344 rats attenuates age-related loss in skeletal muscle-specific force and reduces extracellular space. *J Appl Physiol (1985).* 2003;95(6):2554-2562.

Pernow J, Saria A, Lundberg JM. Mechanisms underlying pre- and postjunctional effects of neuropeptide Y in sympathetic vascular control. *Acta Physiol Scand*. 1986;126(2):239-249.

Pétervári E, Garami A, Soós S, Székely M, Balaskó M. Age-dependence of alpha-MSH-induced anorexia. *Neuropeptides*. 2010;44(4):315-322.

Pétervári E, Rostás I, Soós S, Tenk J, Mikó A, Füredi N, Székely M, Balaskó M. Age versus nutritional state in the development of central leptin resistance. *Peptides*. 2014;56:59-67.

Pétervári E, Szabad AO, Soós S, Garami A, Székely M, Balaskó M. Central alpha-MSH infusion in rats: disparate anorexic vs. metabolic changes with aging. *Regul Pept.* 2011;166(1-3):105-111.

Pétervári E, Szabad AO, Soós S, Garami A, Székely M, Balaskó M. Central alpha-MSH infusion in rats: disparate anorexic vs. metabolic changes with aging. *Regul Pept.* 2011;17;166(1-3):105-111.

Petriz BA, Almeida JA, Gomes CP, Ernesto C, Pereira RW, Franco OL. Exercise performed around MLSS decreases systolic blood pressure and increases aerobic fitness in hypertensive rats. *BMC Physiol*. 2015;15:1.

Pinto S, Roseberry AG, Liu H, Diano S, Shanabrough M, Cai X, Friedman JM, Horvath TL. Rapid rewiring of arcuate nucleus feeding circuits by leptin. Science. 2004;304(5667):110-115.

Pinto YM, Paul M, Ganten D. Lessons from rat models of hypertension: from Goldblatt to genetic engineering. *Cardiovasc Res*. 1998;39(1):77-88.

Porter K, Hayward LF. Stress-induced changes in c-Fos and corticotropin releasing hormone immunoreactivity in the amygdala of the spontaneously hypertensive rat. *Behav Brain Res*. 2011;216(2):543-551.

Ramachandrappa S, Gorrigan RJ, Clark AJ, Chan LF. The melanocortin receptors and their accessory proteins. *Front Endocrinol (Lausanne).* 2013;4:9.

Rautiainen S, Wang L, Lee IM, Manson JE, Buring JE, Sesso HD. Dairy consumption in association with weight change and risk of becoming overweight or obese in middle-aged and older women: a prospective cohort study. *Am J Clin Nutr*. 2016;103(4):979-988.

Redondo P, García-Foncillas J, Okroujnov I, Bandrés E. *α*-MSH regulates interleukin-10 expression by human keratinocytes. *Archives of Dermatological Research*.1998;290(8):425–428.

Renquist BJ, Lippert RN, Sebag JA, Ellacott KL, Cone RD. Physiological roles of the melanocortin MC_3 receptor. *Eur J Pharmacol*. 2011;660(1):13-20.

Richard D, Monge-Roffarello B, Chechi K, Labbé SM, Turcotte EE. Control and physiological determinants of sympathetically mediated brown adipose tissue thermogenesis. *Front. Endocrinol. (Lausanne)* 2012;3:36.

Rigamonti AE, Bonomo SM, Scanniffio D, Cella SG, Müller EE. Orexigenic effects of a growth hormone secretagogue and nitric oxide in aged rats and dogs: correlation with the hypothalamic expression of some neuropeptidergic/receptorial effectors mediating food intake. *J Gerontol A Biol Sci Med Sci.* 2006;61(4):315-322.

Roberts SB, Fuss P, Heyman MB, Evans WJ, Tsay R, Rasmussen H, Fiatarone M, Cortiella J, Dallal GE, Young VR. Control of food intake in older men. *JAMA* 1994;272(20):1601-1606.

Rodrigues AR, Almeida H, Gouveia AM. Alpha-MSH signalling via melanocortin 5 receptor promotes lipolysis and impairs re-esterification in adipocytes. *Biochim Biophys Acta* 2013;1831:1267–1275.

Rolls BJ, Dimeo KA, Shide DJ. Age-related impairments in the regulation of food intake. *Am. J. Clin. Nutr*. 1995;62:923-931.

Romanovsky AA, Blatteis CM. Heat stroke: opioid-mediated mechanisms. *J Appl Physiol (1985).* 1996;81(6):2565-2570.

Romanovsky AA, Ivanov AI, Székely M. Neural route of pyrogen signaling to the brain. *Clin Infect Dis.* 2000;31 Suppl 5:S162-167.

Roselli-Rehfuss L, Mountjoy KG, Robbins LS, Mortrud MT, Low MJ, Tatro JB, Entwistle ML, Simerly RB, Cone RD. Identification of a receptor for gamma melanotropin and other proopiomelanocortin peptides in the hypothalamus and limbic system. *Proc Natl Acad Sci U S A.* 1993;90(19):8856-8860.

Rostás I, Tenk J, Mikó A, Füredi N, Soós S, Solymár M, Lengyel A, Székely M, Gaszner B, Feller D, Pétervári E, Balaskó M. Age-related changes in acute central leptin effects on energy balance are promoted by obesity. *Exp Gerontol.* 2016;85:118-127.

Sánchez E, Rubio VC, Thompson D, Metz J, Flik G, Millhauser GL, Cerdá-Reverter JM. Phosphodiesterase inhibitor-dependent inverse agonism of agouti-related protein on melanocortin 4 receptor in sea bass (Dicentrarchus labrax). *Am J Physiol Regul Integr Comp Physiol.* 2009;296(5):R1293-306.

Sato T, Asahi Y, Toide K, Nakayama N. Insulin resistance in skeletal muscle of the male Otsuka Long-Evans Tokushima Fatty rat, a new model of NIDDM. *Diabetologia*. 1995;38(9):1033-1041.

Savastano DM, Tanofsky-Kraff M, Han JC, Ning C, Sorg RA, Roza CA, Wolkoff LE, Anandalingam K, Jefferson-George KS, Figueroa RE, Sanford EL, Brady S, Kozlosky M, Schoeller DA, Yanovski JA. Energy intake and energy expenditure among children with polymorphisms of the melanocortin-3 receptor. *Am J Clin Nutr*. 2009;90:912–920.

Scantlebury MH, Chun KC, Ma SC, Rho JM, Kim DY. Adrenocorticotropic hormone protects learning and memory function in epileptic Kcna1-null mice. *Neurosci Lett*. 2017; 645:14-18.

Scarlett JM, Marks DL. The use of melanocortin antagonists in cachexia of chronic disease. *Expert Opin Investig Drugs*. 2005;14(10):1233-1239.

Scarpace PJ, Matheny M, Zhang Y, Shek EW, Prima V, Zolotukhin S, Tümer N. Leptin-induced leptin resistance reveals separate roles for the anorexic and thermogenic responses in weight maintenance. *Endocrinology*. 2002;143(8):3026-3035.

Scarpace PJ, Tümer N. Peripheral and hypothalamic leptin resistance with age-related obesity. *Physiol Behav*. 2001;74(4-5):721-727.

Schwartzberg DG, Nakane PK. ACTH-related peptide containing neurons within the medulla oblongata of the rat. Brain Res. 1983;276(2):351-356.

Seidah, NG, Chretien M. Pro-protein convertases of subtilisin/kexin family. *Methods Enzymol*. 1994;244:175–188.

Serra-Prat M, Palomera E, Clave P, Puig-Domingo M: Effect of age and frailty on ghrelin and cholecystokinin responses to a meal test. Am. *J. Clin. Nutr*. 2009;89(5):1410–1417.

Shek EW, Scarpace PJ. Resistance to the anorexic and thermogenic effects of centrally administrated leptin in obese aged rats. *Regul Pept*. 2000;92(1-3):65-71.

Shen Y, Tian M, Zheng Y, Gong F, Fu AK, Ip NY. Stimulation of the Hippocampal POMC/MC4R Circuit Alleviates Synaptic Plasticity Impairment in an Alzheimer's Disease Model. *Cell Rep.* 2016;17(7):1819-1831.

Shen WJ, Yao T, Kong X, Williams KW, Liu T. Melanocortin neurons: Multiple routes to regulation of metabolism. *Biochim Biophys Acta*. 2017;1863(10 Pt A):2477-2485.

Shutter JR, Graham M, Kinsey AC, Scully S, Luthy R, Stark KL. Hypothalamic expression of ART, a novel gene related to agouti, is up-regulated in obese and diabetic mutant mice. *Genes & Development*. 1997;11:593–602.

Silver AJ, Flood JF, Morley JE: Effect of gastrointestinal peptides on ingestion in old and young mice. *Peptides* 1988;9:221–225.

Singru PS, Fekete C, Lechan RM. Neuroanatomical evidence for participation of the hypothalamic dorsomedial nucleus (DMN) in regulation of the hypothalamic paraventricular nucleus (PVN) by alpha-melanocyte stimulating hormone. *Brain Res.* 2005;1064(1-2):42-51.

Singru PS, Wittmann G, Farkas E, Zséli G, Fekete C, Lechan RM. Refeeding-activated glutamatergic neurons in the hypothalamic paraventricular nucleus (PVN) mediate effects of melanocortin signaling in the nucleus tractus solitarius (NTS). *Endocrinology* 2012;153(8):3804-3814.

Slominski A, Ermak G, Mihm M. ACTH receptor, CYP11A1, CYP17 and CYP21A2 genes are expressed in skin. *J Clin Endocrinol Metab.* 1996;81:2746–2749.

Slominski A, Wortsman J, Luger T, Paus R, Solomon S. Corticotropin releasing hormone and proopiomelanocortin involvement in the cutaneous response to stress. *Physiological Reviews*. 2000;80(3):979–1020.

Smith EM, Blalock JE. Human lymphocyte production of corticotropin and endorphin-like substances: association with leukocyte interferon. *Proc Natl Acad Sci USA* 1981;78:7530–7534.

Smith MA, Hisadome K, Al-Qassab H, Heffron H, Withers DJ, Ashford ML. Melanocortins and agouti-related protein modulate the excitability of two arcuate nucleus neuron populations by alteration of resting potassium conductances. *J Physiol*. 2007;578(2):425-438.

So AY, Bernal TU, Pillsbury ML, Yamamoto KR, Feldman BJ. Glucocorticoid regulation of the circadian clock modulates glucose homeostasis. *Proc Natl Acad Sci U S A.* 2009;106(41):17582–17587.

Ste Marie L, Miura GI, Marsh DJ, Yagaloff K, Palmiter RD. A metabolic defect promotes obesity in mice lacking melanocortin-4 receptors. *Proc Natl Acad Sci U S A.* 2000;97(22):12339-12344.

Swart I, Jahng JW, Overton JM, Houpt TA. Hypothalamic NPY, AGRP, and POMC mRNA responses to leptin and refeeding in mice. *Am J Physiol Regul Integr Comp Physiol*. 2002;283(5): R1020-R1026.

Sweerts BW, Jarrott B, Lawrence AJ. The effect of acute and chronic restraint on the central expression of prepro-neuropeptide Y mRNA in normotensive and hypertensive rats. *J Neuroendocrinol*. 2001;13(7):608-617.

Swinburn BA, Ravussin E. 1994. Energy and macronutrient metabolism. *Bailliere's Clin. Endocrinol. Metab.* 1994;8(3):527-548.

Szekely M, Petervari E, Pakai E, Hummel Z, Szelenyi Z. Acute, subacute and chronic effects of central neuropeptide Y on energy balance in rats. *Neuropeptides* 2005;39:103-115.

Székely M, Soós Sz, Pétervári E, Balaskó M. Nutritional Impact on Anabolic and Catabolic Signaling. In: Molecular Basis of Nutrition and Aging. (Eds: Malavolta Marco, Mocchegiani Eugenio), Amsterdam; Boston; Heidelberg: Academic Press, 2016;Chapter 14, pp:189-204.

Székely M, Szelényi Z. Regulation of energy balance by peptides: a review. *Curr Protein Pept Sci*. 2005;6(4):327-353. Review.

Szelényi Z, Székely M. Comparison of the effector mechanisms during endotoxin fever in the adult rabbit. *Acta Physiol Acad Sci Hung*. 1979;54(1):33-41.

Tai MH, Weng WT, Lo WC, Chan JY, Lin CJ, Lam HC, Tseng CJ. Role of nitric oxide in alpha-melanocyte-stimulating hormoneinduced hypotension in the nucleus tractus solitarii of the spontaneously hypertensive rats. *J. Pharmacol. Exp. Ther*. 2007;321(2)455–461.

Takano S, Kanai S, Hosoya H, Ohta M, Uematsu H, Miyasaka K. Orexin-A does not stimulate food intake in old rats. *Am J Physiol Gastrointest Liver Physiol*. 2004;287:G1182–G1187.

Tao YX. Constitutive activity in melanocortin-4 receptor: biased signaling of inverse agonists. *Adv Pharmacol*. 2014; 70:135-54.

Tardif SD, Mansfield KG, Ratnam R, Ross CN, Ziegler TE. The marmoset as a model of aging and age-related diseases. *ILAR J*. 2011;52(1):54-65.

Taylor A, Namba K. In vitro induction of CD25? CD4? regulatory T cells by the neuropeptide alpha-melanocyte stimulating hormone (alpha-MSH). *Immunol Cell Biol.* 2001;79:358–367.

Taylor AW, Kitaichi N, Biros D. Melanocortin 5 receptor and ocular immunity. *Cell Mol Biol (Noisy-le-grand)* 2006; 52:53–59.

Taylor AW, Lee D. Applications of the role of a-MSH in ocular immune privilege. *Adv Exp Med Biol.* 2010; 681:143–149.

Tenk J, Ildikó Rostás I, Füredi N, Mikó A, Solymár M, Soós S, Gaszner B, Feller D, Székely M, Pétervári E, Balaskó M. Age-related changes in central effects of corticotropin-releasing factor (CRF) suggest a role for this mediator in aging anorexia and cachexia. *GeroScience*. 2017;39(1): 61–72.

Tenk J, Rostás I, Füredi N, Mikó A, Soós S, Solymár M, Gaszner B, Székely M, Pétervári E, Balaskó M. Acute central effects of corticotropin-releasing factor (CRF) on energy balance: Effects of age and gender. *Peptides.* 2016;85:63-72.

Tenover JL 1999. Trophic factors and male hormone replacement. In: Hazzard, W.R., Blass, J.P., Ettinger, W.H., Halter, J.B., Ouslander, J.G. (Eds.). Principles of Geriatric Medicine & Gerontology, McGraw-Hill, New York, pp. 1029-1040.

Thistlethwaite D, Darling JA, Fraser R, Mason PA, Rees LH, Harkness RA. Familial glucocorticoid deficiency. Studies of diagnosis and pathogenesis. *Arch Dis Child* 1975; 50:291–297.

Vaisse C, Clement K, Durand E, Hercberg S, Guy-Grand B, Froguel P. Melanocortin-4 receptor mutations are a frequent and heterogeneous cause of morbid obesity. *J Clin Invest.* 2000;106:253-262.

Vaisse C, Clement K, Guy-Grand B, Froguel P. A frameshift mutation in human MC4R is associated with a dominant form of obesity. *Nat Genet*. 1998;20(2):113-114.

Vasheghani-Farahani A, Majidzadeh-A K, Masoudkabir F, Karbalai S, Koleini M, Aiatollahzade-Esfahani F, Pashang M, Hakki E. Sagittal abdominal diameter to triceps skinfold thickness ratio: a novel anthropometric index to predict premature coronary atherosclerosis. *Atherosclerosis* 2013;227:329-333.

Vehapoğlu A, Türkmen S, Terzioğlu Ş. Alpha-Melanocyte-Stimulating Hormone and Agouti-Related Protein: Do They Play a Role in Appetite Regulation in Childhood Obesity? *J Clin Res Pediatr Endocrinol.* 2016;8(1):40-47.

Verty AN, Allen AM, Oldfield BJ. The endogenous actions of hypothalamic peptides on brown adipose tissue thermogenesis in the rat. *Endocrinology.* 2010;151(9):4236-4246.

Wang D, He X, Zhao Z, Feng Q, Lin R, Sun Y, Ding T, Xu F, Luo M, Zhan C. Whole-brain mapping of the direct inputs and axonal projections of POMC and AgRP neurons. *Front Neuroanat*. 2015;9:40.

Wang J, Thornton JC, Kolesnik S, Pierson RN. Anthropometry in body composition. An overview. *Ann N Y Acad Sci. 2000;*904: 317–326.

Whirledge S, Cidlowski JA. A Role for Glucocorticoids in Stress-Impaired Reproduction: Beyond the Hypothalamus and Pituitary. *Endocrinology*. 2013;154(12): 4450–4468.

Wikberg JE, Mutulis F. Targeting melanocortin receptors: an approach to treat weight disorders and sexual dysfunction. *Nat Rev Drug Discov*. 2008;7:307–323.

Williams G, Cai XJ, Elliott JC, Harrold JA. Anabolic neuropeptides. *Physiol Behav.* 2004; 81:211–222.

Winkels RM, Jolink-Stoppelenburg A, de Graaf K, Siebelink E, Mars M, de Groot L: Energy intake compensation after 3 weeks of restricted energy intake in young and elderly men. *J. Am. Med. Dir. Assoc.* 2011;12(4):277–286.

Wolden-Hanson T, Marck BT, Matsumoto AM. Blunted hypothalamic neuropeptide gene expression in response to fasting, but preservation of feeding responses to AgRP in aging male Brown Norway rats. *Am J Physiol Regul Integr Comp Physiol*. 2004:(1): R138-46.

Wolden-Hanson T. Mechanisms of the anorexia of aging in the Brown Norway rat. *Physiol Behav.* 2006;88(3):267-276.

Woo ND, Mukherjee K, Ganguly PK. Norepinephrine levels in paraventricular nucleus of spontaneously hypertensive rats: role of neuropeptide Y. Am J Physiol. 1993;265:H893–H898.

World Health Organization: Obesity and overweight fact sheet. Geneva, Switzerland Retrieved from: http://www.who.int/mediacentre/factsheets/fs311/en/ (2014).

World Health Organization: Obesity and overweight fact sheet. Geneva, Switzerland Retrieved from: http://www.who.int/mediacentre/factsheets/fs311/en/ (2015).

World Health Organization:10 facts on ageing and the life course. Geneva, Switzerland Retrieved from: http://www.who.int/features/factfiles/ageing/en/ (2012).

Yamakage H, Ito R, Tochiya M, Muranaka K, Tanaka M, Matsuo Y, Odori S, Kono S, Shimatsu A, Satoh-Asahara N. The utility of dual bioelectrical impedance analysis in detecting intra-abdominal fat area in obese patients during weight reduction therapy in comparison with waist circumference and abdominal CT. *Endocr. J.* 2014;61:807-819.

Ye DW, Liu C, Liu TT, Tian XB, Xiang HB. Motor cortex-periaqueductal gray-spinal cord neuronal circuitry may involve in modulation of nociception: a virally mediated transsynaptic tracing study in spinally transected transgenic mouse model. *PLoS One*. 2014;9(2): e89486.

Ye ZY, Li DP. Activation of the melanocortin-4 receptor causes enhanced excitation in presympathetic paraventricular neurons in obese Zucker rats. *Regul Pept.* 2011;166(1-3):112-120.

Yeo GS, Farooqi IS, Aminian S, Halsall DJ, Stanhope RG, O'Rahilly S. A frameshift mutation in MC4R associated with dominantly inherited human obesity. *Nat Genet*. 1998:111–112.

Yilmaz Z, Davis C, Loxton NJ, Kaplan AS, Levitan RD, Carter JC, Kennedy JL. Association between M C4R rs17782313 polymorphism and overeating behaviors. *Int J Obes (Lond)*. 2015;39(1):114-20.

Yilmaz Z, Kaplan AS, Tiwari AK, Levitan RD, Piran S, Bergen AW, Kaye WH, Hakonarson H, Wang K, Berrettini WH, Brandt HA, Bulik CM, Crawford S, Crow S, Fichter MM, Halmi KA, Johnson CL, Keel PK, Klump KL, Magistretti P, Mitchell JE, Strober M, Thornton LM, Treasure J, Woodside DB, Knight J, Kennedy JL. The role of leptin, melanocortin, and neurotrophin system genes on body weight in anorexia nervosa and bulimia nervosa. *J Psychiatr Res*. 2014;55:77-86.

Yin X, Zhu YH, Xu SF. Expression of preproopiomelanocortin mRNA and preprodynorphin mRNA in brain of spontaneously hypertensive rats. *Acta Pharmacol Sin*. 1997;18:391–394.

Zegers D, Beckers S, de Freitas F, Peeters AV, Mertens IL, Verhulst SL, Rooman RP, Timmermans JP, Desager KN, Massa G, Van Gaal LF, Van Hul W. Identification of three novel genetic variants in the melanocortin-3 receptor of obese children. *Obesity (Silver Spring)* 2011;19:152–159.

Zhan C, Zhou J, Feng Q, Zhang JE, Lin S, Bao J, Wu P, Luo M. Acute and long-term suppression of feeding behavior by POMC neurons in the brainstem and hypothalamus, respectively. *J Neurosci*. 2013;33(8):3624-3632.

Zhang L, Li WH, Anthonavage M, Pappas A, Rossetti D, Cavender D, Seiberg M, Eisinger M. Melanocortin-5 receptor and sebogenesis. *Eur J Pharmacol*. 2011;660(1):202-206.

Zhang Y, Matheny M, Tümer N, Scarpace PJ. Aged-obese rats exhibit robust responses to a melanocortin agonist and antagonist despite leptin resistance. *Neurobiol Aging.* 2004;25(10):1349-1360.

Zséli G, Vida B, Martinez A, Lechan RM, Khan AM, Fekete C. Elucidation of the anatomy of a satiety network: Focus on connectivity of the parabrachial nucleus in the adult rat. *J Comp Neurol.* 2016;524(14):2803-2827.

11. PUBLICATIONS

List of publications the PhD thesis is based on [Cumulative impact factor (IF): 13.158]

Nóra Füredi, Alexandra Mikó, Balázs Gaszner, Diána Feller, Ildikó Rostás, Judit Tenk, Margit Solymár, Márta Balaskó, Erika Pétervári. Activity of the hypothalamic melanocortin system decreases in middle-aged and increases in old rats. *Journals of Gerontology - Series A: Biological Sciences* 2017 Nov 1. doi: 10.1093/gerona/glx213.
IF: 5.957
Independent citations: 1

Furedi N, Miko A, Aubrecht B, Gaszner B, Feller D, Rostas I, Tenk J, Soos S, Balasko M, Balogh A, Pap M, Petervari E. Regulatory Alterations of Energy Homeostasis in Spontaneously Hypertensive Rats (SHR). *J Mol Neurosci*. 2016;59(4):521-530.
IF: 2.229

Rostás I, **Füredi N**, Tenk J, Mikó A, Solymár M, Soós S, Székely M, Pétervári E, Balaskó M. Age-related alterations in the central thermoregulatory responsiveness to alpha-MSH. *J Therm Biol.* 2015;49-50:9-15.
IF: 1.621
Independent citations: 1

Tekus E, Miko A, **Furedi N,** Rostas I, Tenk J, Kiss T, Szitter I, Balasko M, Helyes Z, Wilhelm M, Petervari E. Body fat of rats of different age-groups and nutritional states: assessment by micro-CT and skinfold thickness. *J Appl Physiol.* 2017:jap.00884.2016.
IF: 3.351 (2016)

List of other publications (cumulative IF: 27.498)

Balaskó M, Rostás I, **Füredi N**, Mikó A, Tenk J, Cséplő P, Koncsecskó-Gáspár M, Soós S, Székely M, Pétervári E. Age and nutritional state influence the effects of cholecystokinin on energy balance. *Exp Gerontol*. 2013;48(11):1180-1188.
IF: 3.529
Independent citations: 7

Pétervári E, Rostás I, Soós S, Tenk J, Mikó A, **Füredi N**, Székely M, Balaskó M. Age versus nutritional state in the development of central leptin resistance. *Peptides.* 2014;56:59-67.
IF: 2.618
Independent citations: 7

Mikó A, **Füredi N**, Tenk J, Rostás I, Soós S, Solymár M, Székely M, Balaskó M, Brunner SM, Kofler B, Pétervári E. Acute central effects of alarin on the regulation on energy homeostasis. *Neuropeptides*. 2016;pii: S0143-4179(16)30087-7.
IF: 2.486

Tenk J, Rostás I**, Füredi N**, Mikó A, Soós S, Solymár M, Gaszner B, Székely M, Pétervári E, Balaskó M. Acute central effects of corticotropin-releasing factor (CRF) on energy balance: Effects of age and gender. *Peptides*. 2016 ;85:63-72.
IF: 2.778

Rostás I, Tenk J, Mikó A, **Füredi N**, Soós S, Solymár M, Lengyel A, Székely M, Gaszner B, Feller D, Pétervári E, Balaskó M. Age-related changes in acute central leptin effects on energy balance are promoted by obesity. *Exp Gerontol*. 2016;85:118-127.
IF: 3.340 (2016)
Independent citations: 4

Tenk J, Mátrai P, Hegyi P, Rostás I, Garami A, Szabó I, Solymár M, Pétervári E, Czimmer J, Márta K, Mikó A, **Füredi N**, Párniczky A, Zsiborás C, Balaskó M. In Obesity, HPA Axis Activity Does Not Increase with BMI, but Declines with Aging: A Meta-Analysis of Clinical Studies. *PLoS One*. 2016;11(11):e0166842.
IF: 2.806

Tenk J, Rostás I, **Füredi N**, Mikó A, Solymár M, Soós S, Gaszner B, Feller D, Székely M, Pétervári E, Balaskó M. Age-related changes in central effects of corticotropin-releasing factor (CRF) suggest a role for this mediator in aging anorexia and cachexia. *Geroscience.* 2017;39(1):61-72.
IF: 2.123 (2016)
Independent citations: 3

Füredi N, Nagy Á, Mikó A, Berta G, Kozicz T, Pétervári E, Balaskó M, Gaszner B. Melanocortin 4 receptor ligands modulate energy homeostasis through urocortin 1 neurons of the centrally projecting Edinger-Westphal nucleus. *Neuropharmacology*. 2017;118:26-37.
IF: 5.012 (2016)

Rostás I, Pótó L, Mátrai P, Hegyi P, Tenk J, Garami A, Illés A, Solymár M, Pétervári E, Szűcs Á, Párniczky A, Pécsi D, Rumbus Z, Zsiborás C, **Füredi N,** Balaskó M.: In middle-aged and old obese patients, training intervention reduces leptin level: A meta-analysis. *PLoS One*. 2017 12(8):e0182801.
IF: 2.806 (2016)